Exoplanets of low-mass stars

(mostly M dwarfs)

Wednesday : **Advantages & Difficulties**

Today : **Individual systems & Statistical properties**

Family album

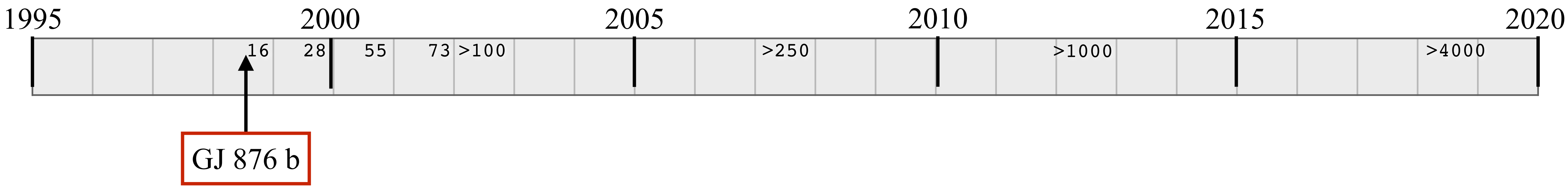

- GJ 876b: 1st M-dwarf host

(Delfosse et al. 1998; Marcy et al. 1998)

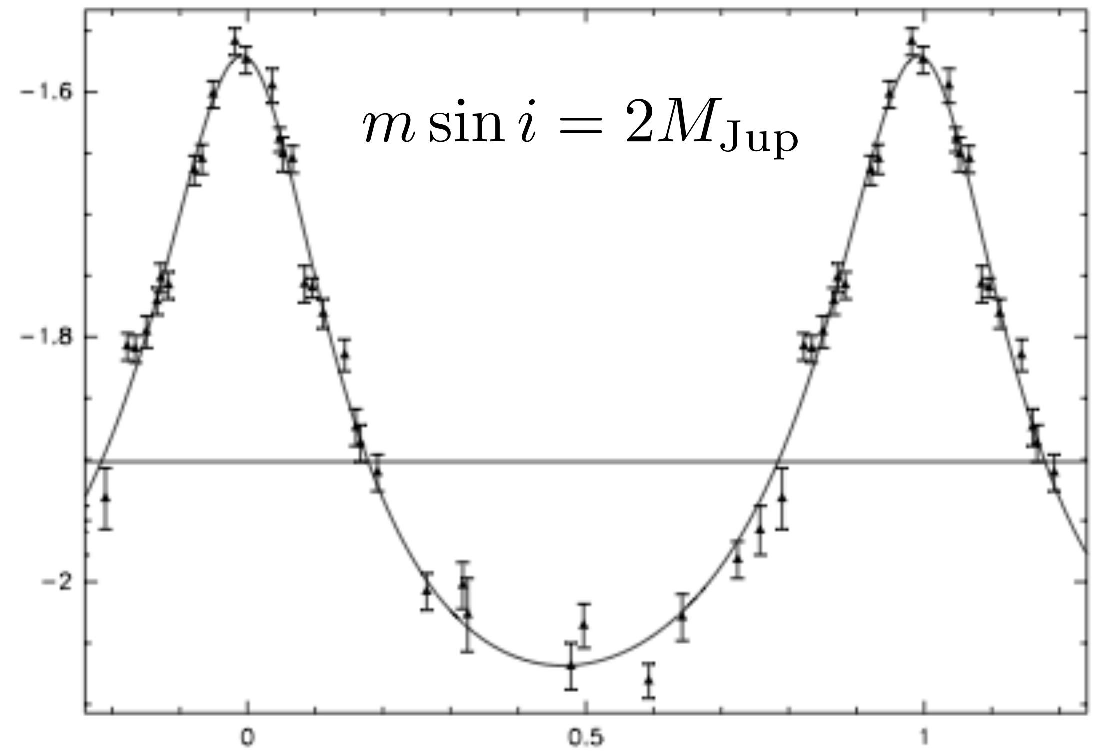

Fig. 1. Combined ELODIE and CORALIE radial velocities for Gl 876. The solid line is the radial velocity curve for the orbital solution.

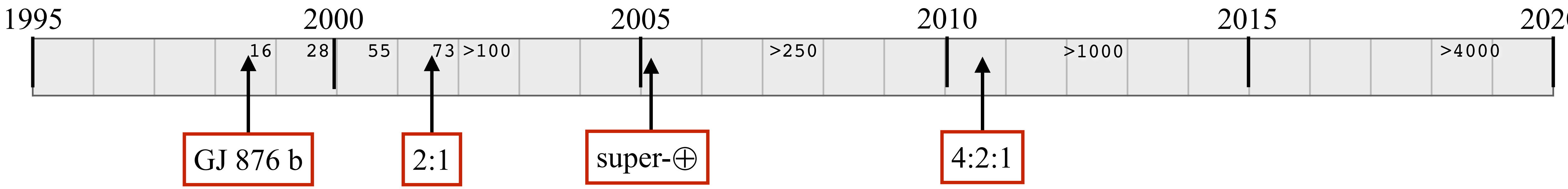

- GJ 876b: 1st M-dwarf host

  (Delfosse et al. 1998; Marcy et al. 1998)

- GJ 876c: pl-pl interactions

  (Marcy et al. 2001)

- GJ 876d: 1st super-Earth

  (Rivera et al. 2005)

- GJ 876e: Laplace resonance

  (Rivera et al. 2010)

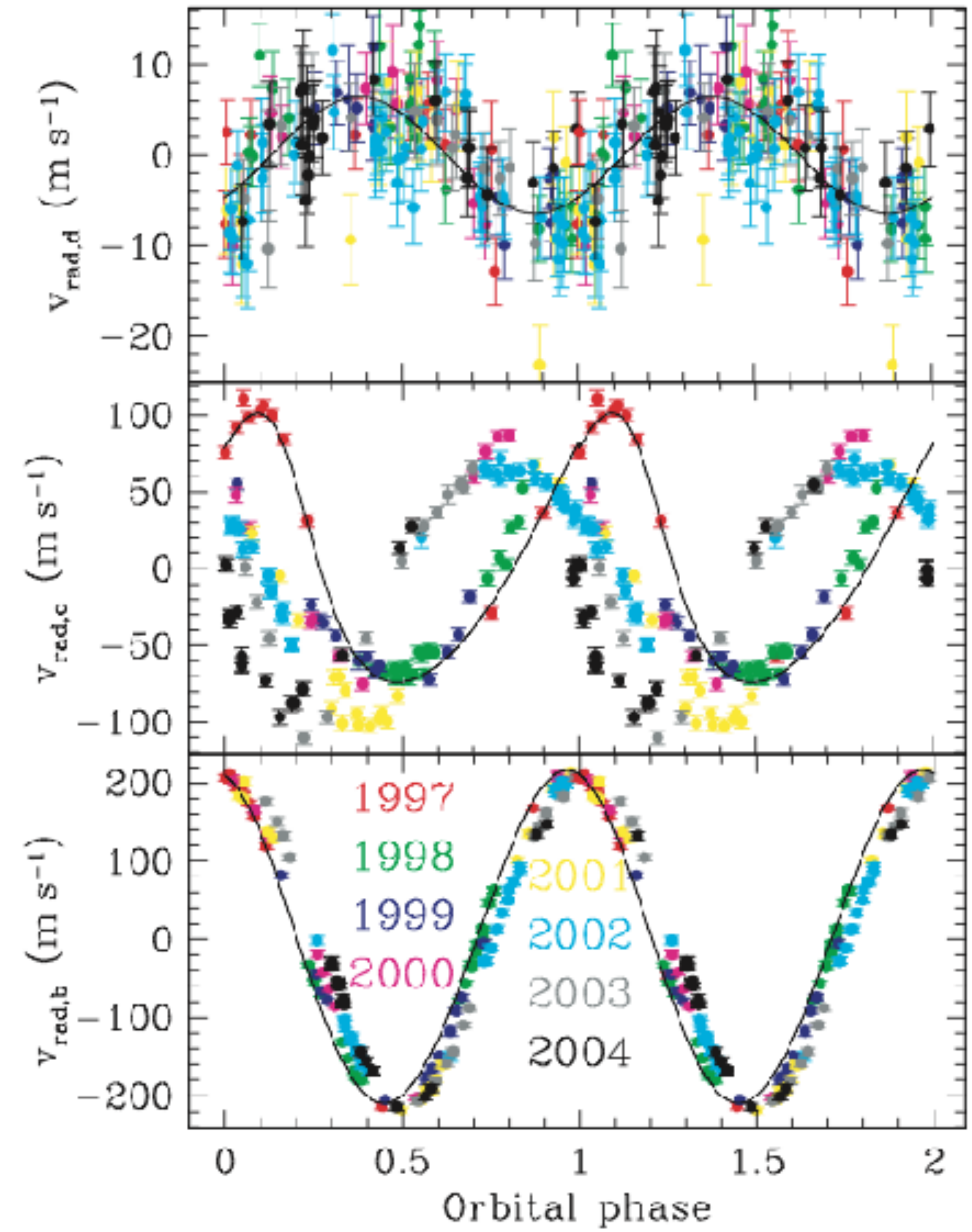

Careful: if pl-pl interactions are overlooked, you end up w/ 6+ planets

(Jenkins et al. 2014, MNRAS 441, 2253)

Planet d might not be rocky because of tidal heating ($10^{19} - 10^{20} W$; compared to $7 \times 10^{17} W$ to melt the planet)

Valencia et al. 2007

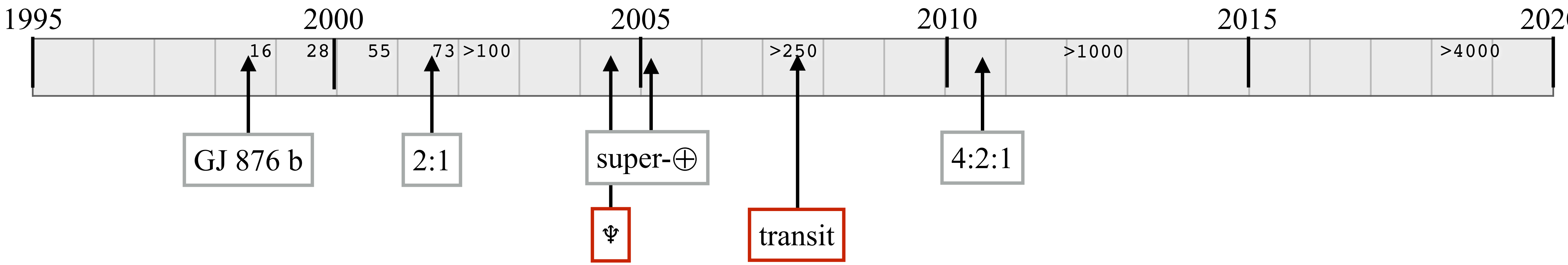

- GJ 436b: one of the 3 first exoNeptune
- caught in transit 3 years later

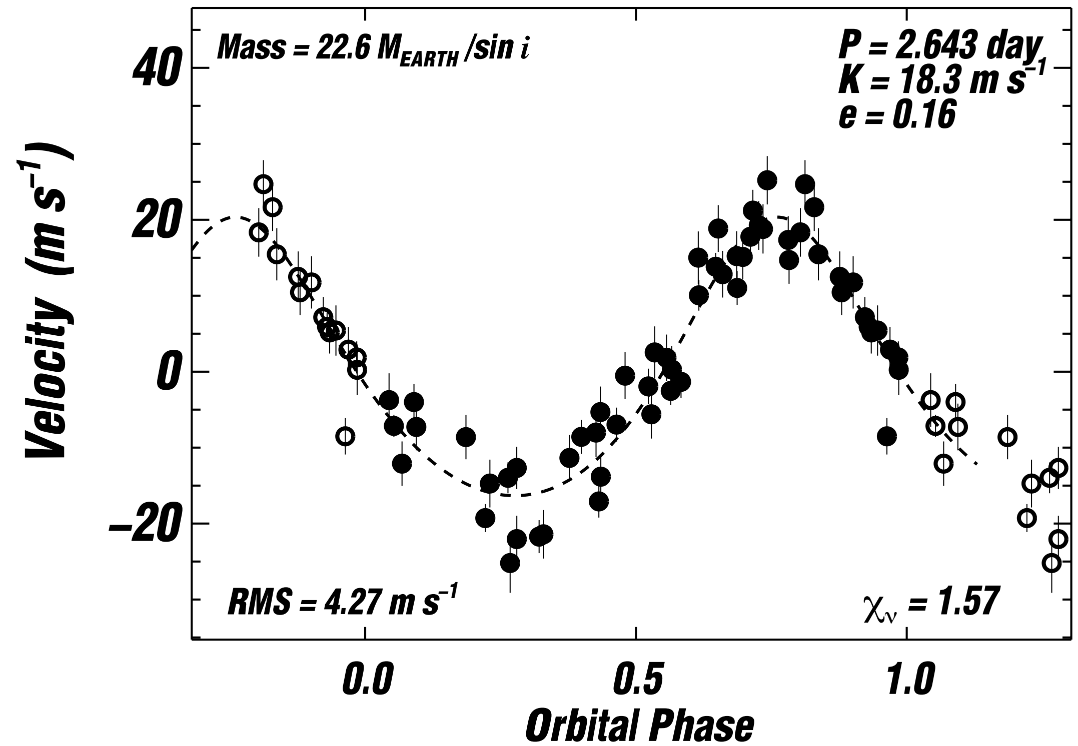

Butler et al. (2004); Maness et al. (2007)

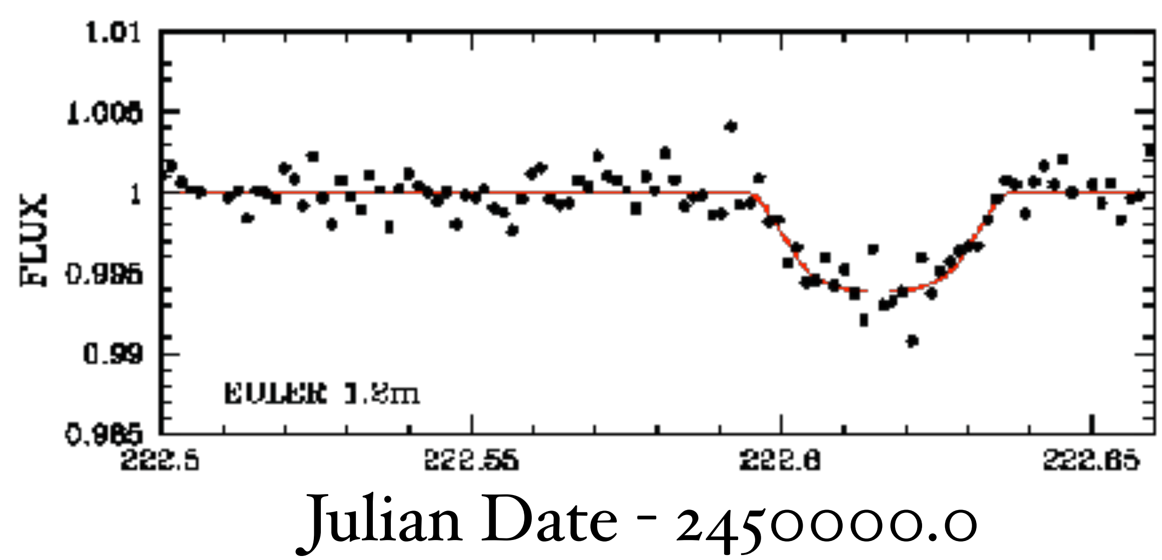

Gillon et al. (2007a)

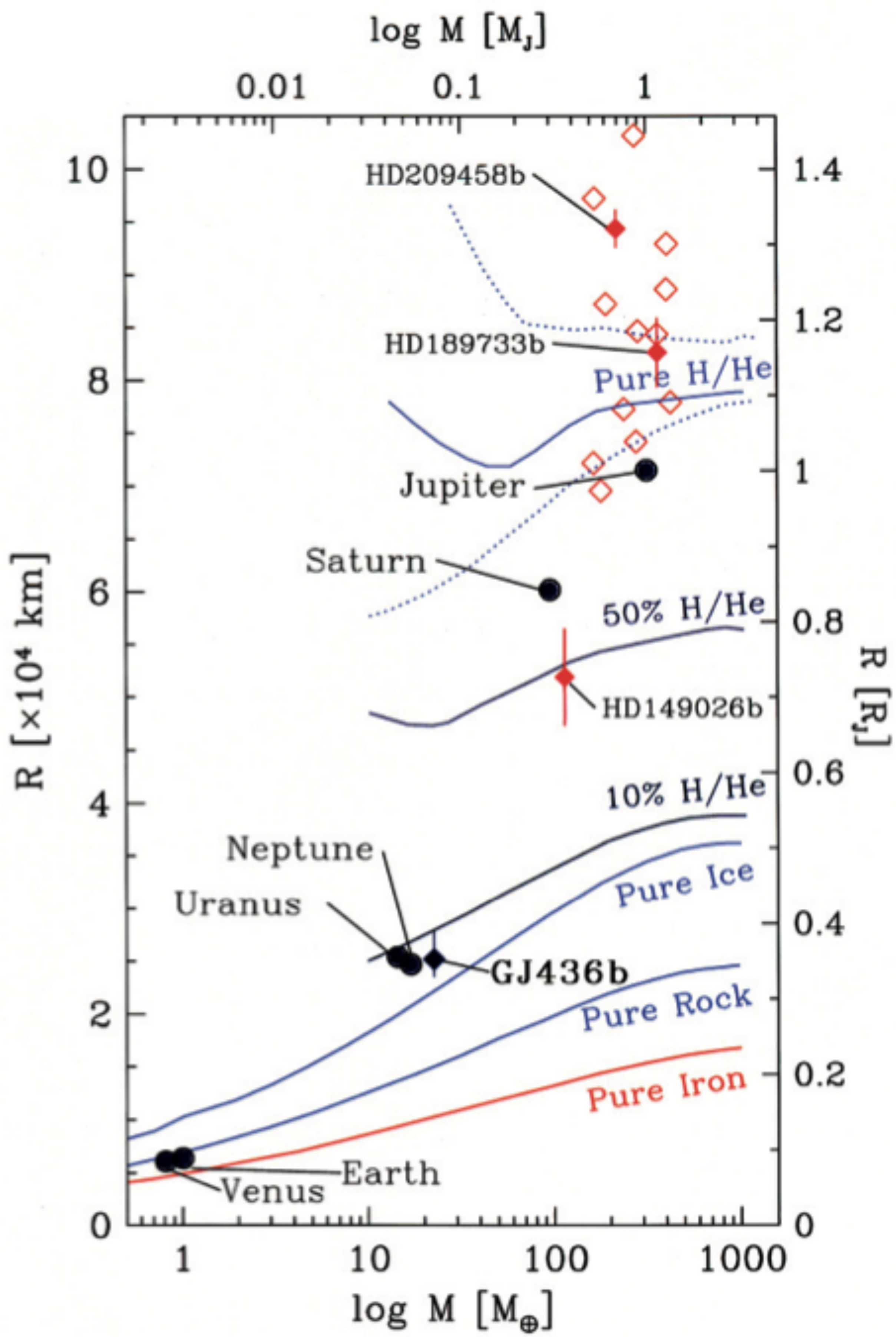

GJ 436 b's Characterization

- radius, mass, density

  Gillon et al. (2007b); Deming (2007); Torres (2007);

- bulk composition   H/He enveloppe

  Adams et al. (2008); Figueira et al. (2008); Nettelmann et al. (2010)

- precise eccentricity (e=0.14+-0.01)

  Demory et al. (2007); Deming (2007);

- search for companion (pertuber ?)

  Ribas et al. (2008); Alonso et al. (2007); Bean & Seifahrt (2008); Mardling (2008); Ballard et al. (2008, 2010); Batygin et al. (2009)

- secondary eclipse spectro.

  CO, H2O, <CH4

  Pont et al. (2009); Stevenson et al. (2010)

- transmission spectro

  CH4 dominated ? Beaulieu et al. (2011)

  No   Gibson et al. (2011)

  No, but CO   Knutson et al. (2011)

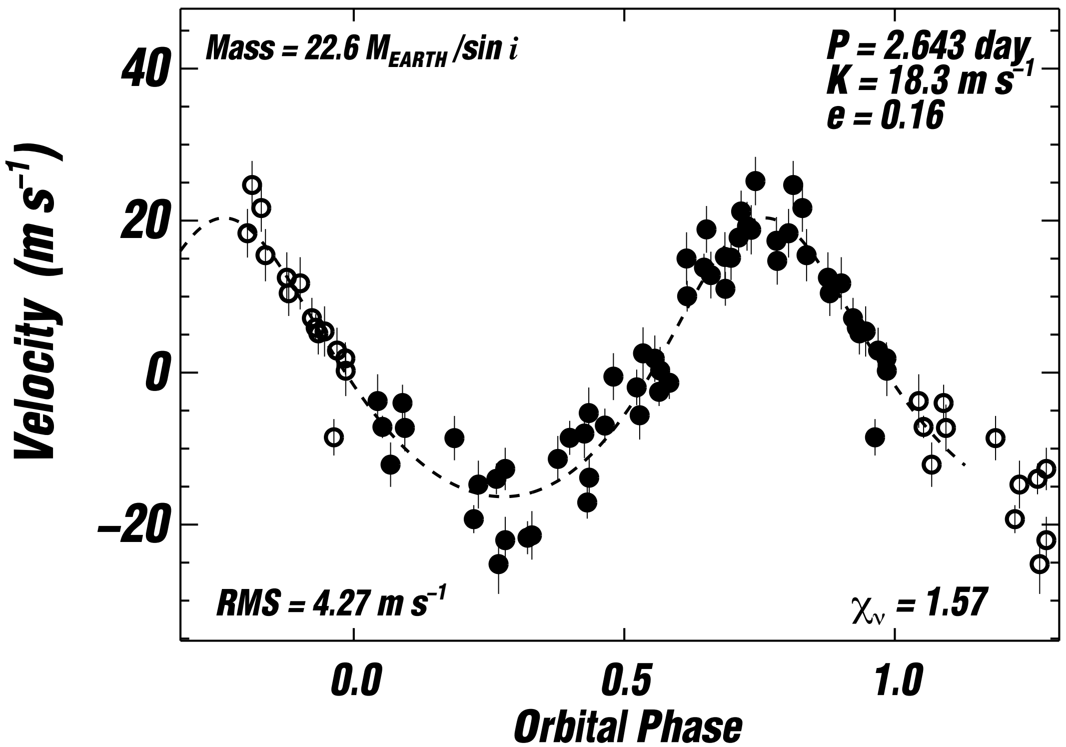

Demory et al. (2007)

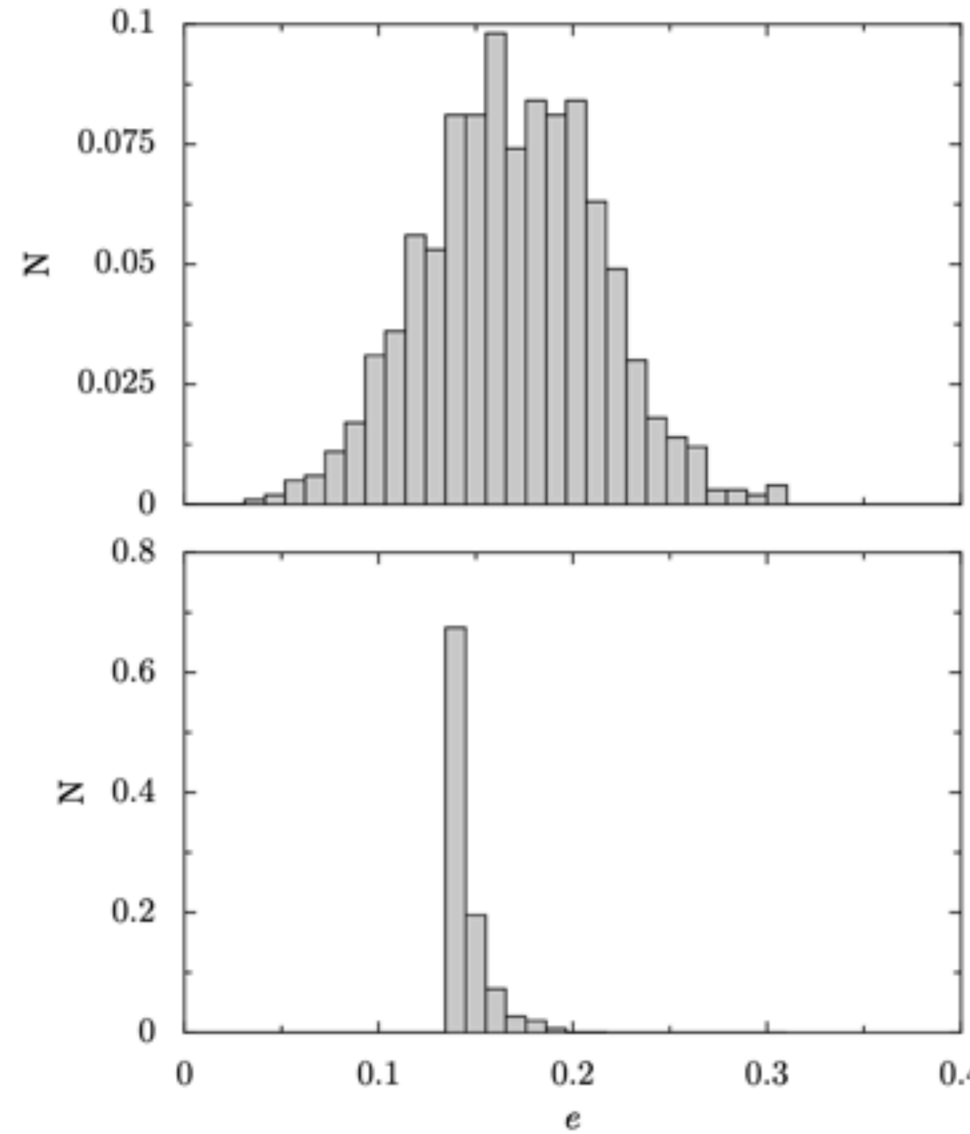

Fig. 3. Probability distributions for the eccentricity resulting from randomly generated datasets including: *Top*: radial velocity data only. *Bottom*: radial velocities + transit and secondary eclipse timings.

Bourier et al. (2017)

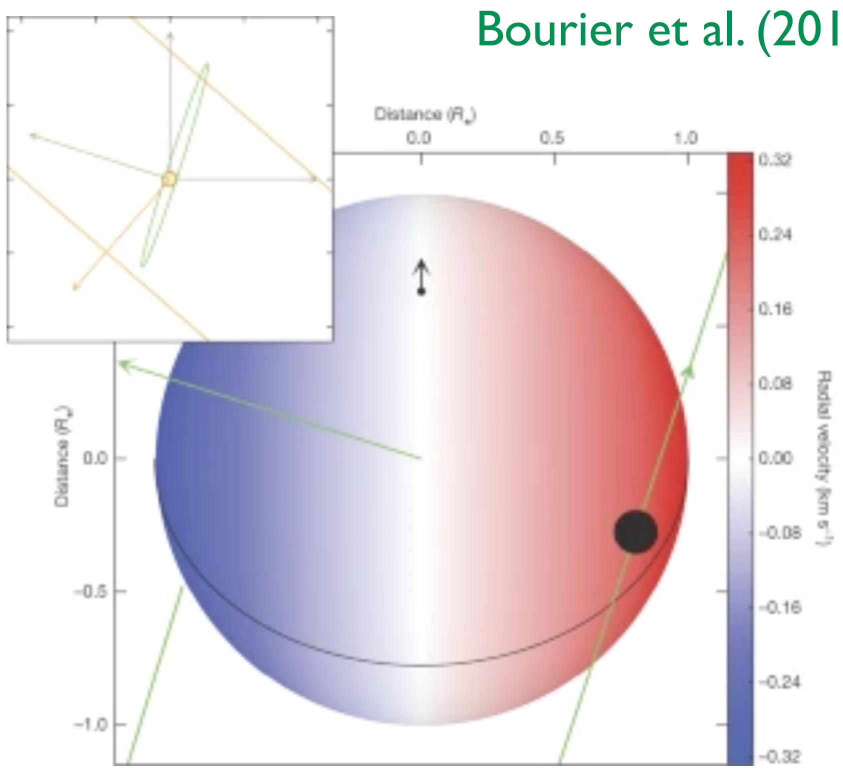

Xavier Bonfils

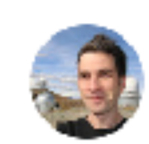

HD 209458

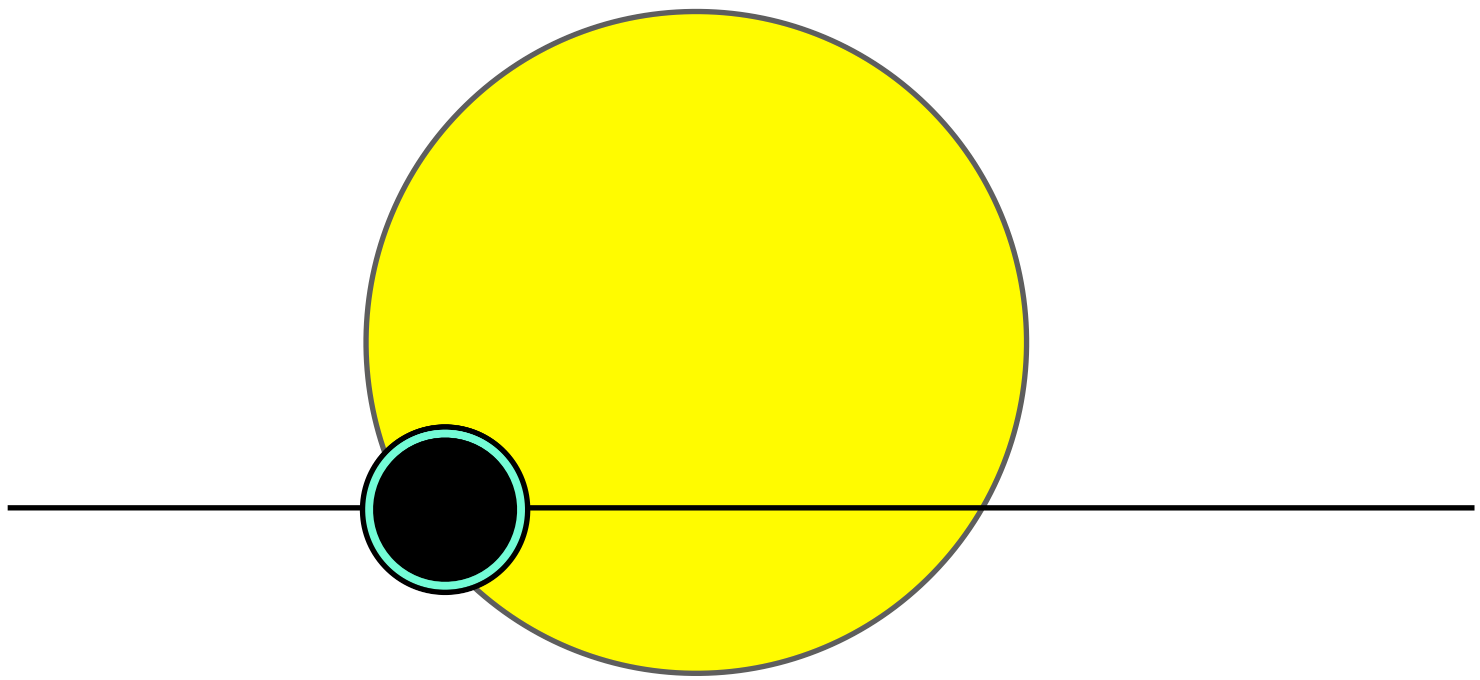

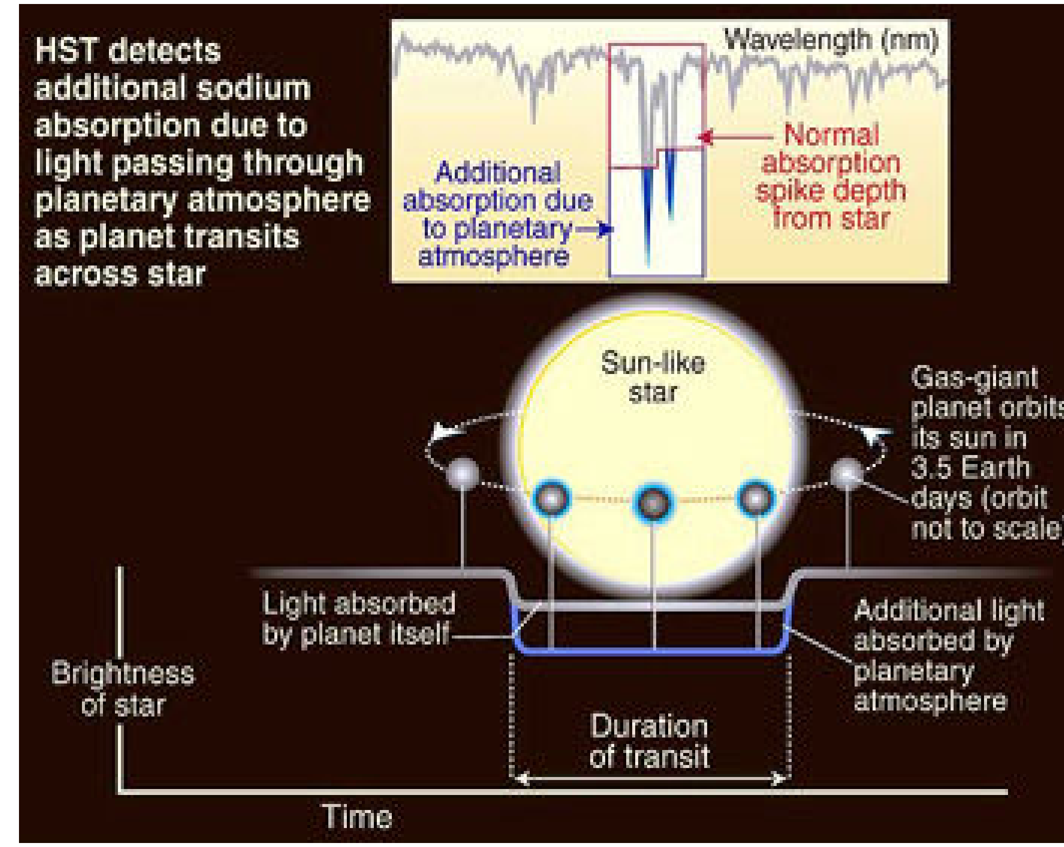

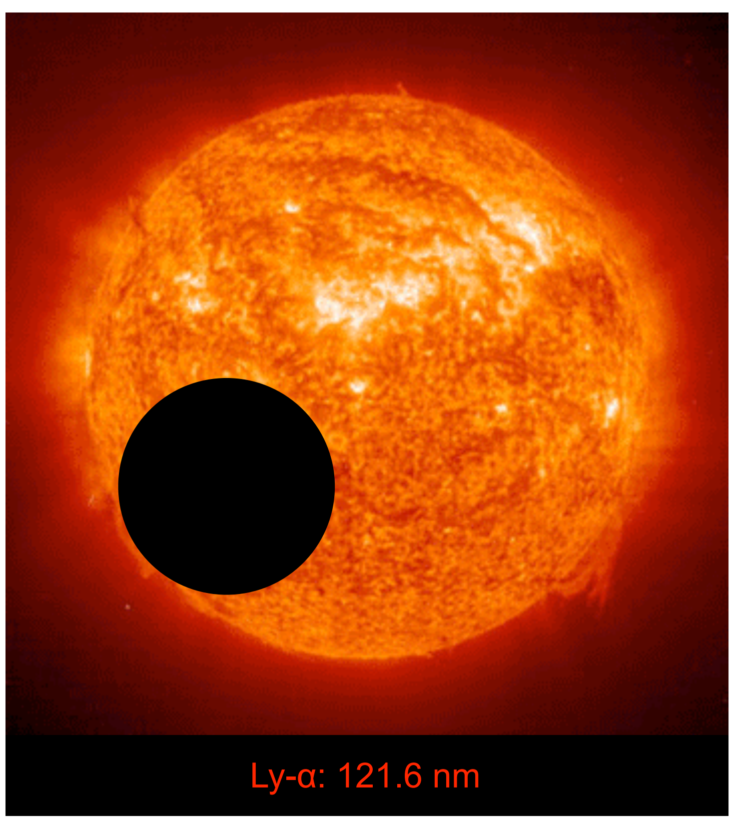

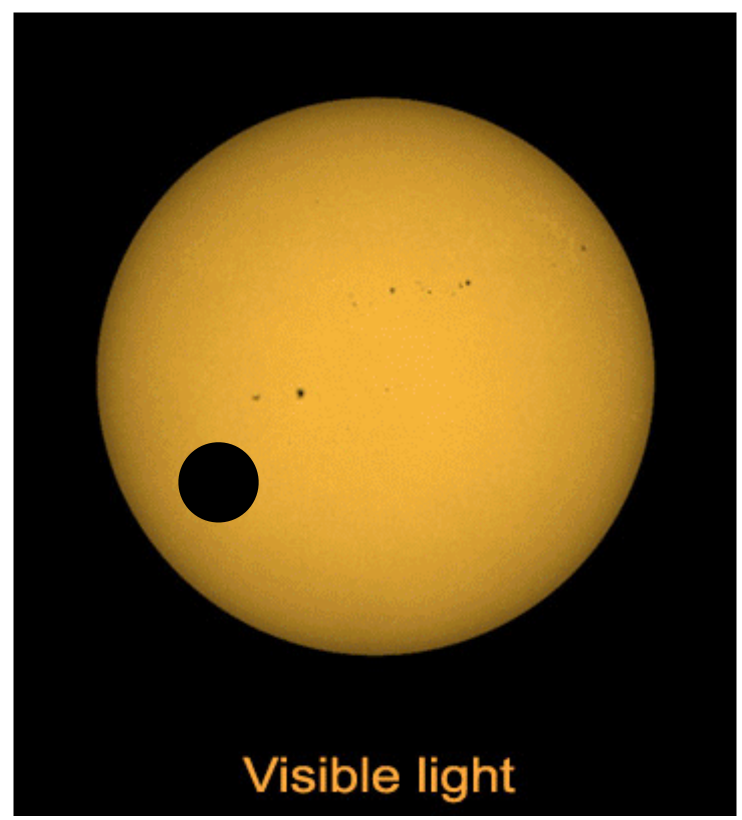

Vidal-Madjar et al. (2003) Charbonneau et al. (2000) Richardson et al. (2006)

Xavier BONFILS

Ehrenreich et al. (2015, Nature 459, 522)

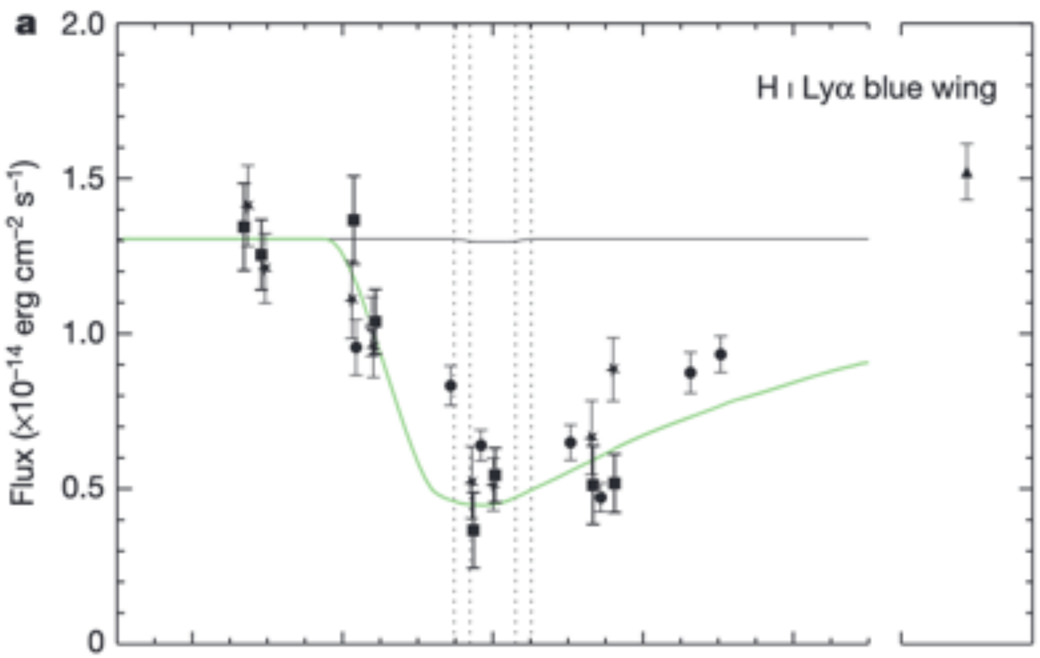

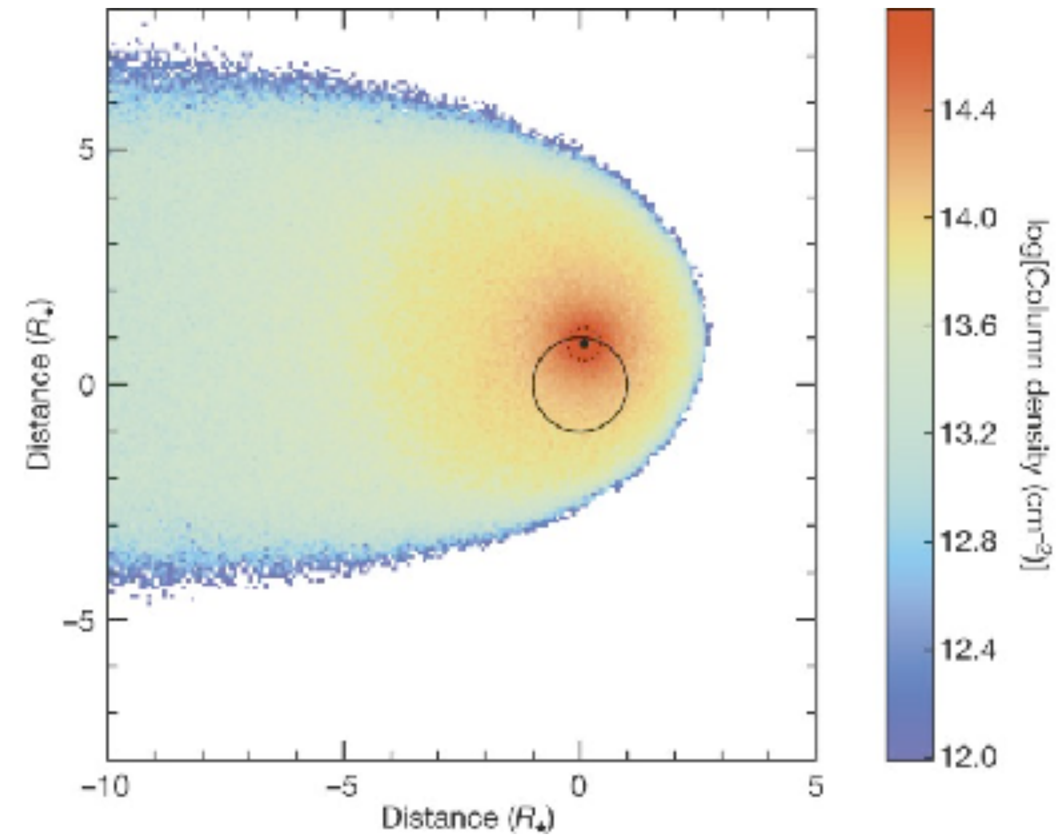

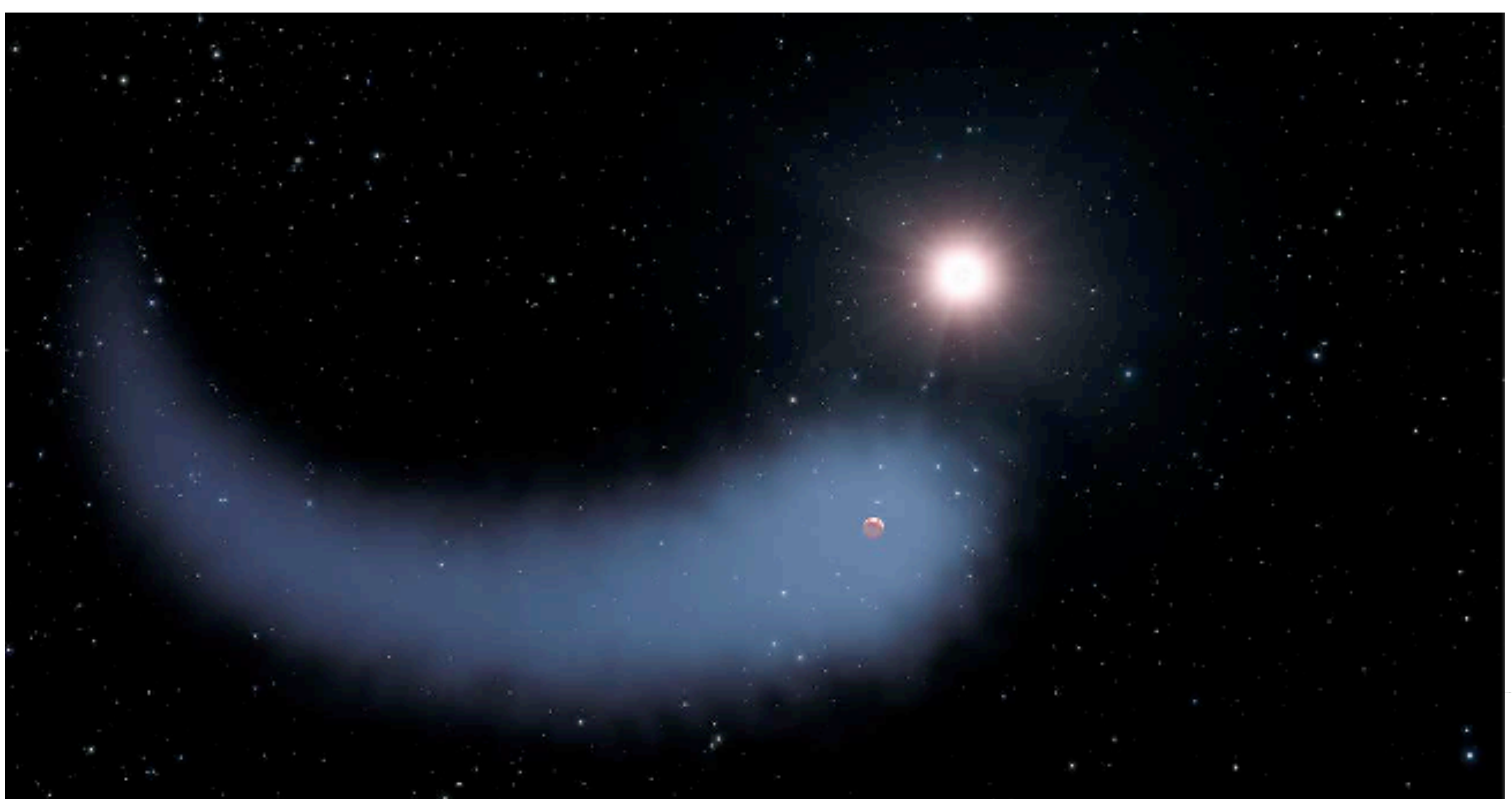

Xavier Bonfils

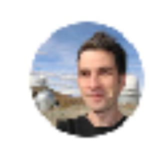

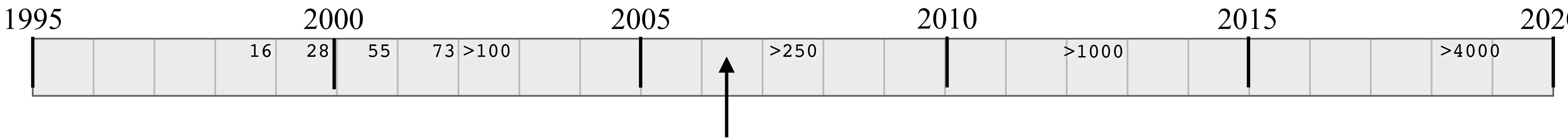

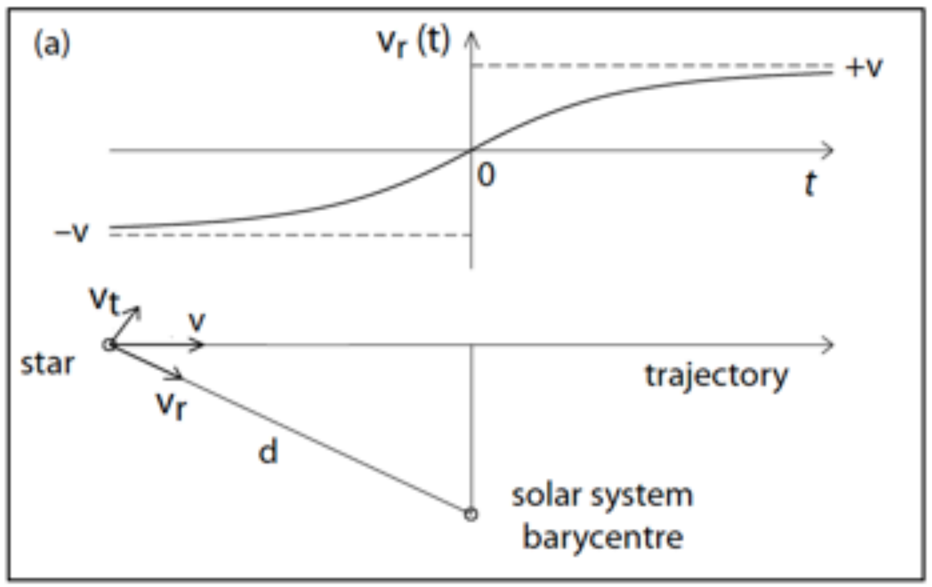

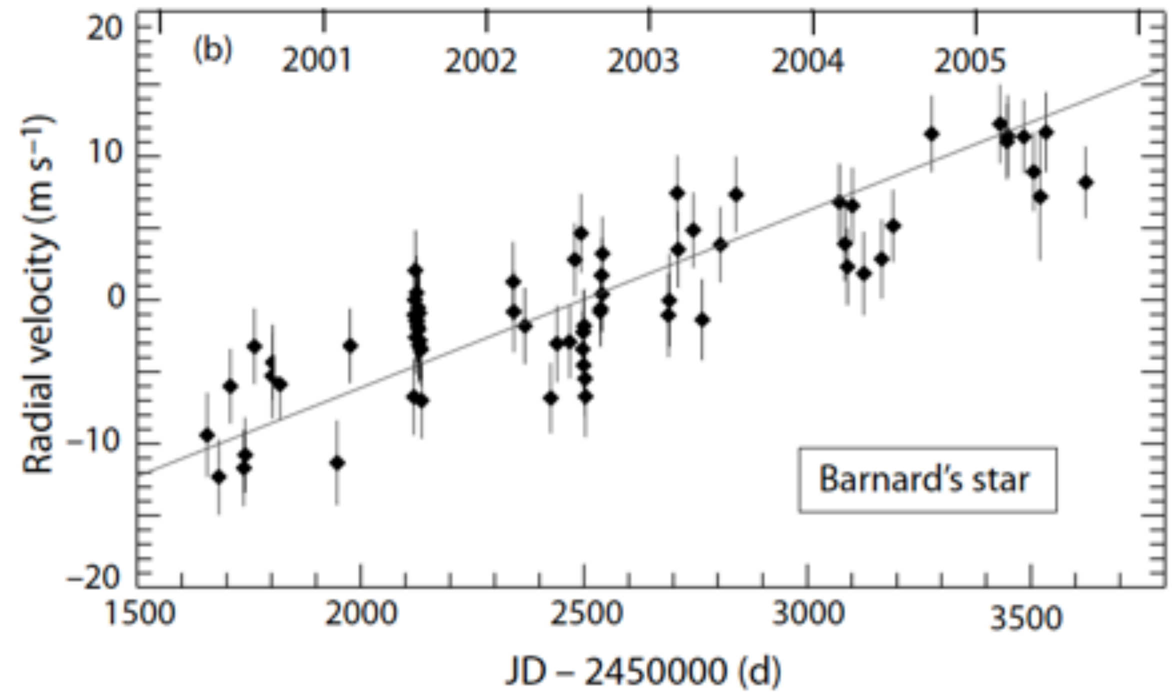

- No planet
- But "secular" acceleration
- Barnard's star has the largest proper motion (and largest secular acceleration)

Kuerster et al. 2006

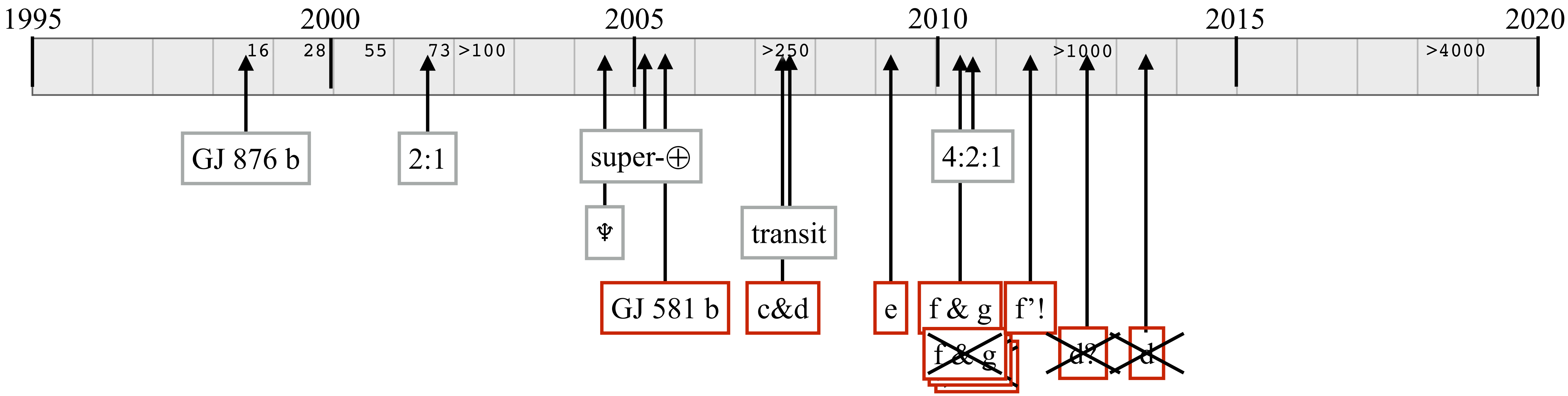

- GJ 581b (Bonfils et al. 2005)
- GJ 581c&d: habitable candidates (Udry et al. 2007)
- GJ 581e: 2 earth-mass planet (Mayor et al. 2009)
- more planets claimed (Vogt et al. 2010, 2012) but quickly disproved (Forveille et al. 2011, +)
- correlated noise casted doubts on 'd' too (Baluev 2013)
- H_α-RV correlation demotes 'd' (Robertson et al. 2014)

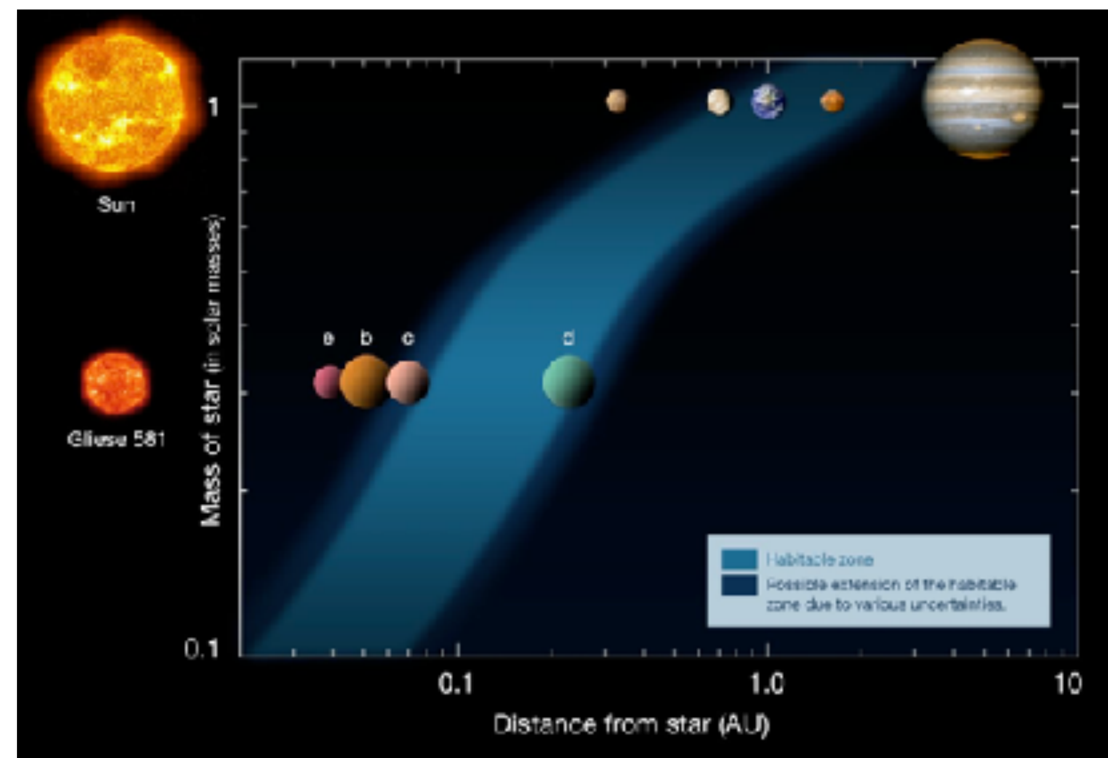

Main lesson here: you can't be sure of a detection if you don't know the rotation

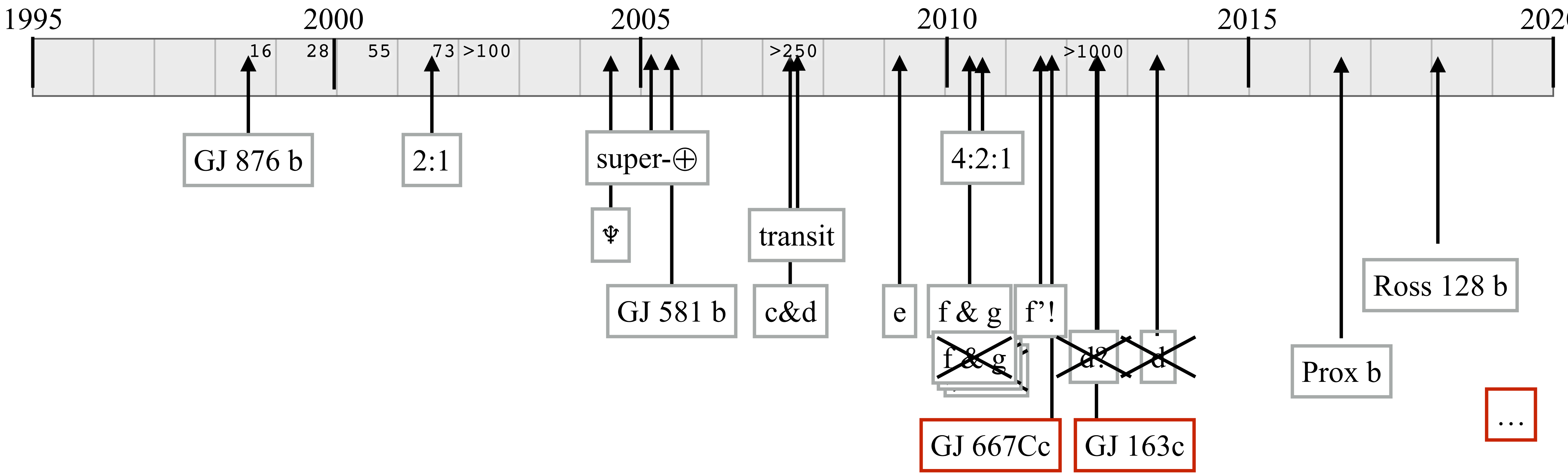

- GJ 667Cc (Bonfils et al. 2011, Delfosse et al. 2013)
- GJ 163c (Bonfils et al. 2012)
- Proxima b (Anglada-Escudé et al. 2016)
- GJ 273c (Astudillo-Defru et al. 2017)
- Ross 128b (Bonfils et al. 2018)

- many others (from HARPS & Kepler)

Miss Earth contest :

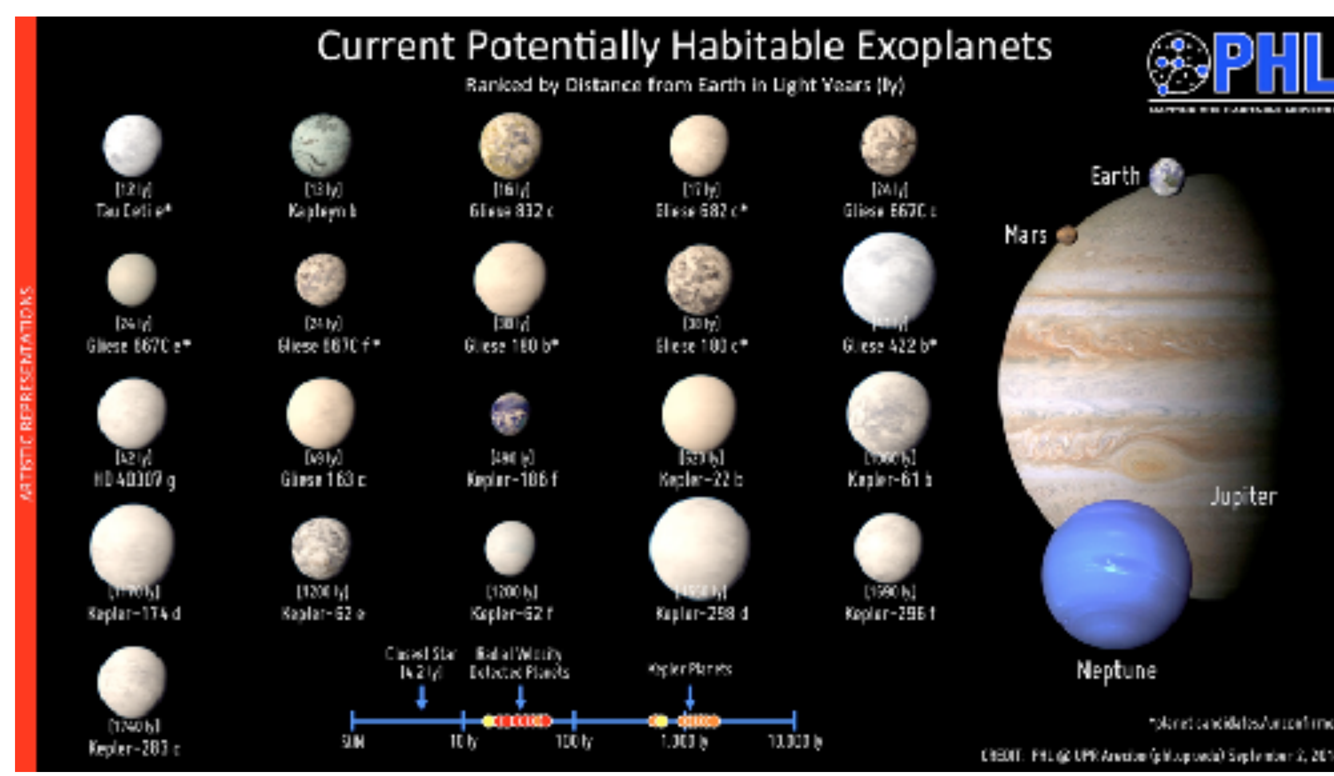

LETTER

doi:10.1038/nature19106

A terrestrial planet candidate in a temperate orbit around Proxima Centauri

Guillem Anglada-Escudé[1], Pedro J. Amado[2], John Barnes[3], Zaira M. Berdiñas[2], R. Paul Butler[4], Gavin A. L. Coleman[1], Ignacio de la Cueva[5], Stefan Dreizler[6], Michael Endl[7], Benjamin Giesers[6], Sandra V. Jeffers[6], James S. Jenkins[8], Hugh R. A. Jones[9], Marcin Kiraga[10], Martin Kürster[11], María J. López-González[2], Christopher J. Marvin[6], Nicolás Morales[2], Julien Morin[12], Richard P. Nelson[1], José L. Ortiz[2], Aviv Ofir[13], Sijme-Jan Paardekooper[1], Ansgar Reiners[6], Eloy Rodríguez[2], Cristina Rodríguez-López[2], Luis F. Sarmiento[6], John P. Strachan[1], Yiannis Tsapras[14], Mikko Tuomi[9] & Mathias Zechmeister[6]

A temperate exo-Earth around a quiet M dwarf at 3.4 parsecs*

X. Bonfils[1], N. Astudillo-Defru[2], R. Díaz[3,4], J.-M. Almenara[2], T. Forveille[1], F. Bouchy[2], X. Delfosse[1], C. Lovis[2], M. Mayor[2], F. Murgas[5,6], F. Pepe[2], N. C. Santos[7,8], D. Ségransan[2], S. Udry[2], and A. Wünsche[1]

eso1736 — Science Release

Closest Temperate World Orbiting Quiet Star Discovered

ESO's HARPS instrument finds Earth-mass exoplanet around Ross 128

15 November 2017

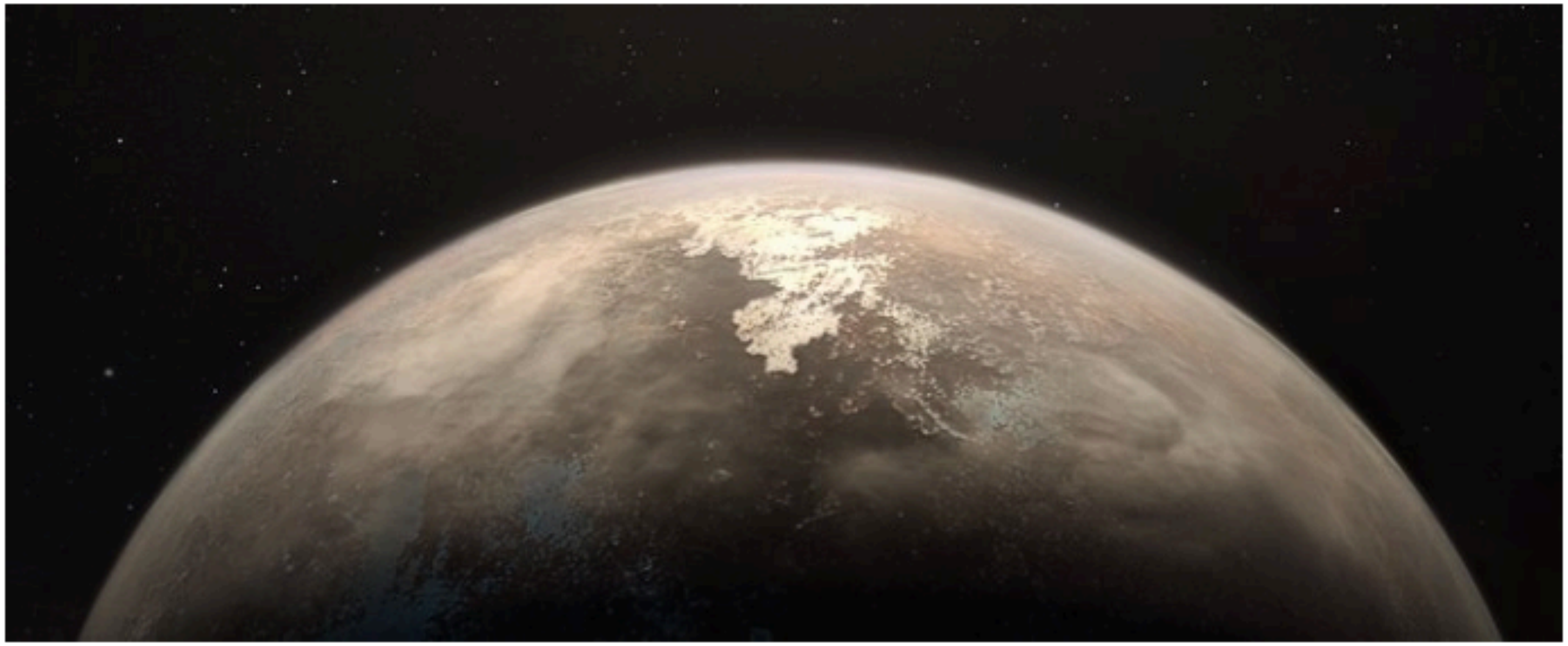

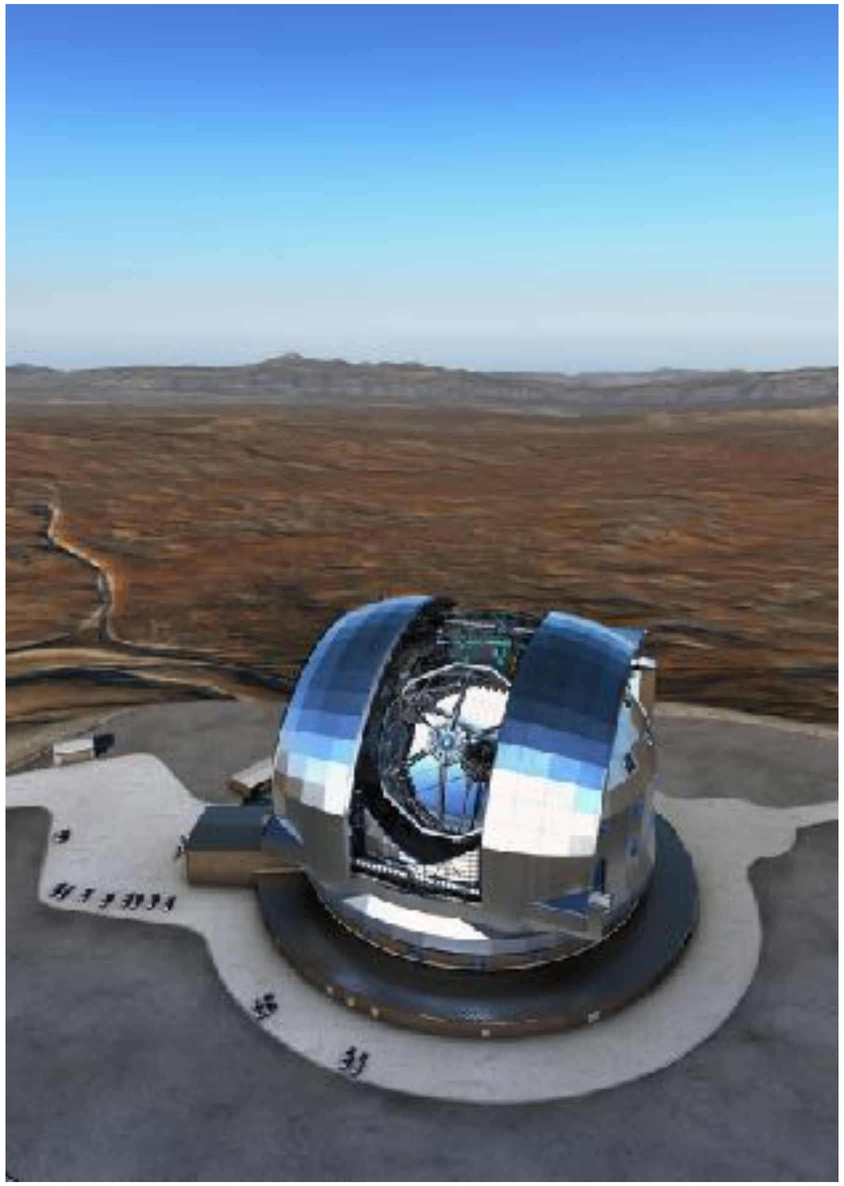

A temperate Earth-sized planet has been discovered only 11 light-years from the Solar System by a team using ESO's unique planet-hunting HARPS instrument. The new world has the designation Ross 128 b and is now the second-closest temperate planet to be detected after Proxima b. It is also the closest planet to be discovered orbiting an inactive red dwarf star, which may increase the likelihood that this planet could potentially sustain life. Ross 128 b will be a prime target for ESO's Extremely Large Telescope, which will be able to search for biomarkers in the planet's atmosphere.

Planets to resolve

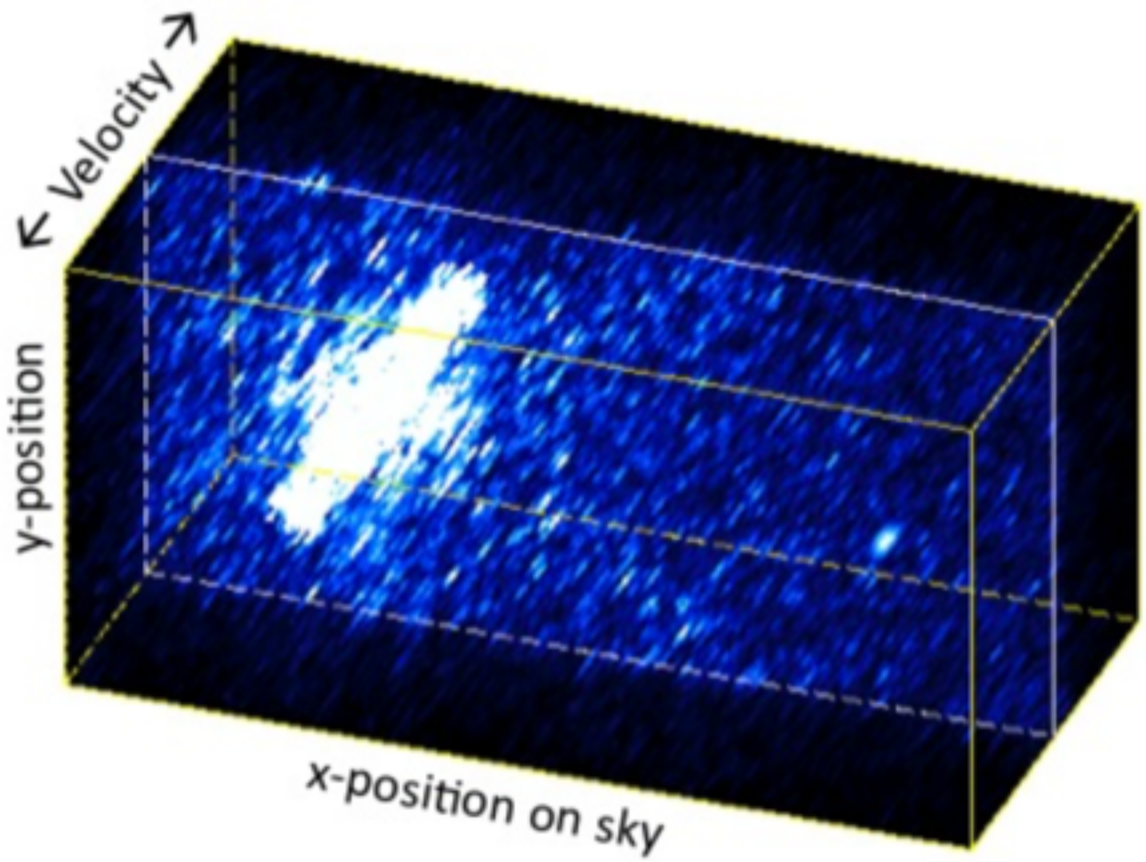

Snellen+15; see also Lovis+17

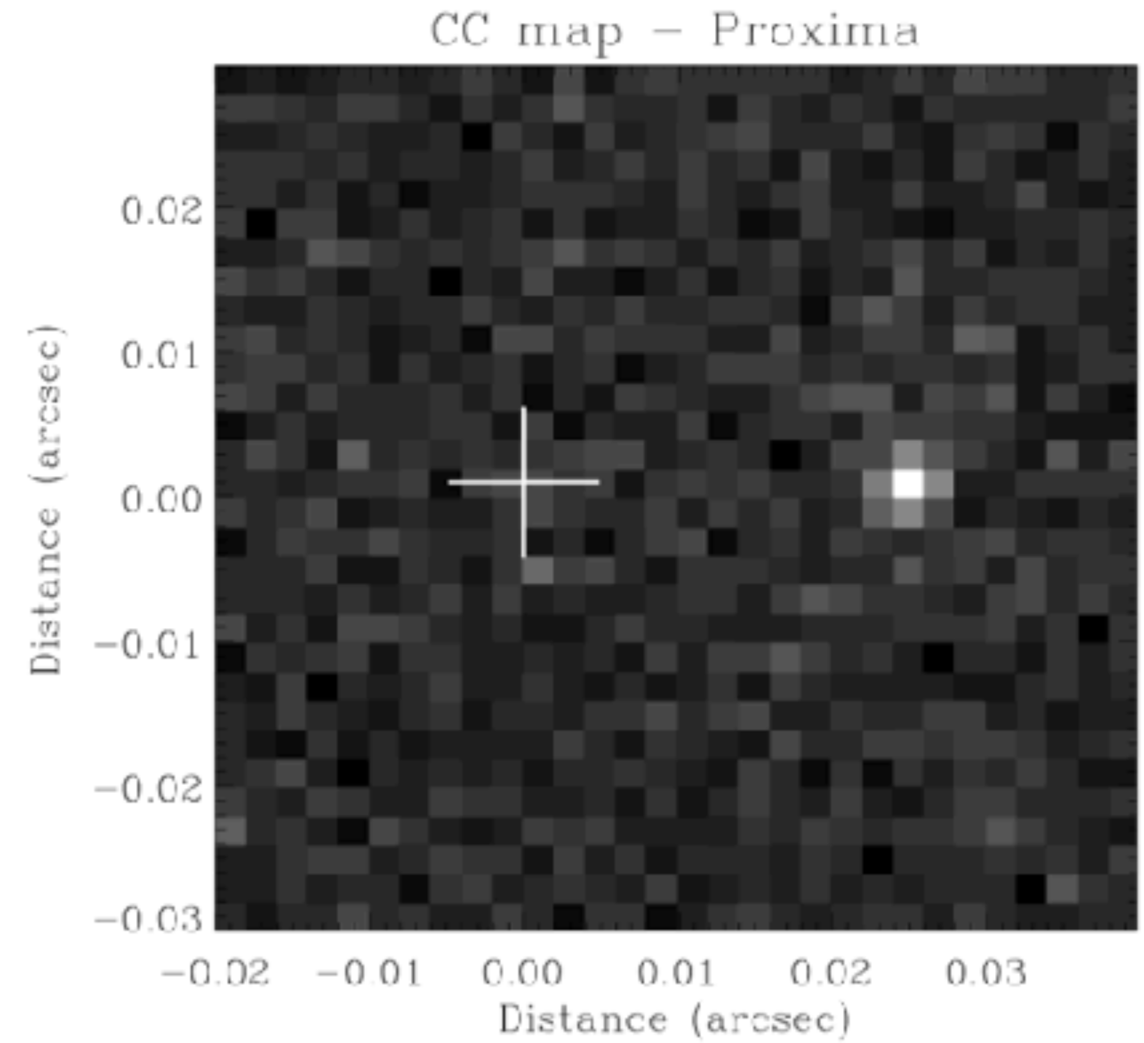

Fig. 6. HDS+HCI cross-correlation map of 10 hours of optical observations with the E-ELT using a R=100,000 IFS and an adaptive optics system producing a Strehl ratio of 0.3. The hypothetical planet with a radius of R=1.5 R_{Earth}, albedo of 0.3, and T_{eq}=280 K such that it is at an orbital radius of 0.032 AU, 25 milliarcseconds from the star. The starlight reflected off the planet is detected at an S/N of ~10.

- for Proxima b, Ross 128b, GJ273b, and other planets closer than ~5pc
- detection of O2 is possible in the near future
- require ELT, HIRES w/ SCAO, a few nights

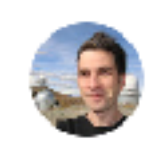

Ground Based / Field Surveys

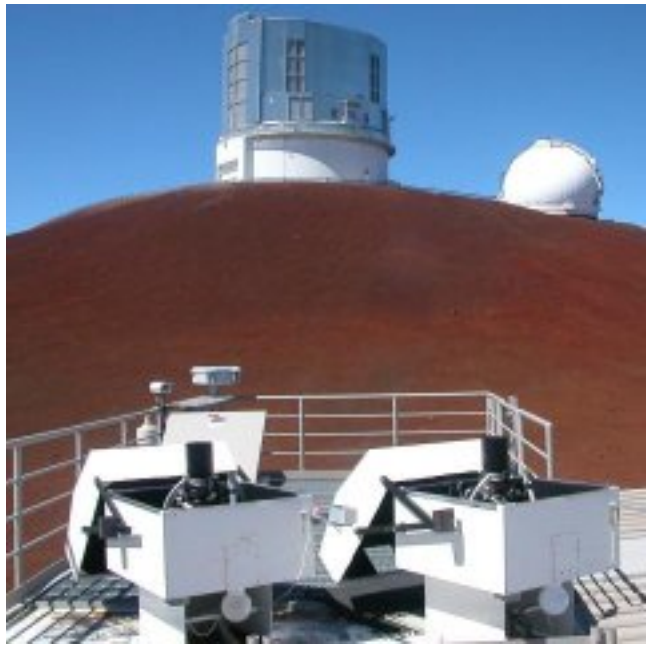

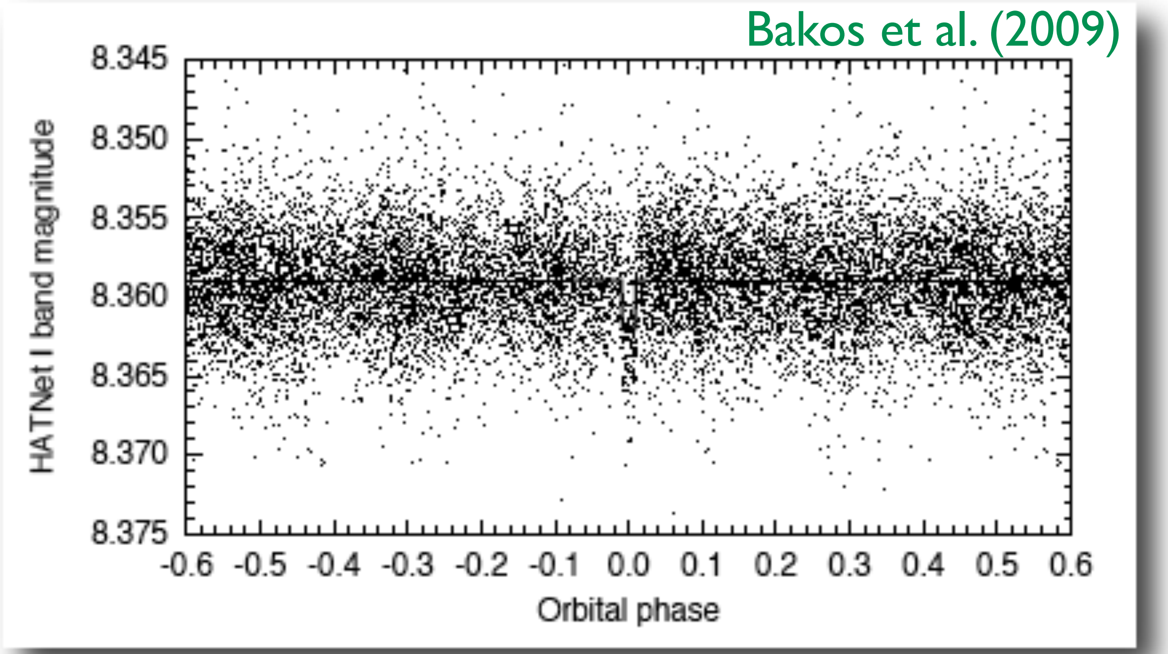

- 11-cm telescopes
- 8x8 deg
- 6 units (3 locations)

- HAT + super-WASP + XO + Tres + OGLE
= 80 detection, dont 1 Neptune

Pictures from oklo.org

SPACE BASED / FIELD SURVEYS

- 26-cm telescope
- 2.7x3.0 deg

- CoRoT-7b : 1.7 Rearth; ~4.8 Mearth
  first transiting super-Earth

- >14 transiting planets
- some @ extremes of the M-P diagram

(mass debated : e.g. Hatzes et al. 2010; Pont et al. 2010)

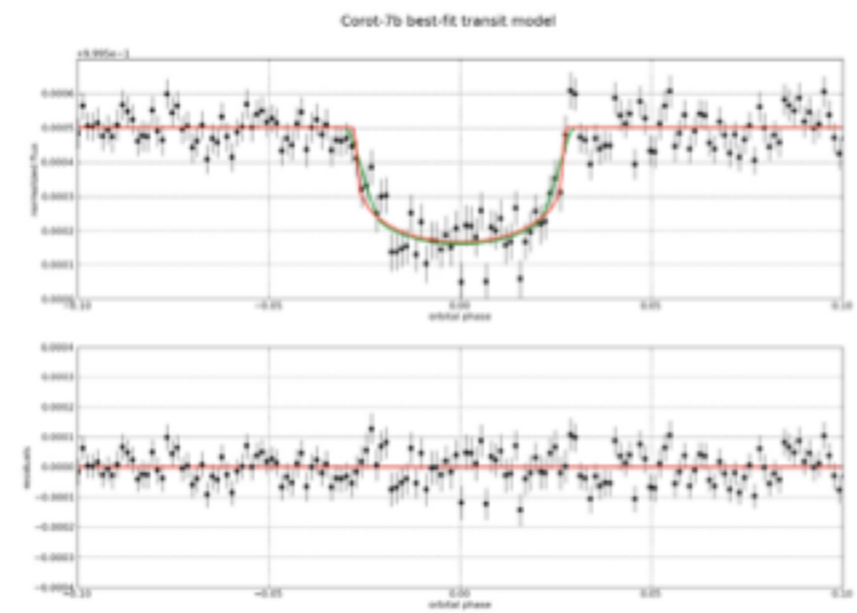

Léger et al. (2009)

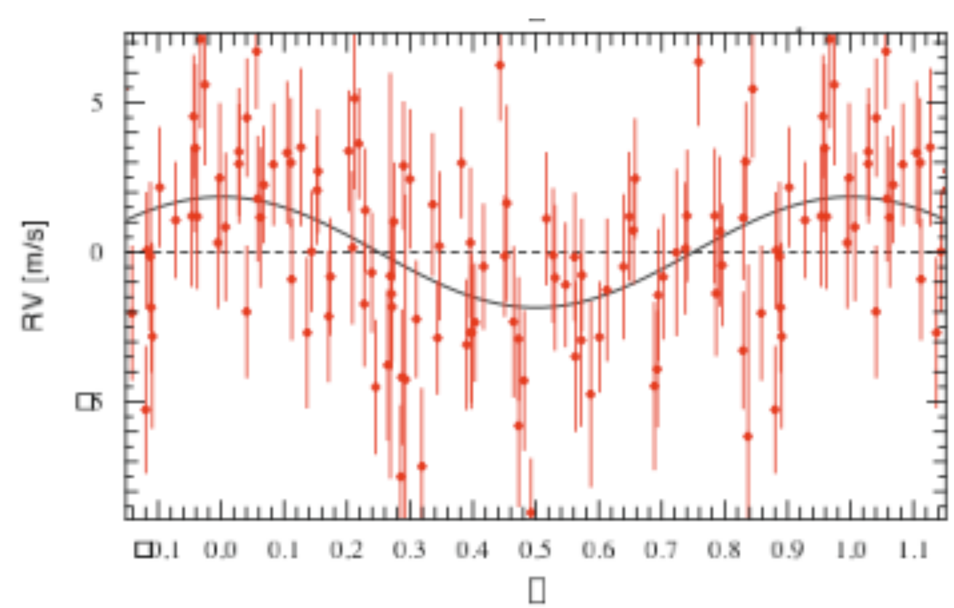

Queloz et al. (2009)

SPACE BASED / FIELD SURVEYS

- 95-cm telescope
- 100 deg^2
- 100,000 stars

- Kepler-4b : ~25 Mearth; 4 Rearth

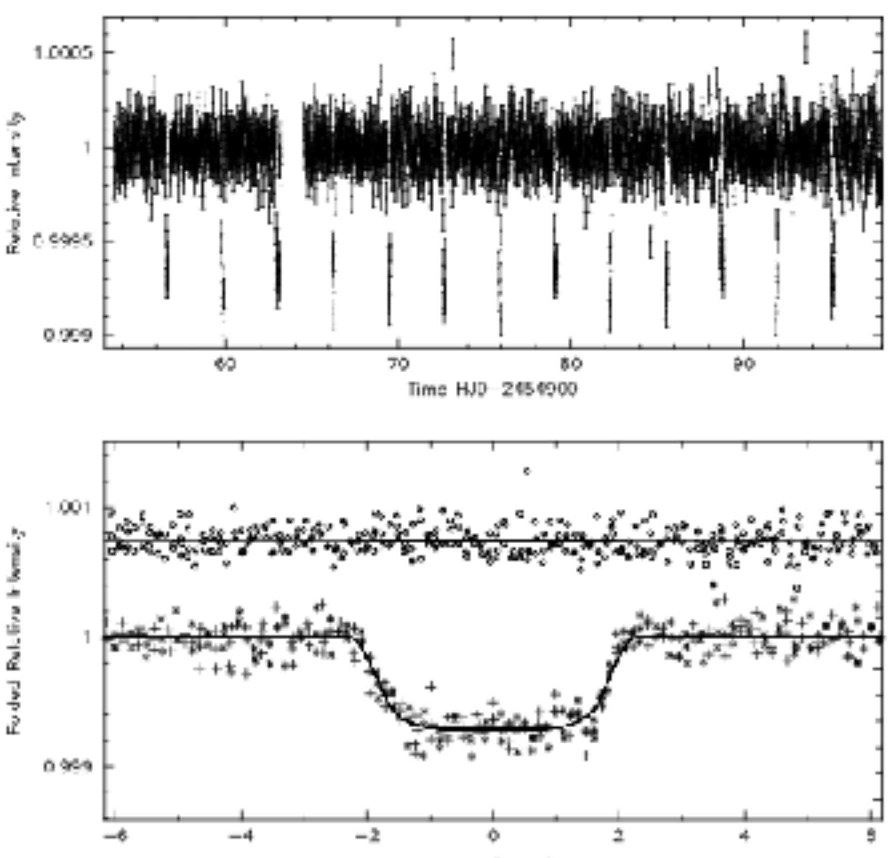

Borucki et al. (2010)

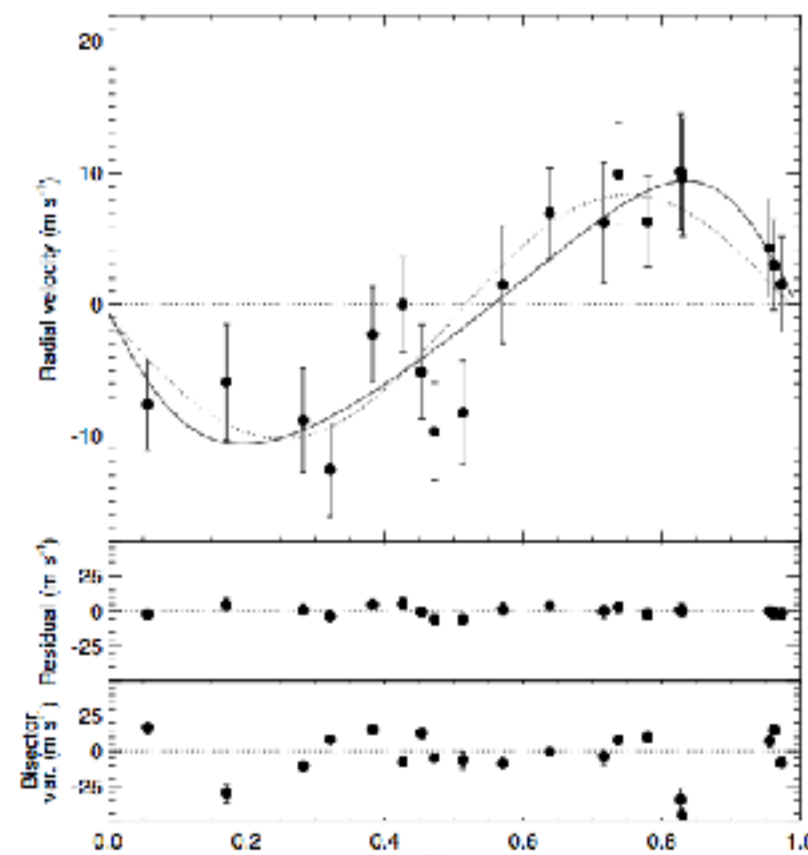

voir aussi KOI-377.03
"**Kepler-9-(d)**" ?
P=1.6 d
R=1.4 Rearth
FAP < 5.9x10^-3
pas de RV / pas de masse

Torres et al. (2010)

GROUND BASED / TARGETED SURVEYS

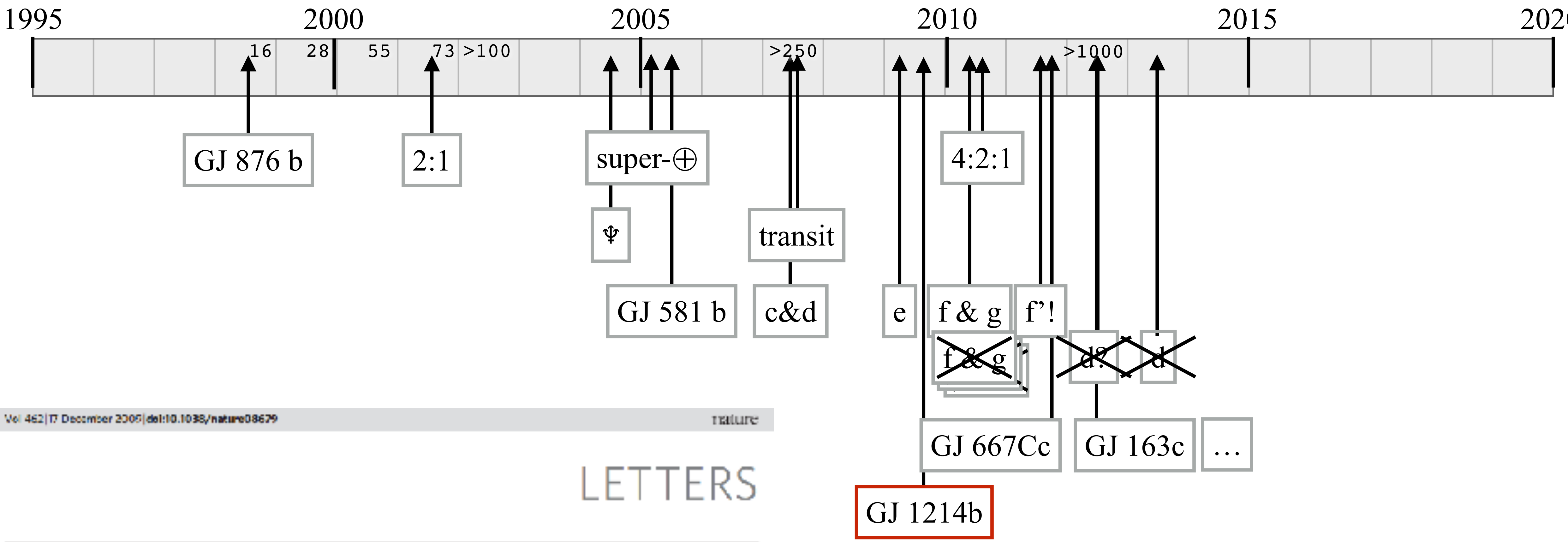

Vol 462 | 17 December 2009 | doi:10.1038/nature08679 nature

LETTERS

A super-Earth transiting a nearby low-mass star

David Charbonneau[1], Zachory K. Berta[1], Jonathan Irwin[1], Christopher J. Burke[1], Philip Nutzman[1], Lars A. Buchhave[1,2], Christophe Lovis[3], Xavier Bonfils[3,4], David W. Latham[1], Stéphane Udry[3], Ruth A. Murray-Clay[1], Matthew J. Holman[1], Emilio E. Falco[1], Joshua N. Winn[5], Didier Queloz[3], Francesco Pepe[3], Michel Mayor[3], Xavier Delfosse[4] & Thierry Forveille[4]

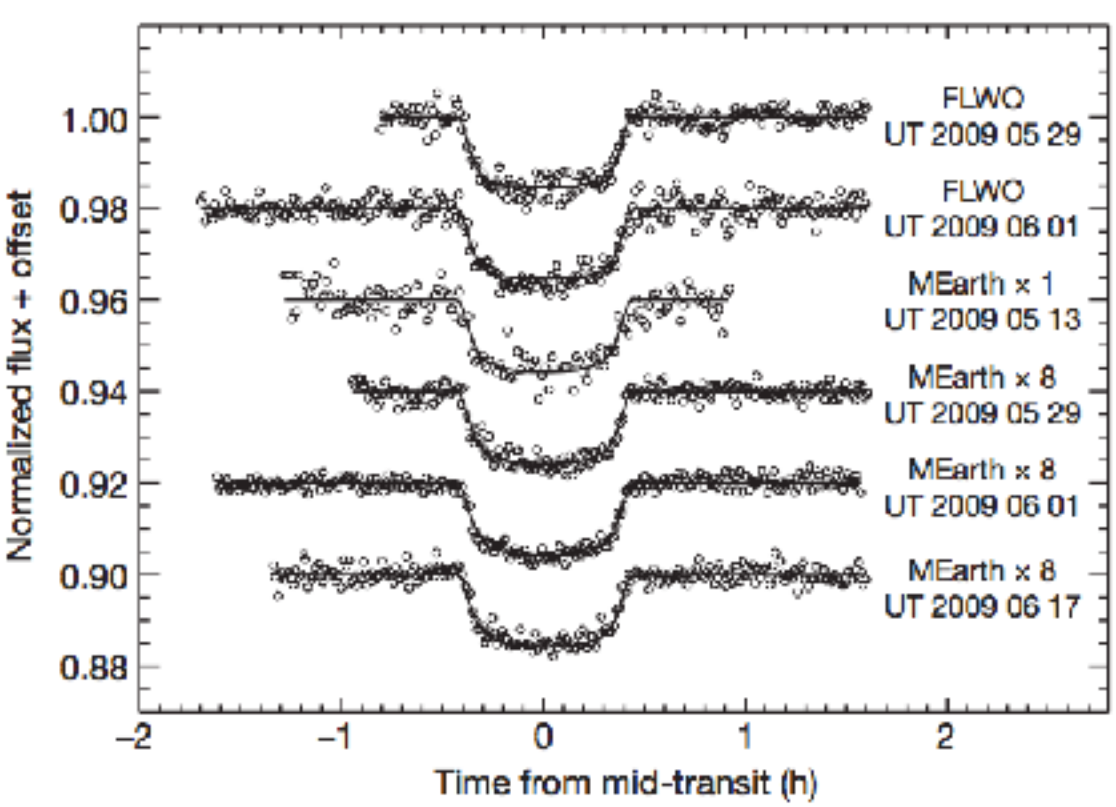

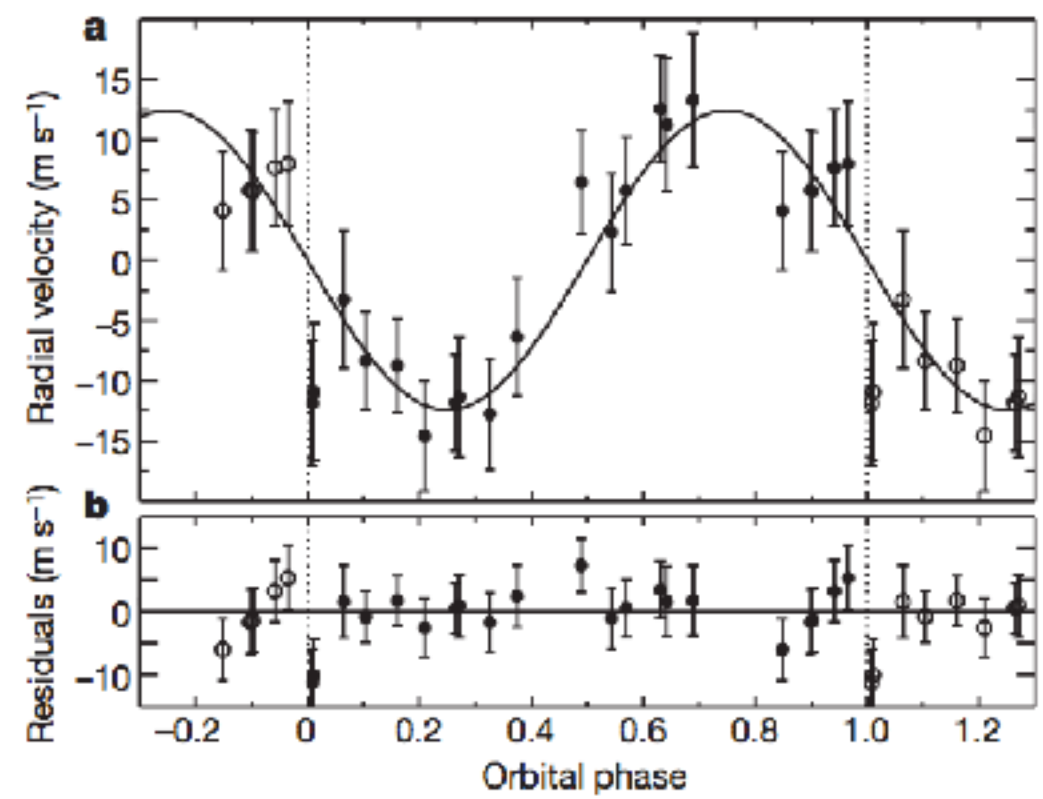

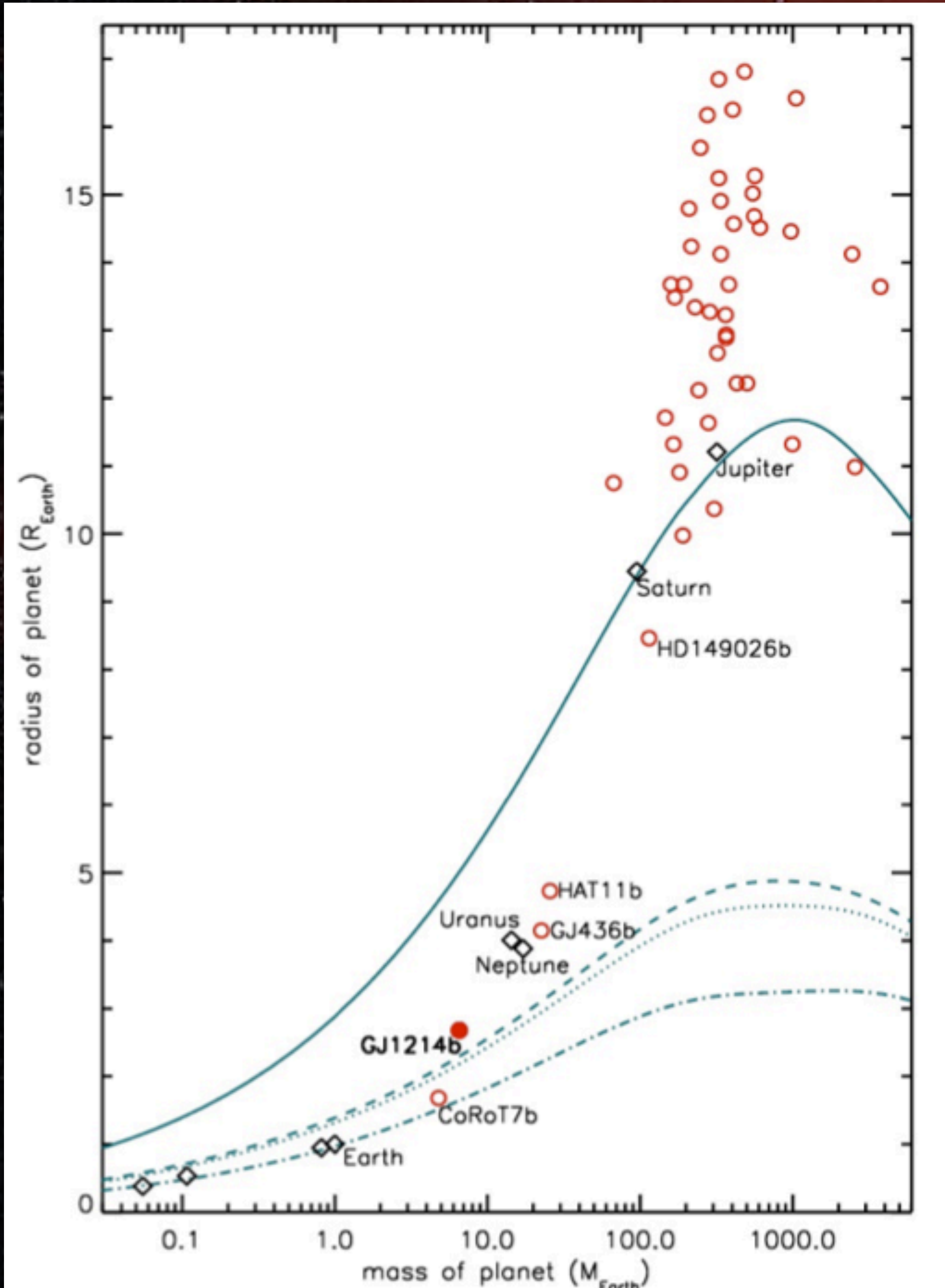
radius of planet (R_{Earth})
mass of planet (M_{Earth})
0
5
10
15
0.1
1.0
10.0
100.0
1000.0
Jupiter
Saturn
HD149026b
HAT11b
Uranus
GJ436b
Neptune
GJ1214b
CoRoT7b
Earth

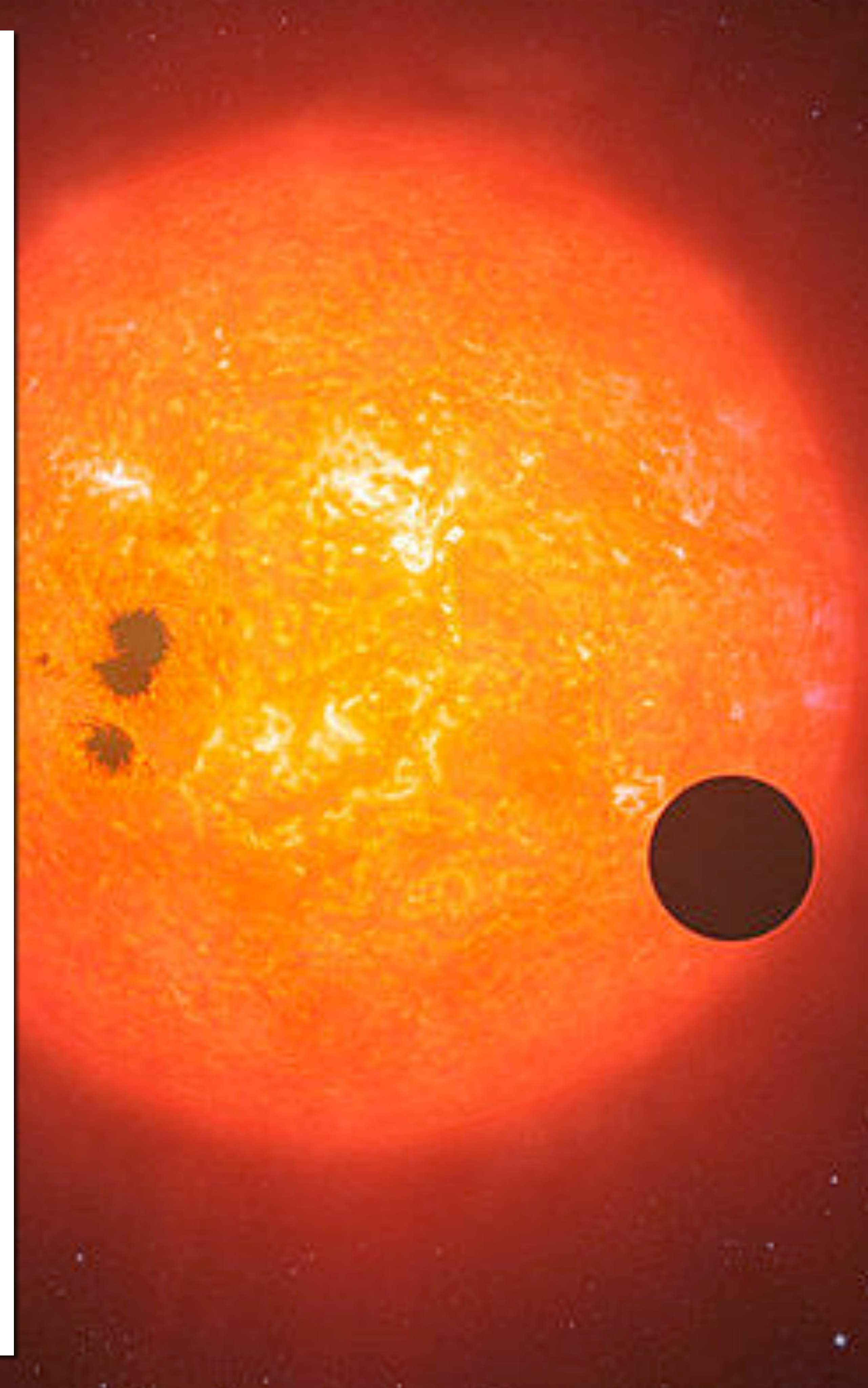

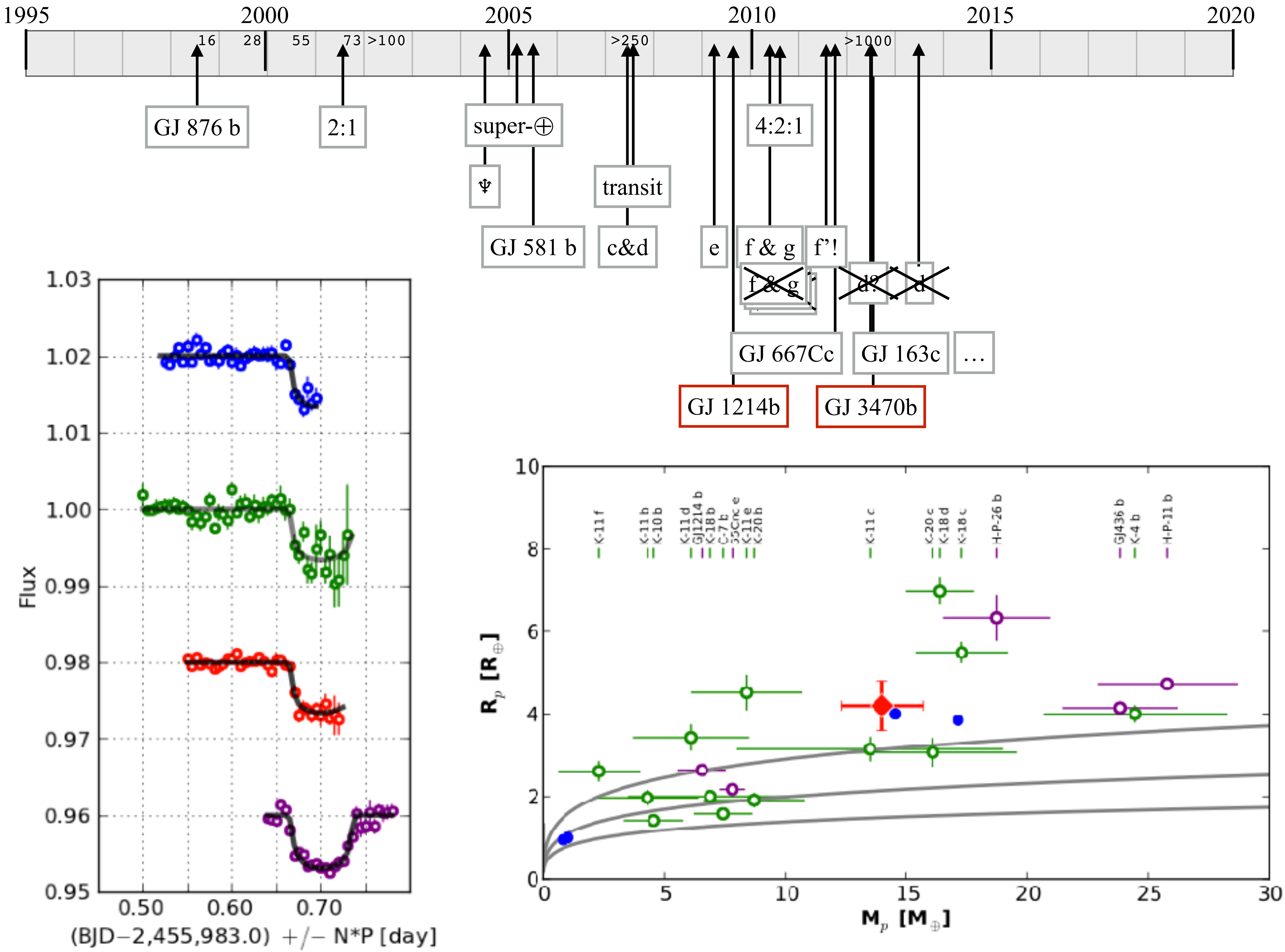

(Bonfils et al. 2012)

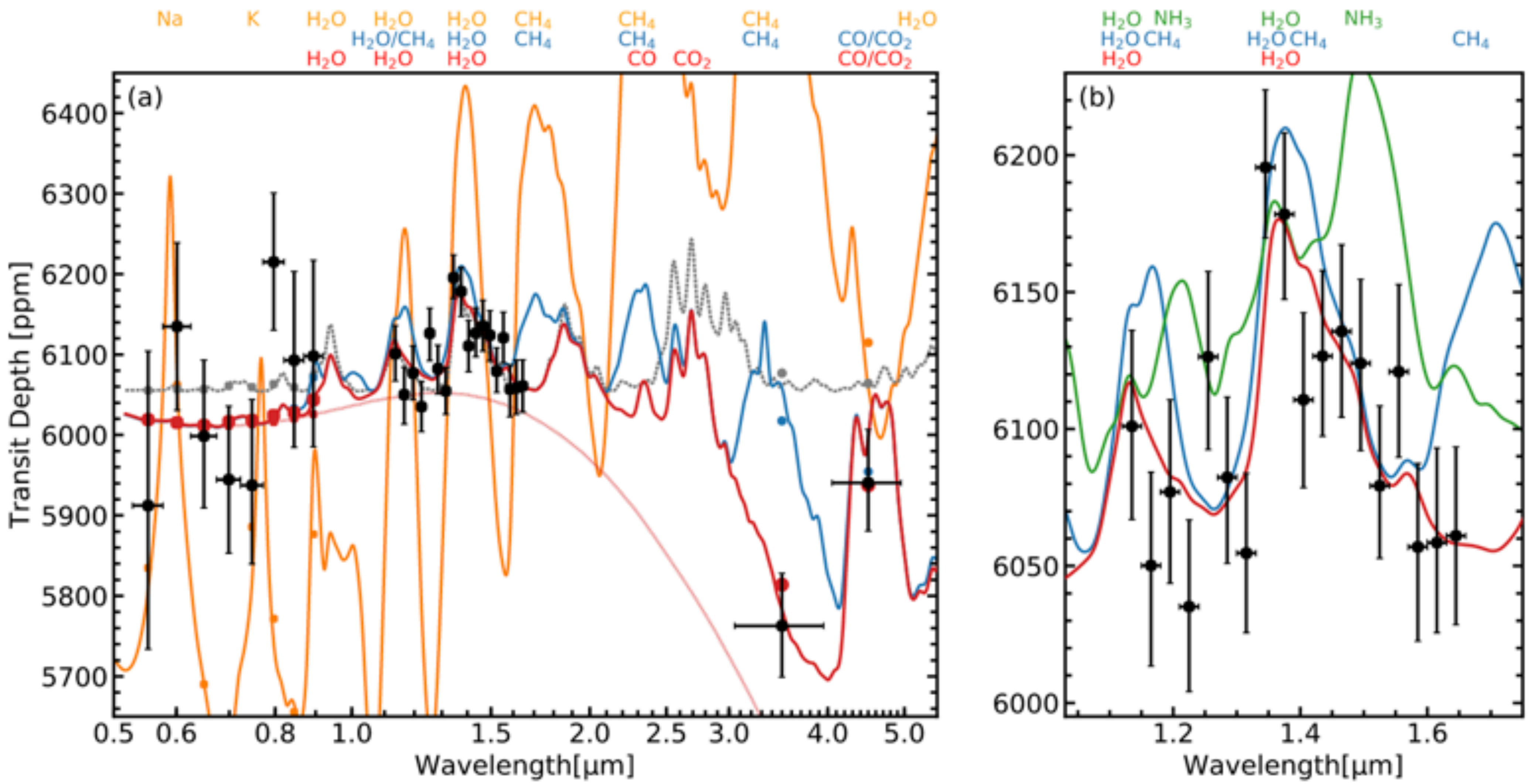

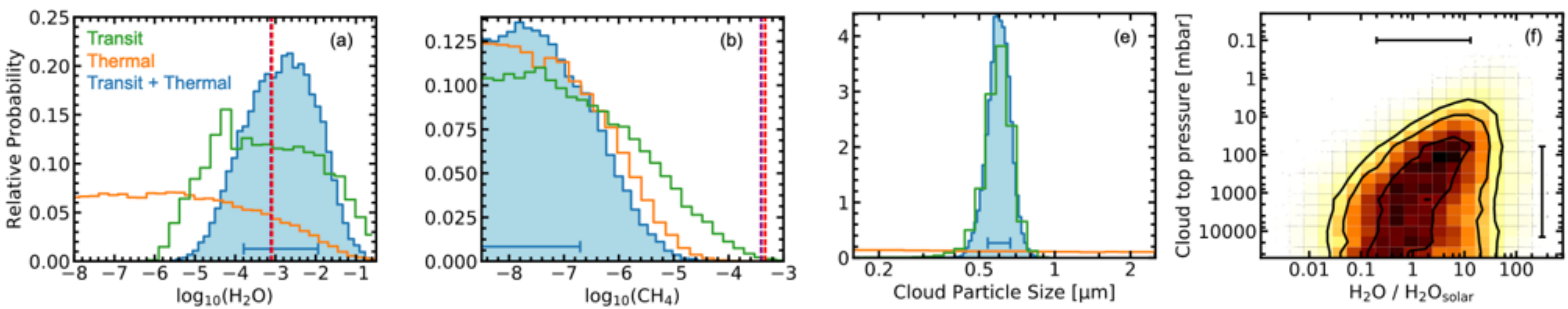

Benneke et al. (2019) see also Tsiaras et al. (2019)

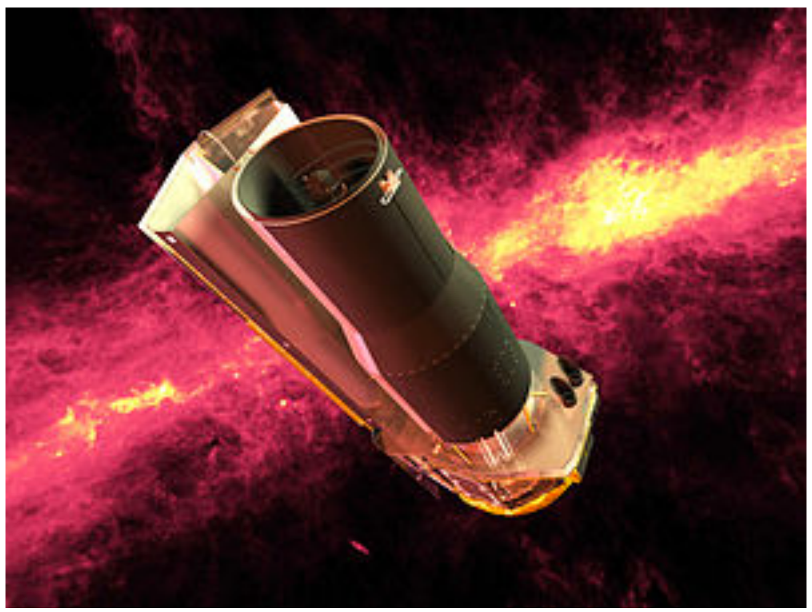

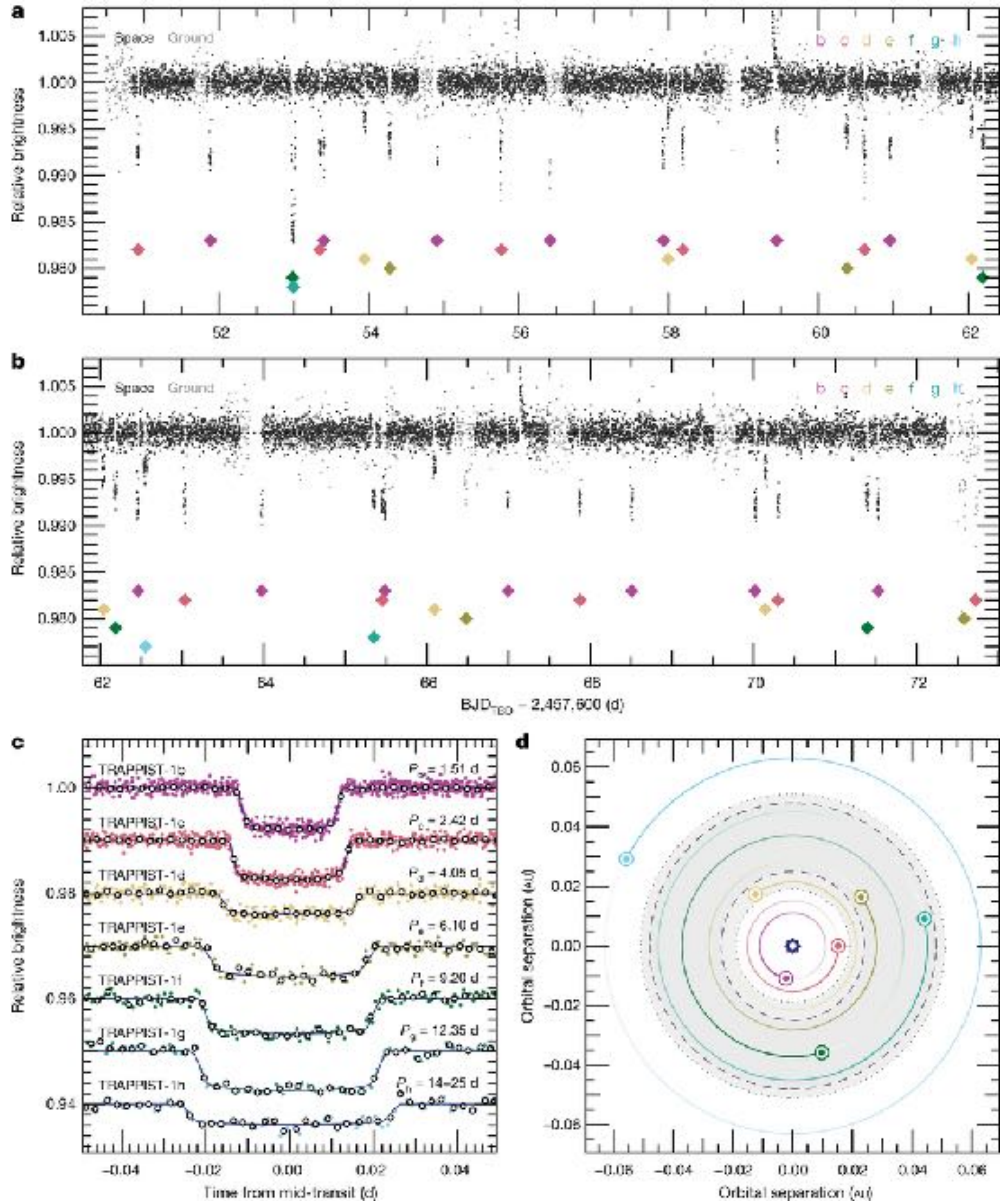
a
b
c
d
Space
Ground
Relative brightness
BJD$_{TDB}$ − 2,457,600 (d)
TRAPPIST-1b
TRAPPIST-1c
TRAPPIST-1d
TRAPPIST-1e
TRAPPIST-1f
TRAPPIST-1g
TRAPPIST-1h
P_b = 1.51 d
P_c = 2.42 d
P_d = 4.05 d
P_e = 6.10 d
P_f = 9.20 d
P_g = 12.35 d
P_h = 14–25 d
Time from mid-transit (d)
Orbital separation (AU)

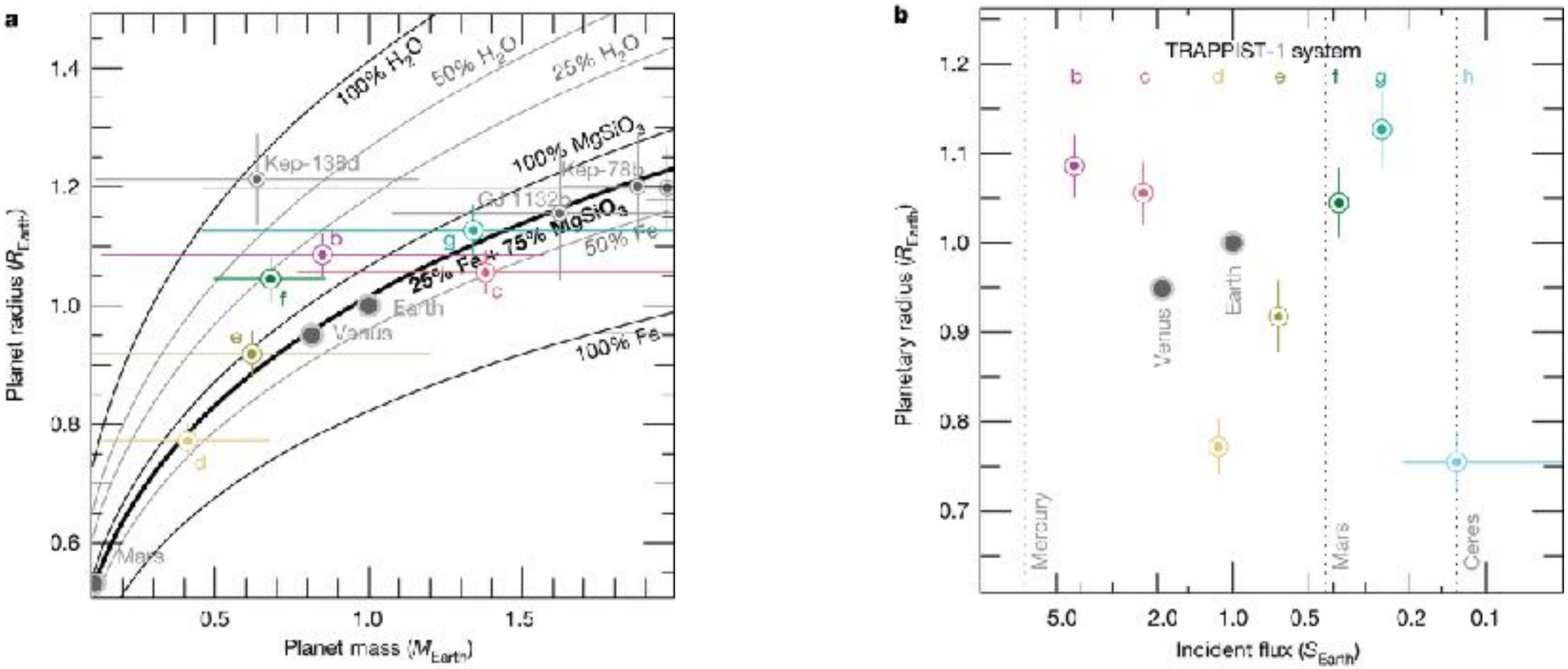

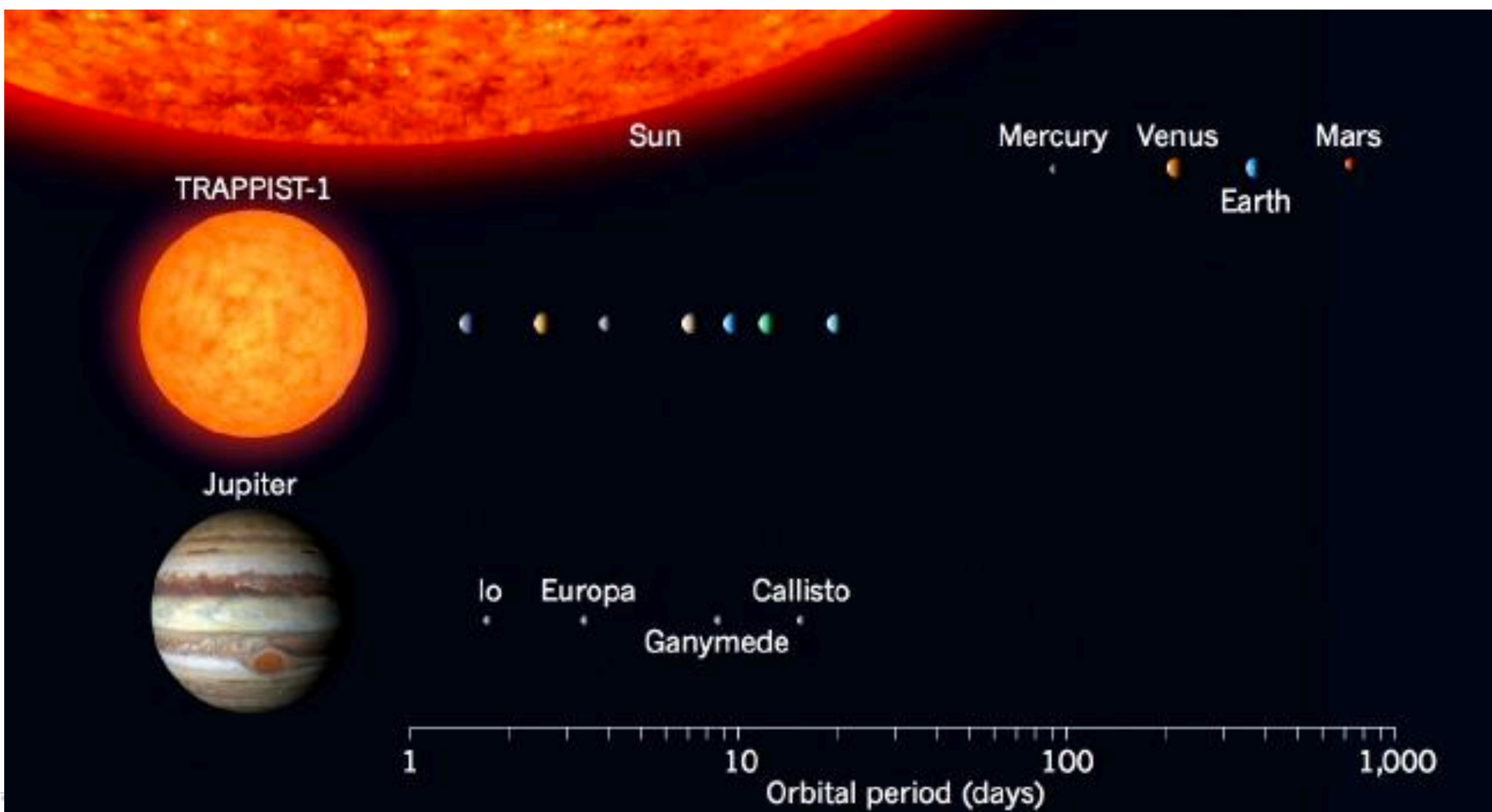

Xavier
ONFILS

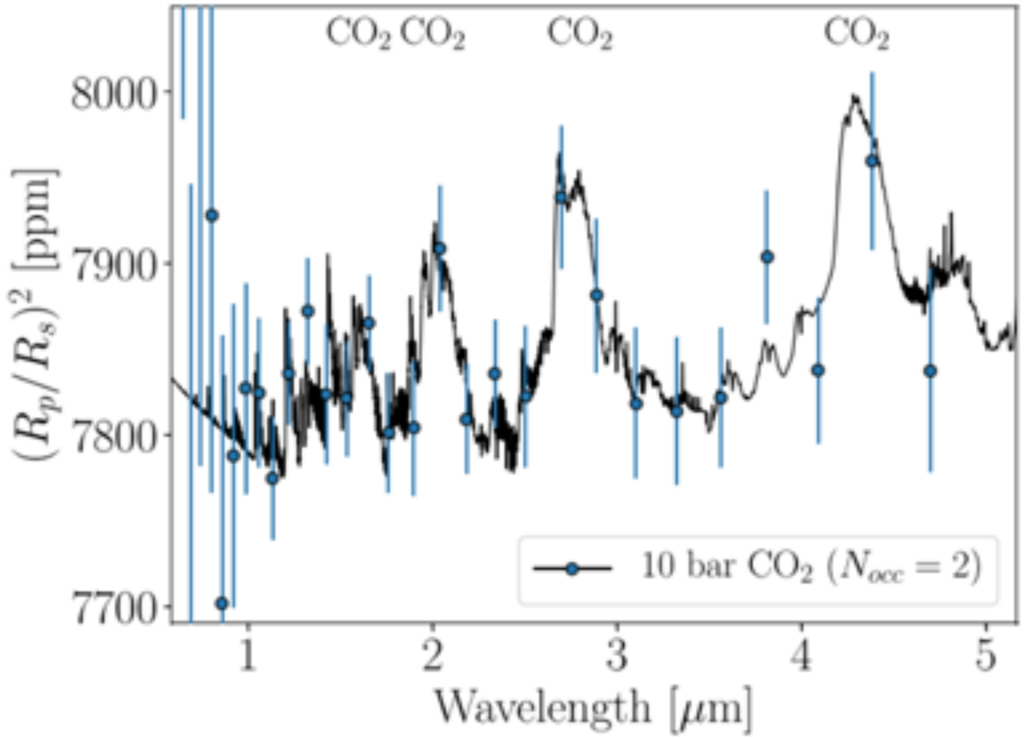

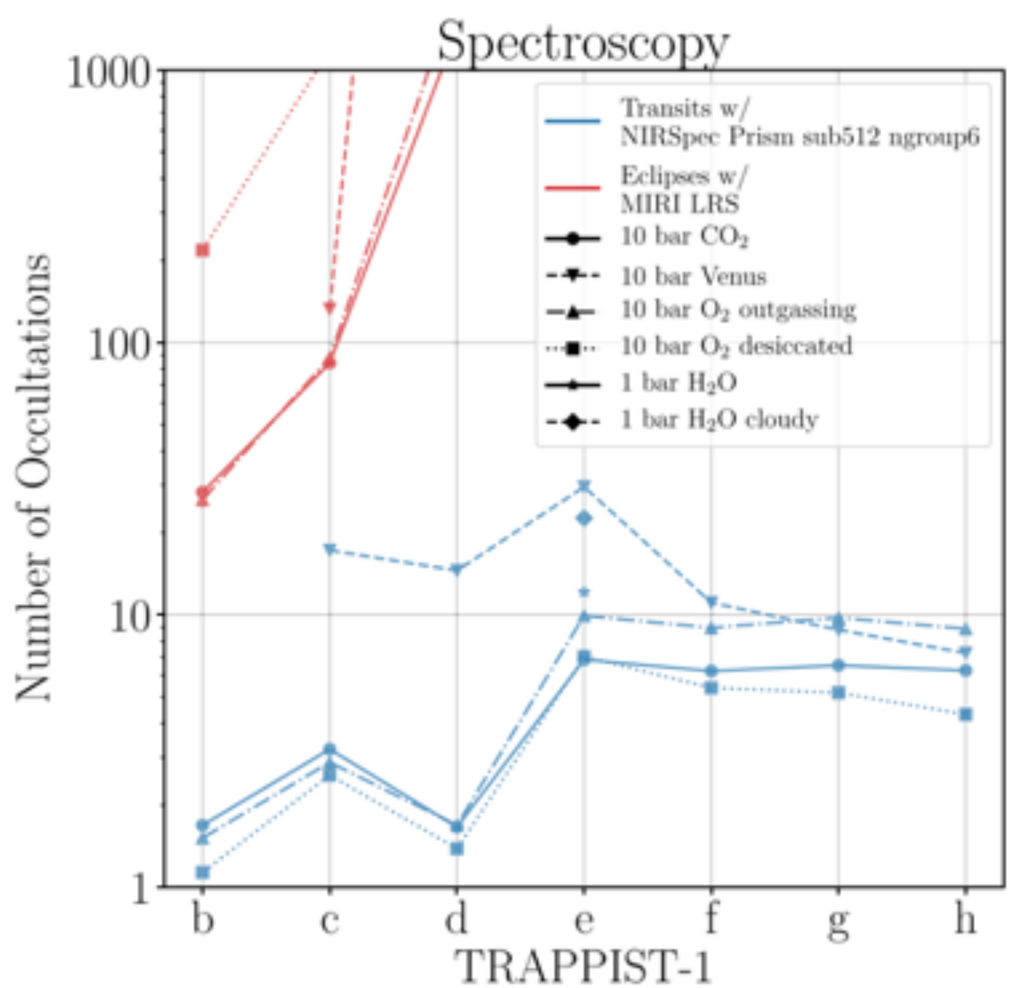

- Amenable to characterization w/ JWST
- Variety of atmosphere detectable w/ a few transits in transmission

Via Gillon et al. (2020)

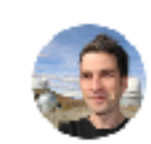

NATURE | LETTER

日本語要約

A temperate rocky super-Earth transiting a nearby cool star

Jason A. Dittmann, Jonathan M. Irwin, David Charbonneau, Xavier Bonfils, Nicola Astudillo-Defru, Raphaëlle D. Haywood, Zachory K. Berta-Thompson, Elisabeth R. Newton, Joseph E. Rodriguez, Jennifer G. Winters, Thiam-Guan Tan, Jose-Manuel Almenara, François Bouchy, Xavier Delfosse, Thierry Forveille, Christophe Lovis, Felipe Murgas, Francesco Pepe, Nuno C. Santos, Stephane Udry, Anaël Wünsche, Gilbert A. Esquerdo, David W. Latham & Courtney D. Dressing

Affiliations | Contributions | Corresponding author

Nature **544**, 333–336 (20 April 2017) | doi:10.1038/nature22055
Received 22 December 2016 | Accepted 09 March 2017 | Published online 19 April 2017

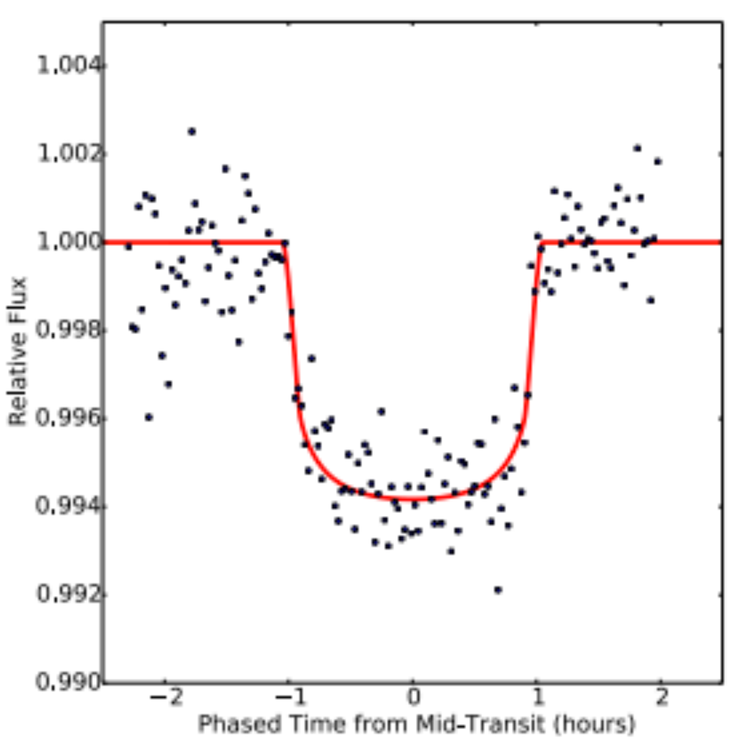

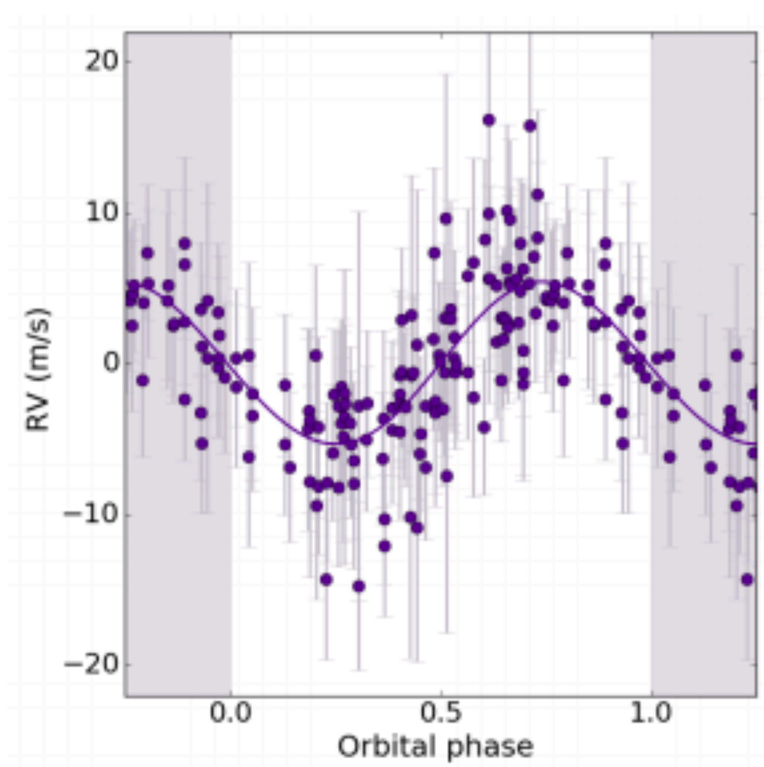

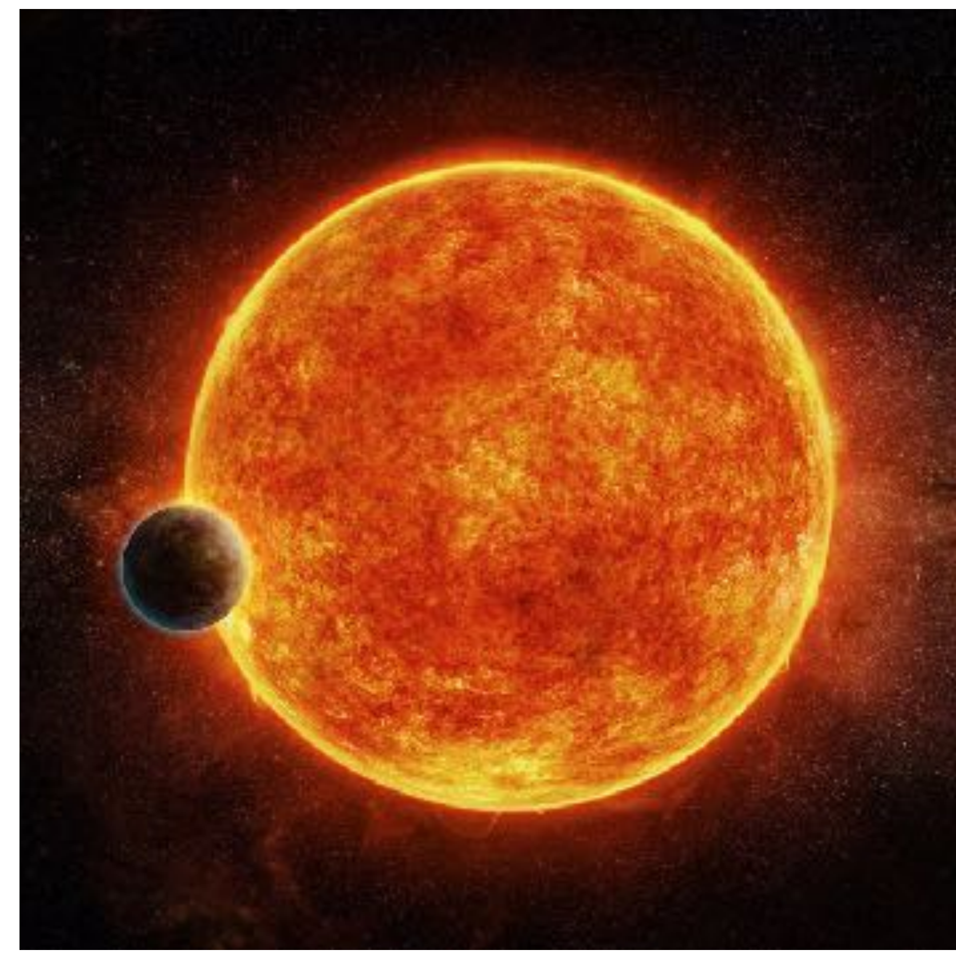

Xavier BONFILS

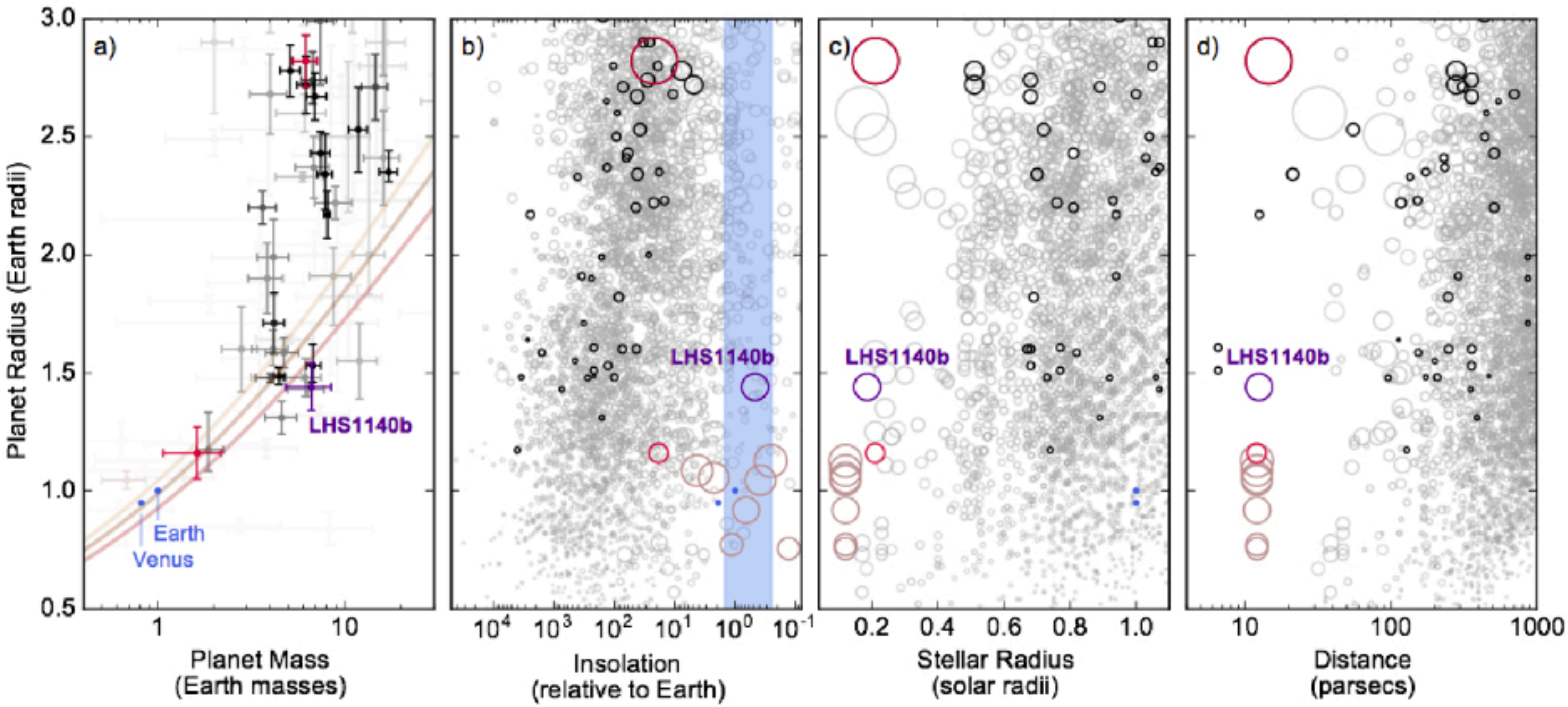
a)
b)
c)
d)
Planet Radius (Earth radii)
3.0
2.5
2.0
1.5
1.0
0.5
LHS1140b
LHS1140b
LHS1140b
LHS1140b
Earth
Venus
1
10
Planet Mass
(Earth masses)
10^4 10^3 10^2 10^1 10^0 10^{-1}
Insolation
(relative to Earth)
0.2 0.4 0.6 0.8 1.0
Stellar Radius
(solar radii)
10
100
1000
Distance
(parsecs)

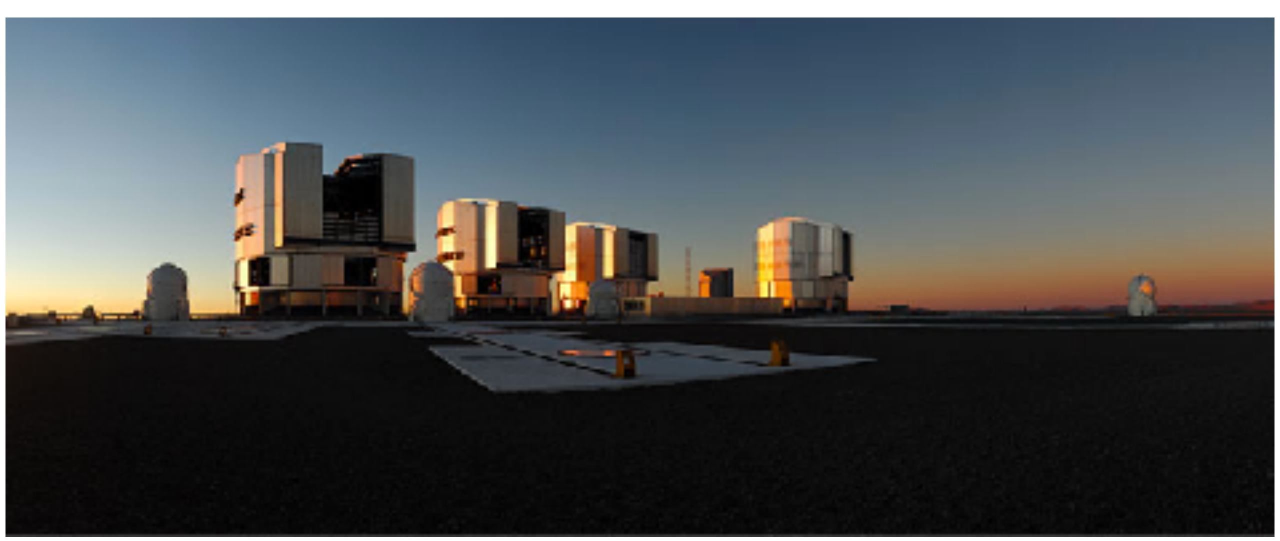

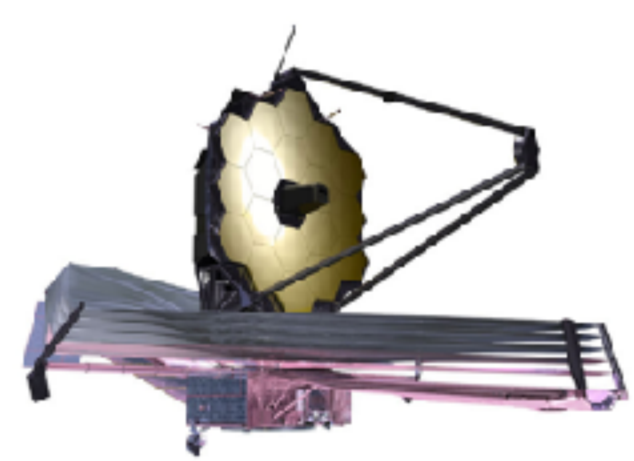

LHS1140 c

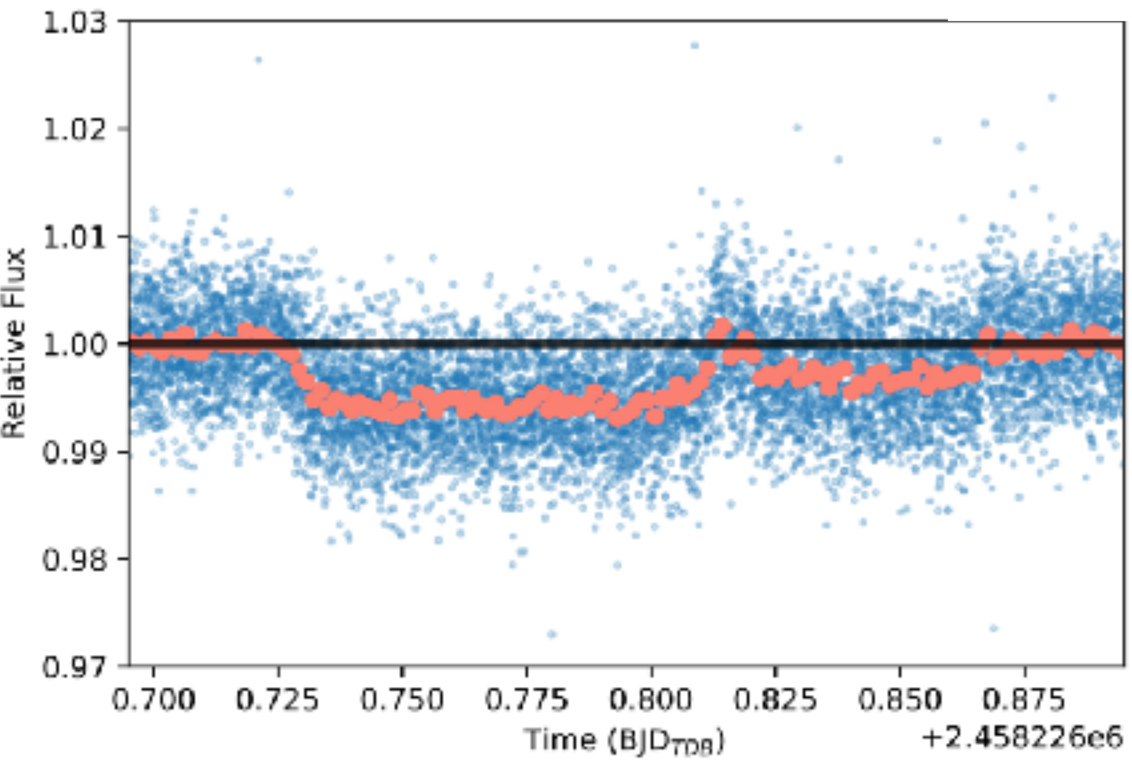

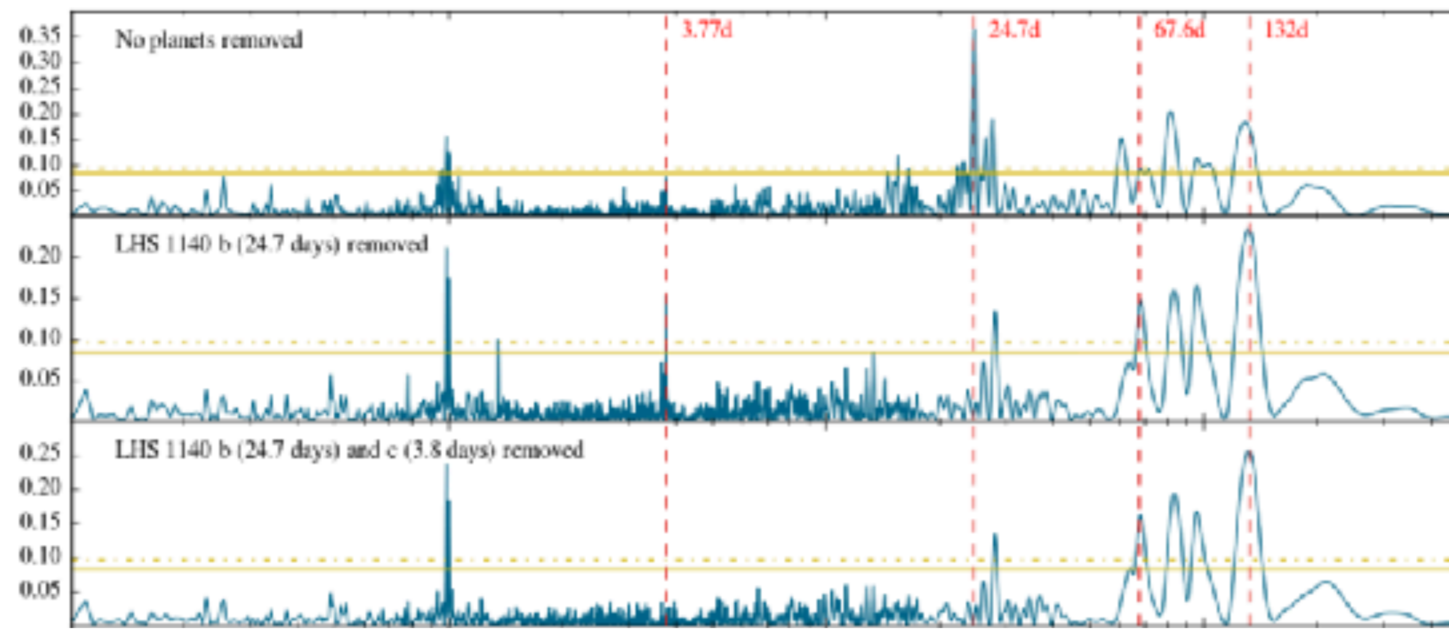

Parameter	LHS 1140 b	LHS 1140 c
Modeled transit and RV parameters		
Orbital period P (days)	24.736959 ± 0.000080	3.777931 ± 0.000003
RV semi-amplitude K (m s^{-1})	4.85 ± 0.55	2.35 ± 0.49
Eccentricity e (90% confidence)	< 0.06	< 0.31
Time of mid-transit t_T (BJD)	2456915.71154 ± 0.00004	2458226.843169 ± 0.000026
Inclination i (deg)	$89.89^{+0.05}_{-0.03}$	$89.92^{+0.06}_{-0.09}$
Planet-to-star radius ratio $r/R_\star$	0.07390 ± 0.00008	0.05486 ± 0.00013
$a/R_\star$ ratio	95.34 ± 1.06	26.57 ± 0.05
Derived planetary parameters		
Mass m (M$_\oplus$)	6.98 ± 0.89	1.81 ± 0.39
Radius r (R$_\oplus$)	1.727 ± 0.032	1.282 ± 0.024
Density ρ (g cm^{-3})	7.5 ± 1.0	4.7 ± 1.1
Surface gravity g (m s^{-2})	23.7 ± 2.7	10.6 ± 2.2
Semi-major axis a (AU)	0.0936 ± 0.0024	0.02675 ± 0.00070
Incident flux S (S$_\oplus$)	0.503 ± 0.030	6.16 ± 0.37
Equilibrium temperature[b] T_{eq} (K)	235 ± 5	438 ± 9

Xavier BONFILS

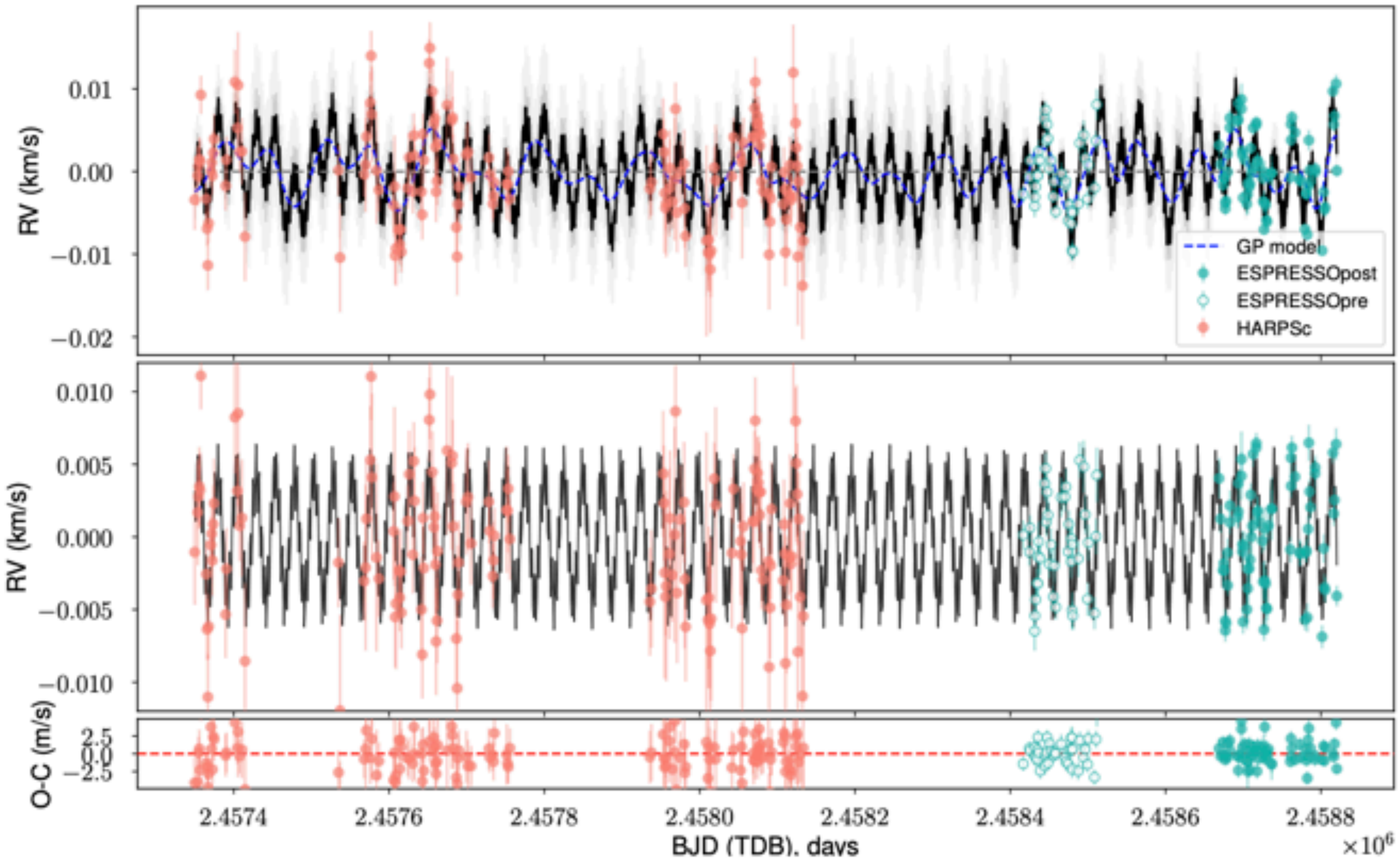

- W/ ESPRESSO
- 4-5x lower photon noise
- a 3rd planet (candidate)
- does it transit ? Unknown…

Lillo-Box et al. (2020)

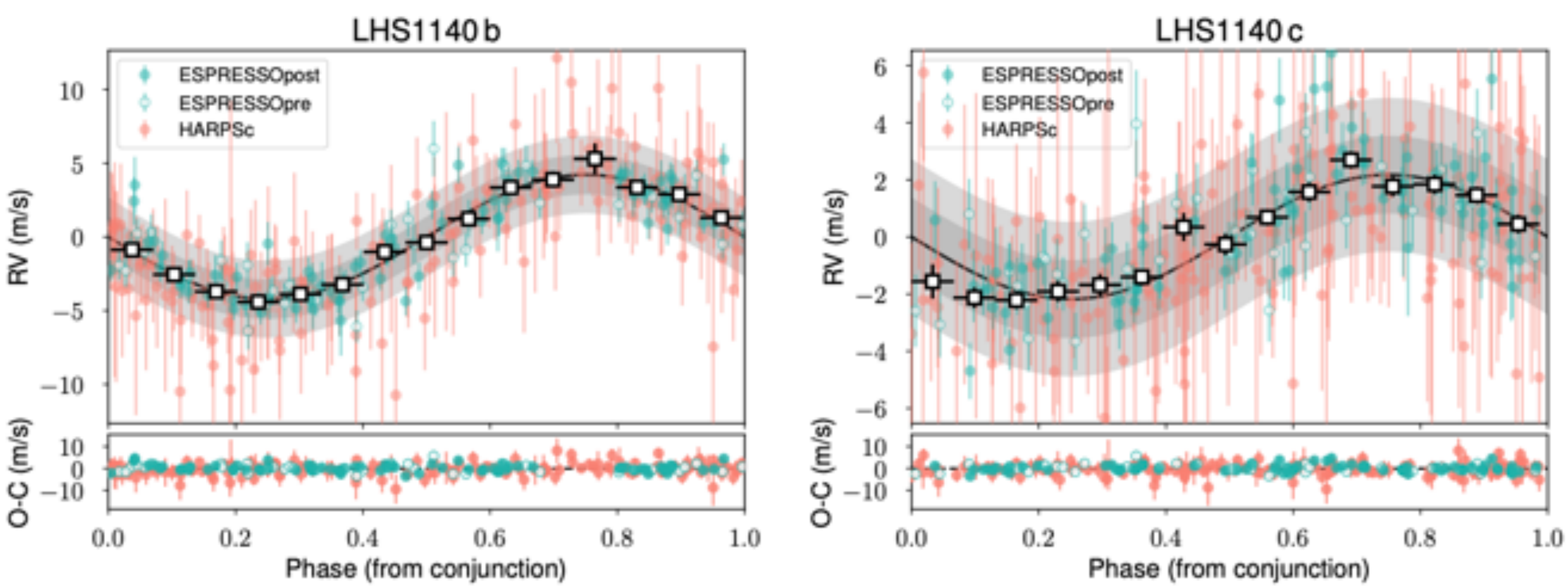

TESS

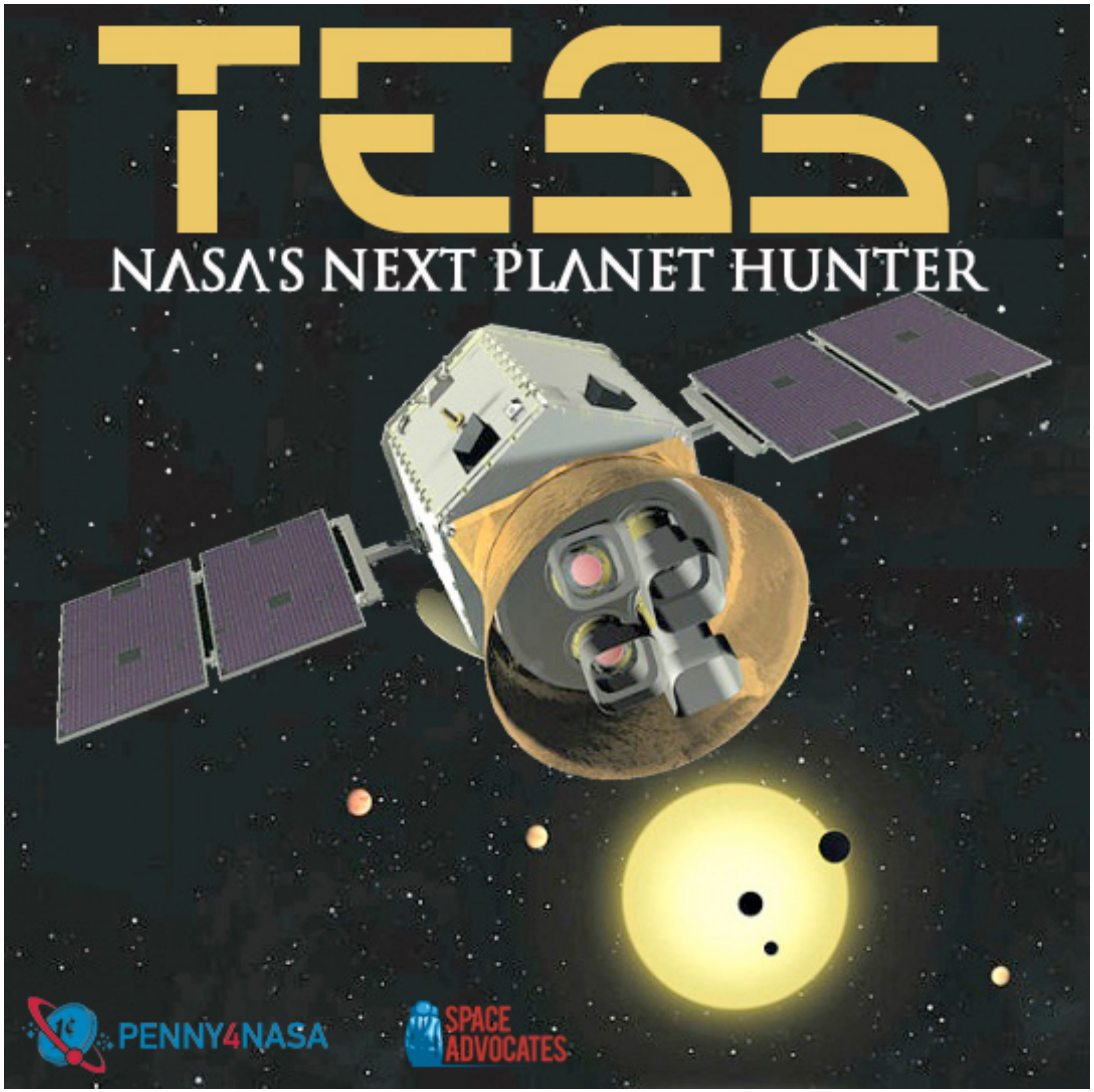

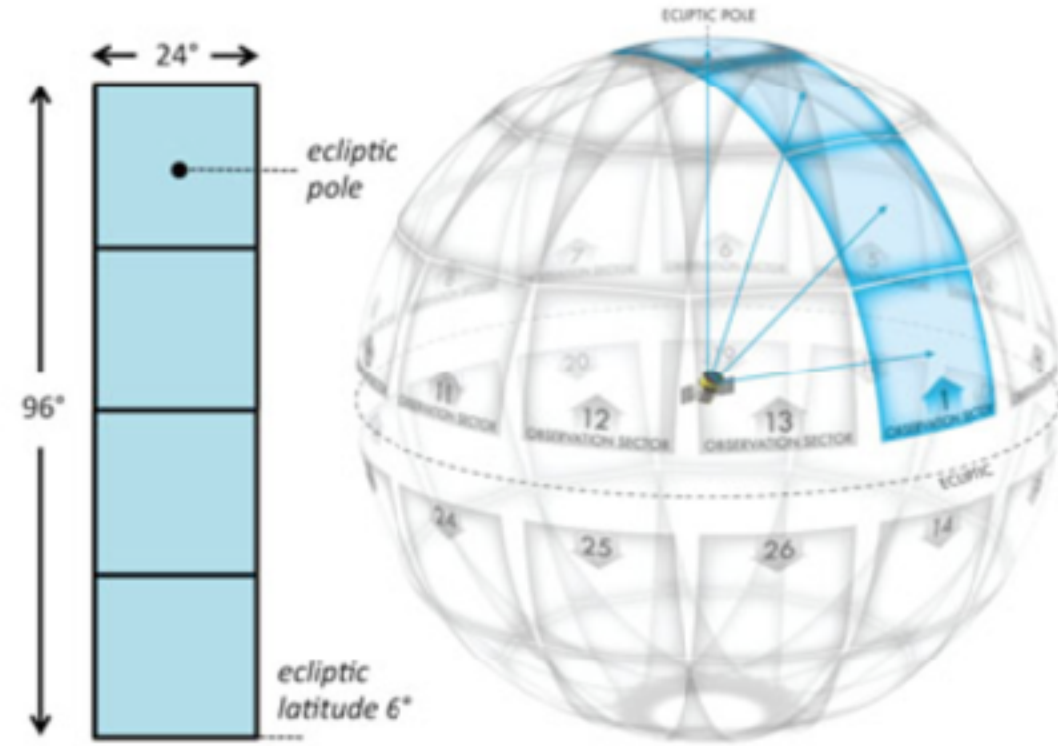

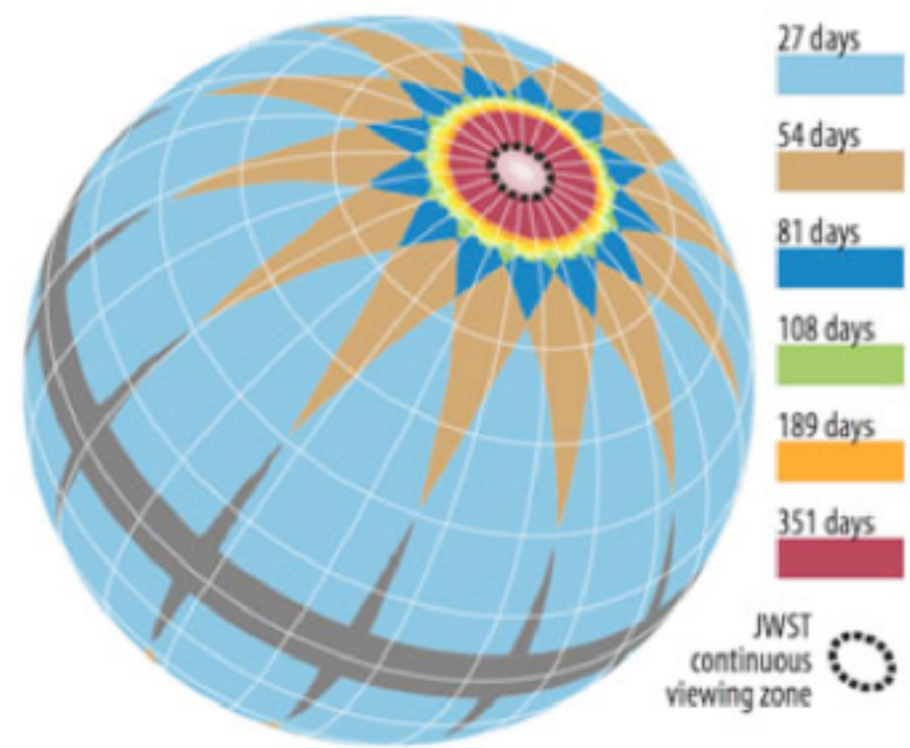

Xavier BONFILS

Sullivan et al. (2015)
http://arxiv.org/abs/1506.03845

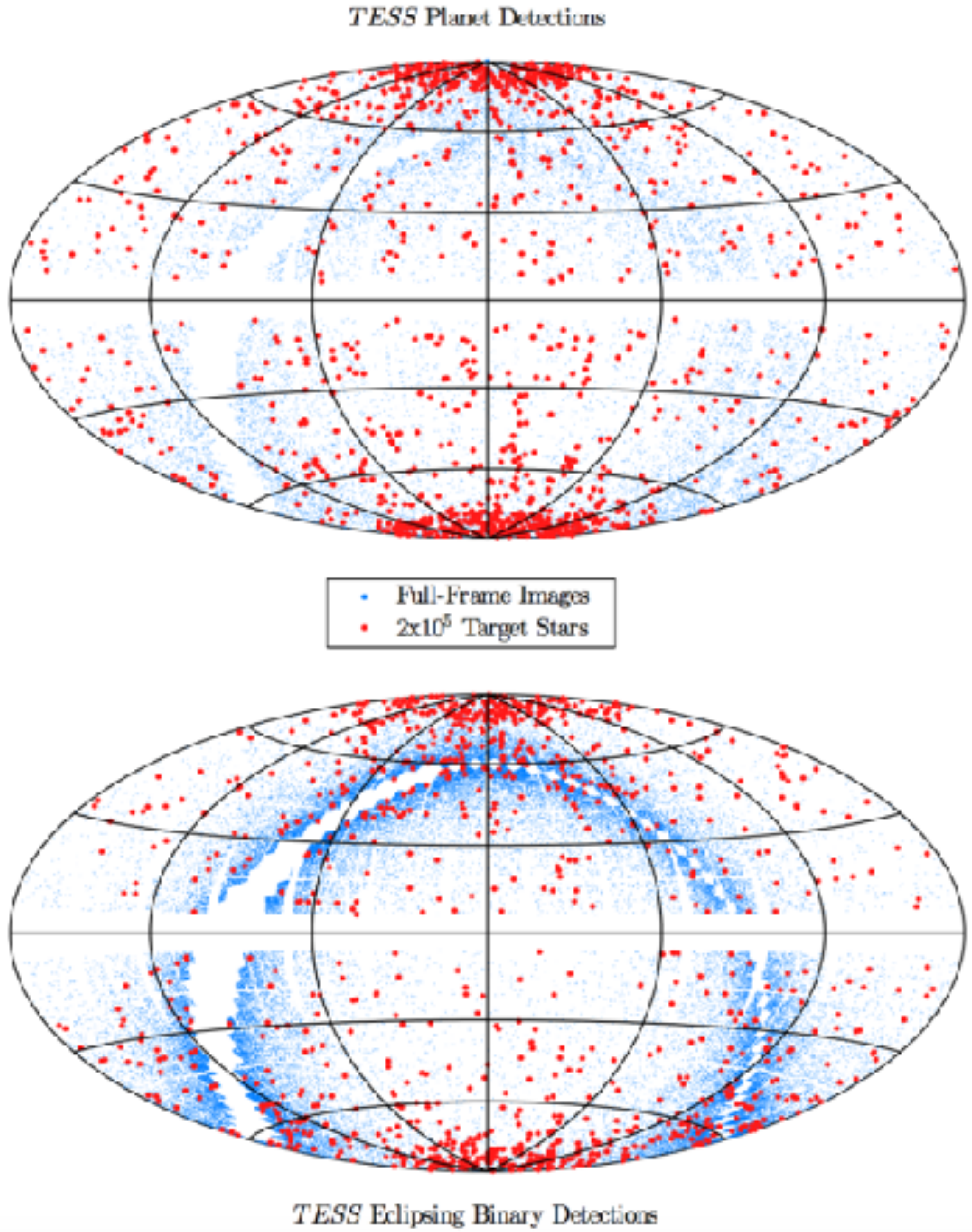

FIG. 19.— Sky maps of the simulated *TESS* detections in equal-area projections of ecliptic coordinates. The lines of latitude are spaced by 30°, and the lines of longitude are spaced by 60°. *Top.*—Planet detections. Red points represent planets detected around target stars (2 min cadence). Blue points represent planets detected around stars that are only observed in the full-frame images (30 min cadence). Note the enhancement in the planet yield near the ecliptic poles, which *TESS* observes for the longest duration. Note also that the inner 6° of the ecliptic is not observed. *Bottom.*—Astrophysical false positive detections, using the same color scheme. For clarity, only 10% of the false positives detected in the full-frame images are shown. (All other categories show 100% of the detections from one trial.) Note the enhancement in the detection rate near the galactic plane, which is stronger for false positives than for planets.

TESS Exoplanets Detected as of 8-2-2021:

- ➡ **4349** TESS Objects of Interest ("TOIs")
  - **3667** Planet Candidates (PCs) remain after false positives removed
  - ~ **800** PCs have $R_{PC} < 4\ R_{\oplus}$
- ➡ See https://exoplanetarchive.ipac.caltech.edu/

TOI-700

Gilbert et al. (2020)

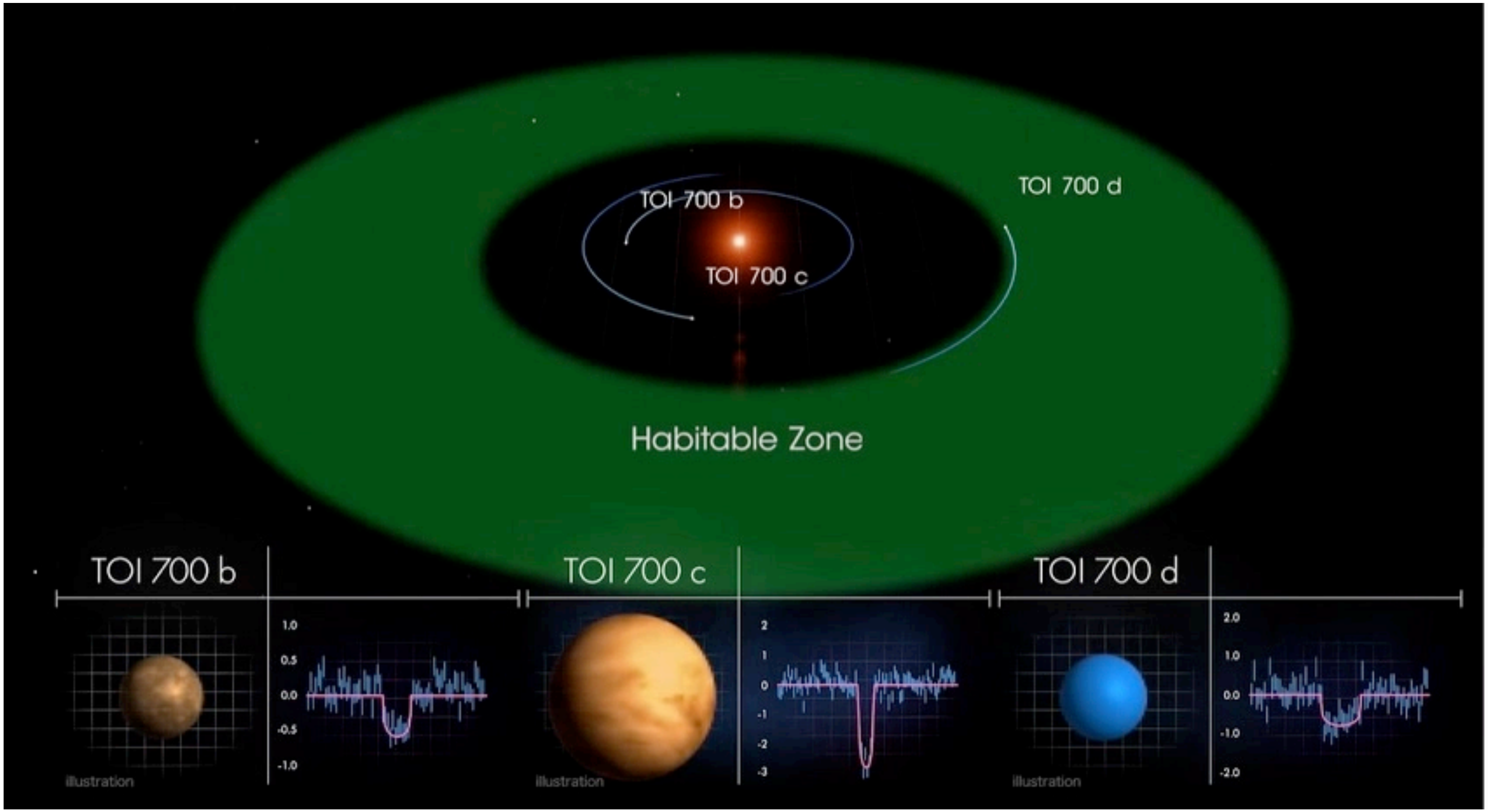

Xavier Bonfils

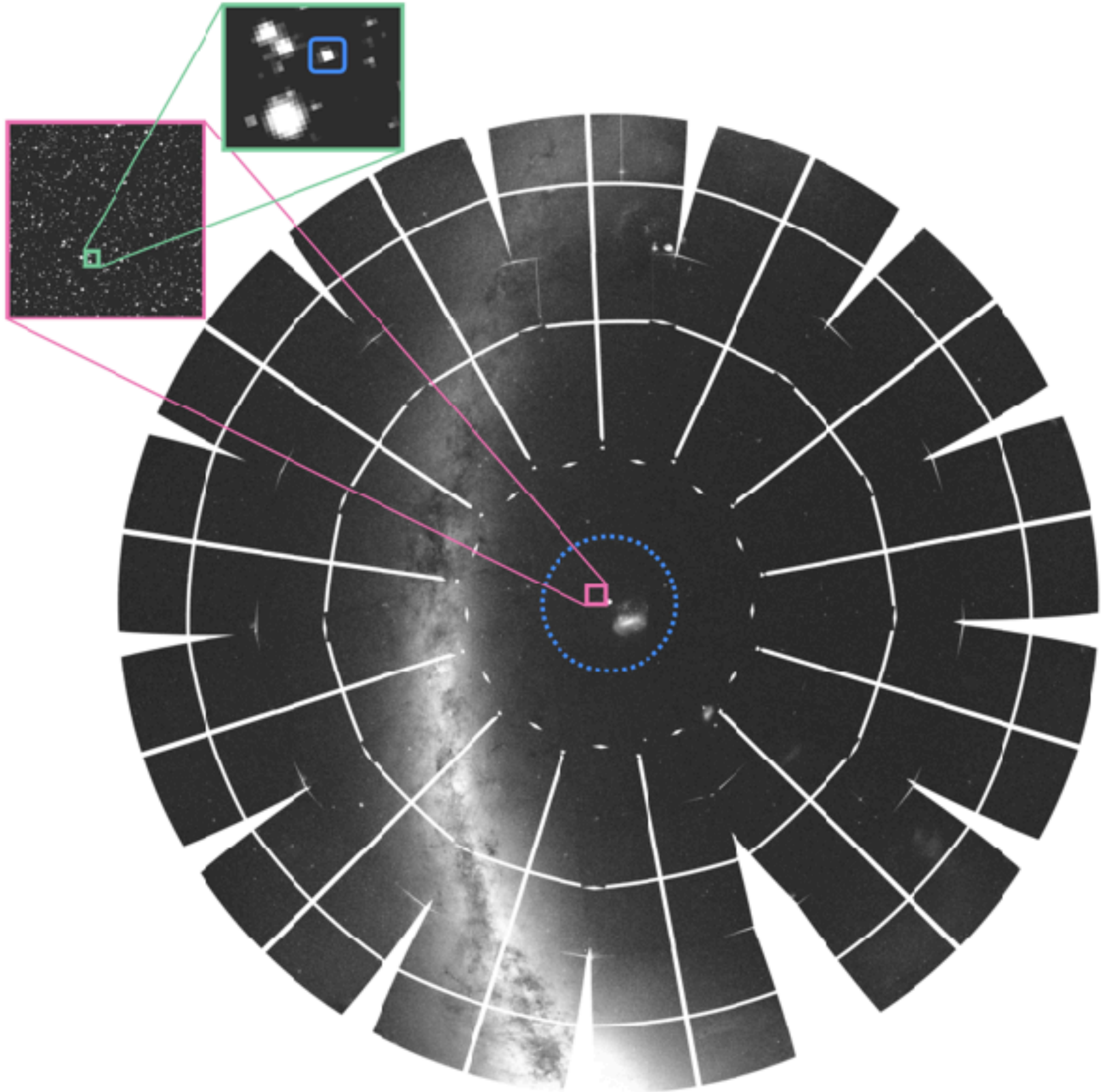

Figure 1. TOI-700 is close to the South Ecliptic Pole and was observed by TESS in 11 of the first 13 sectors of the mission. The field around TOI-700 is relatively uncontaminated, with approximately 1% of the starlight in the region around TOI-700 coming from other stars. The blue dashed line in the figure is the TESS Continuous Viewing Zone (CVZ). The blue square in the upper-left inset shows TOI-700.

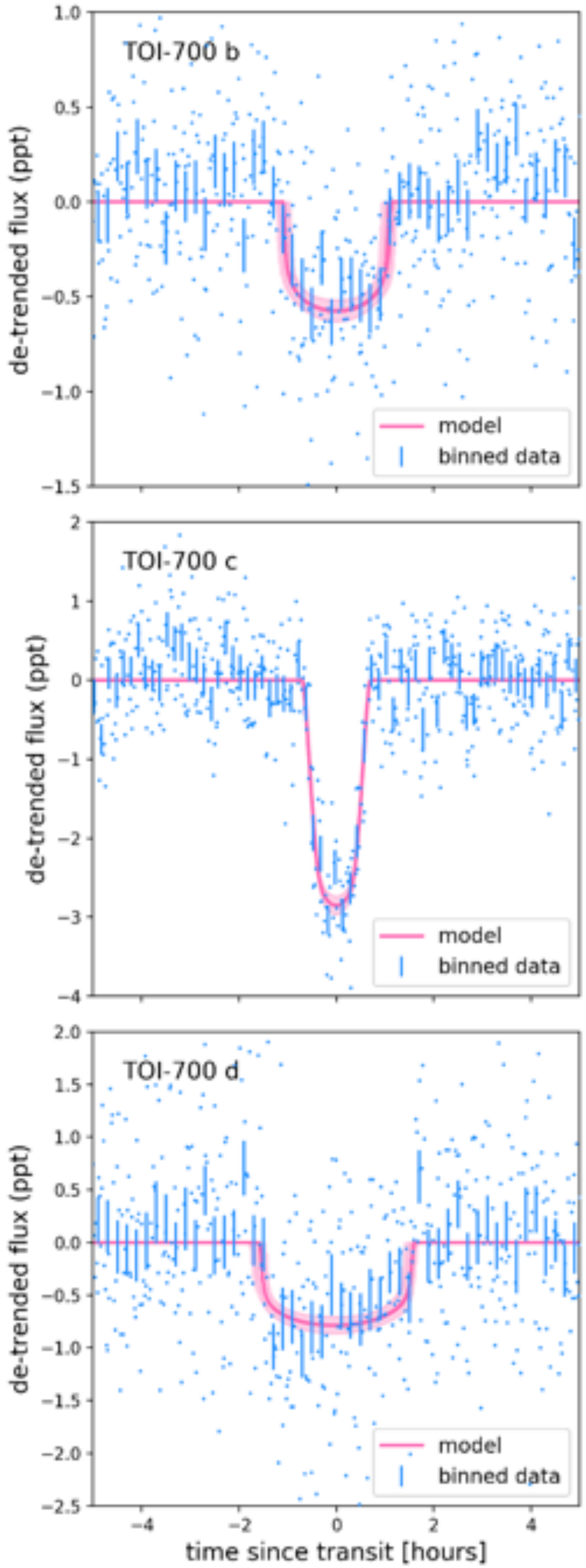

	Derived Parameters		
TOI-700 b			
Period [days]	9.97701	0.00024	0.00028
R_p/R_*	0.0221	0.0011	0.0012
Radius [$R_\oplus$]	1.010	0.094	0.087
Insolation	5.0	1.1	0.9
a/R_*	34.8	1.9	1.9
a [AU]	0.0637	0.0064	0.0060
Inclination (deg)	89.67	0.23	0.32
Duration (hours)	2.15	0.15	0.7
TOI-700 c			
Period [days]	16.051098	0.000089	0.000092
R_p/R_*	0.0574	0.0032	0.0026
Radius [$R_\oplus$]	2.63	0.24	0.23
Insolation	2.66	0.58	0.46
a/R_*	47.8	2.7	2.6
a [AU]	0.0925	0.0088	0.0083
Inclination (deg)	88.90	0.08	0.11
Duration (hours)	1.41	0.14	0.09
TOI-700 d			
Period [days]	37.4260	0.0007	0.0010
R_p/R_*	0.0262	0.0014	0.0015
Radius [$R_\oplus$]	1.19	0.11	0.11
Insolation	0.86	0.19	0.15
a/R_*	84.0	4.7	4.6
a [AU]	0.163	0.015	0.015
Inclination (deg)	89.73	0.15	0.12
Duration (hours)	3.21	0.27	0.26

TOI-175

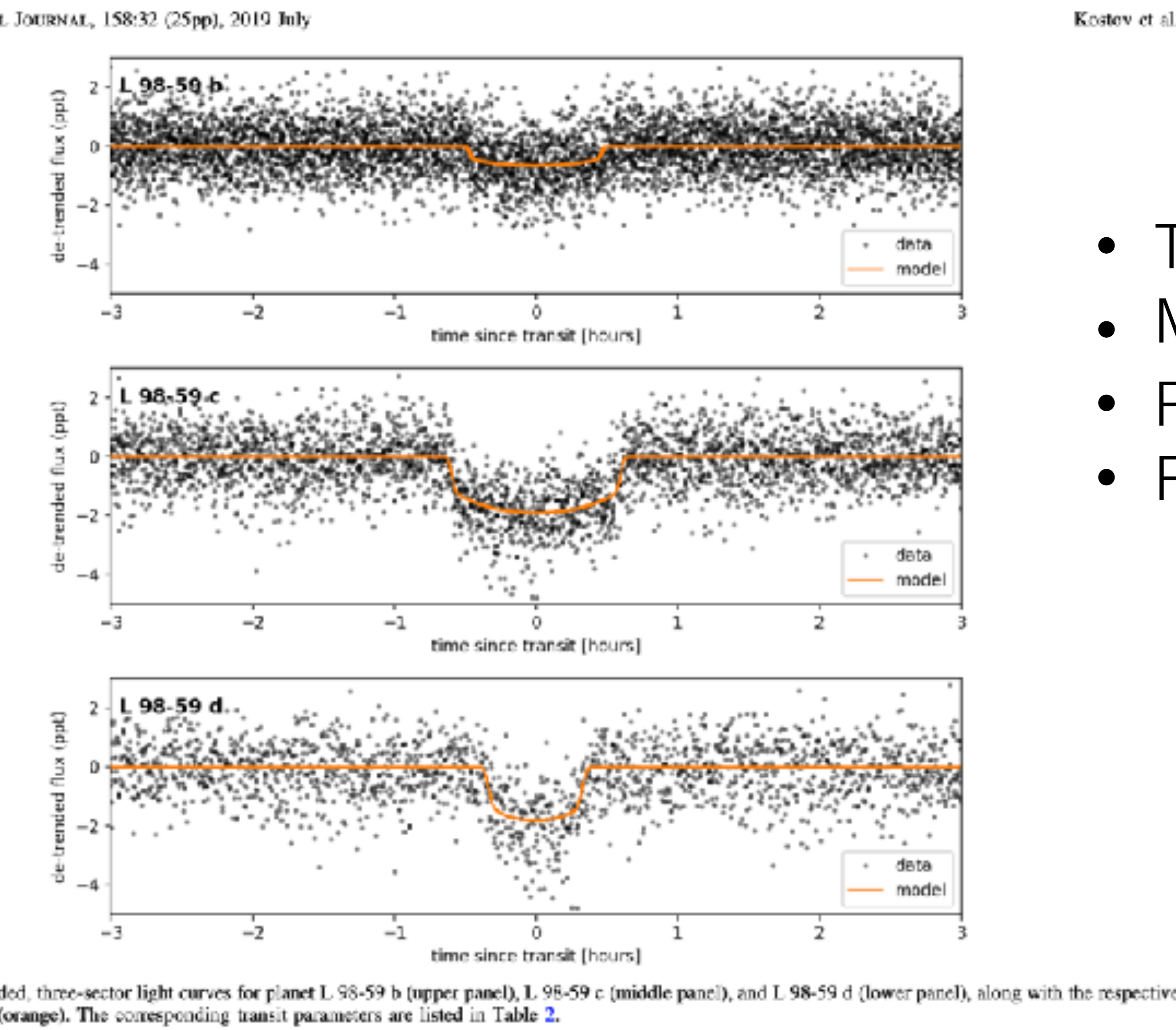

- TESS detection (Kostov et al. 2019)
- M3; V = 11.6 mag; $M_\star = 0.3 M_\odot$
- P=2.2, 3.7, 7.5 d (5:3; 2:1)
- Rp=0.8, 1.3, 1.6 Rearth

Kostov et al. (2019)

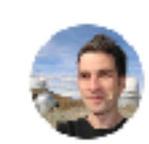

TOI-175

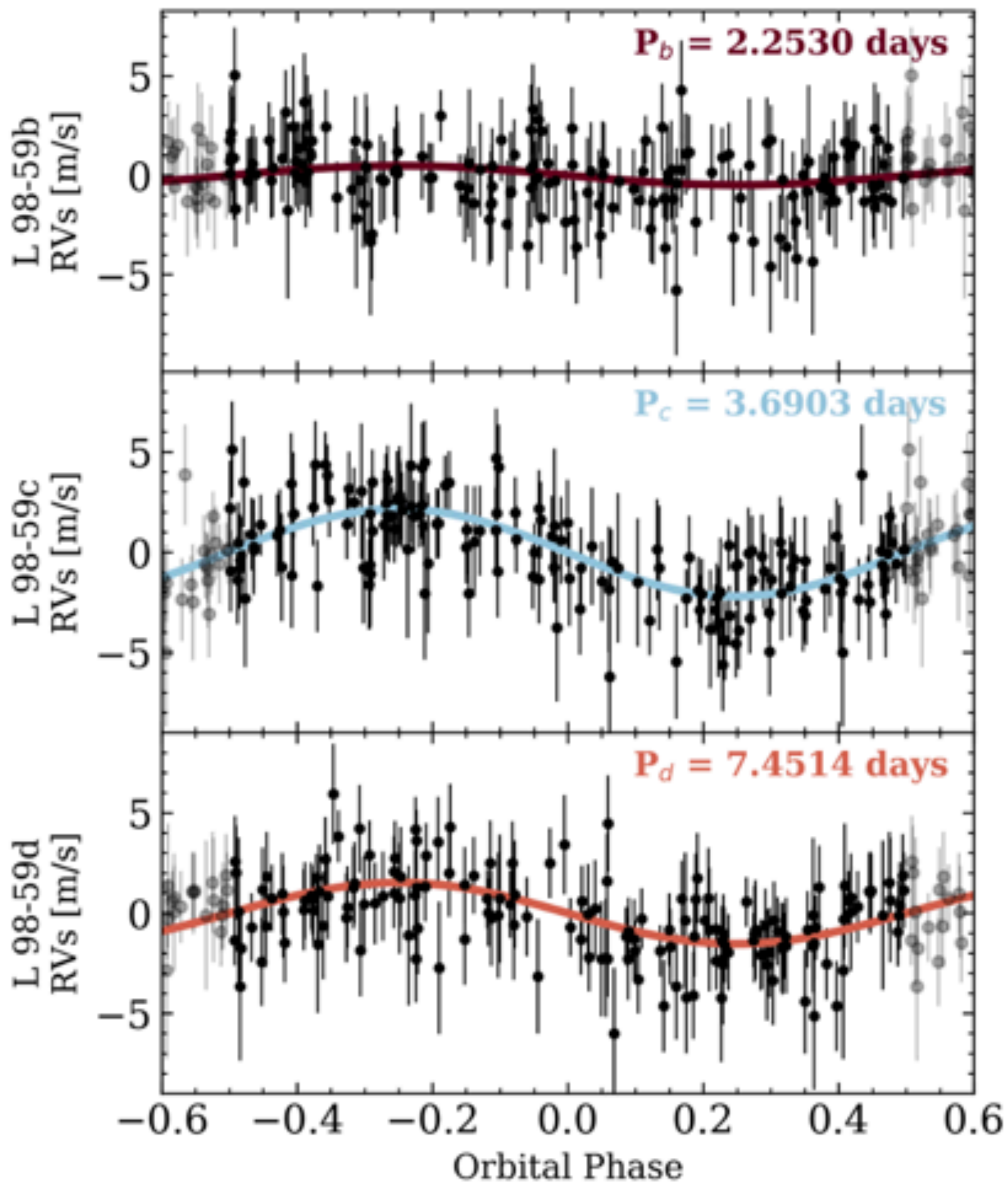

Fig. 3. Phase-folded RVs for each known L 98-59 planet. Each set of RVs has been corrected for stellar activity and the two planets not depicted in its panel. Only the two outermost planets are detected with semi-amplitudes that are inconsistent with 0 m s^{-1}.

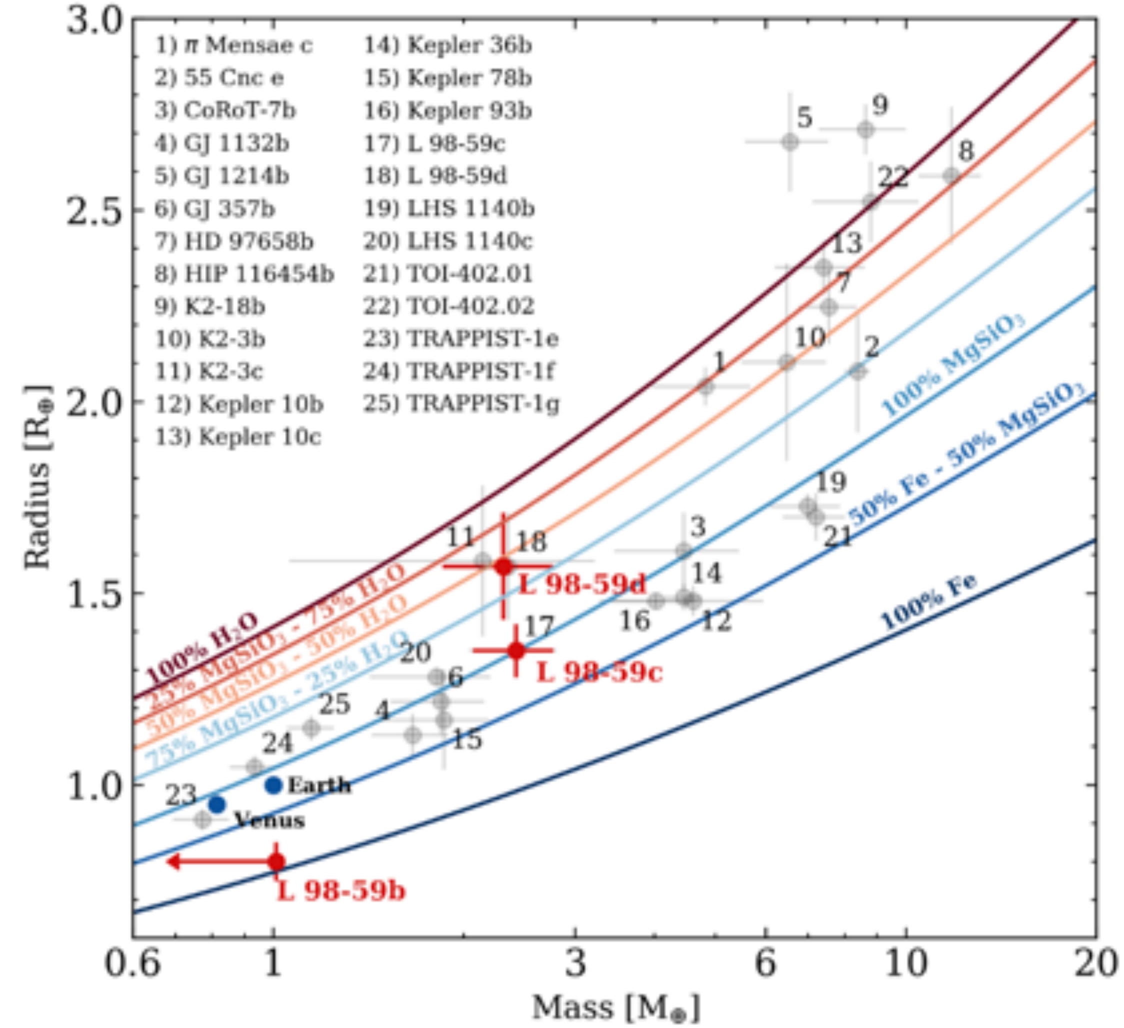

Cloutier et al. (2019)

Xavier Bonfils

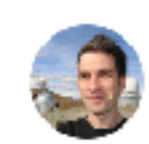

TOI-175

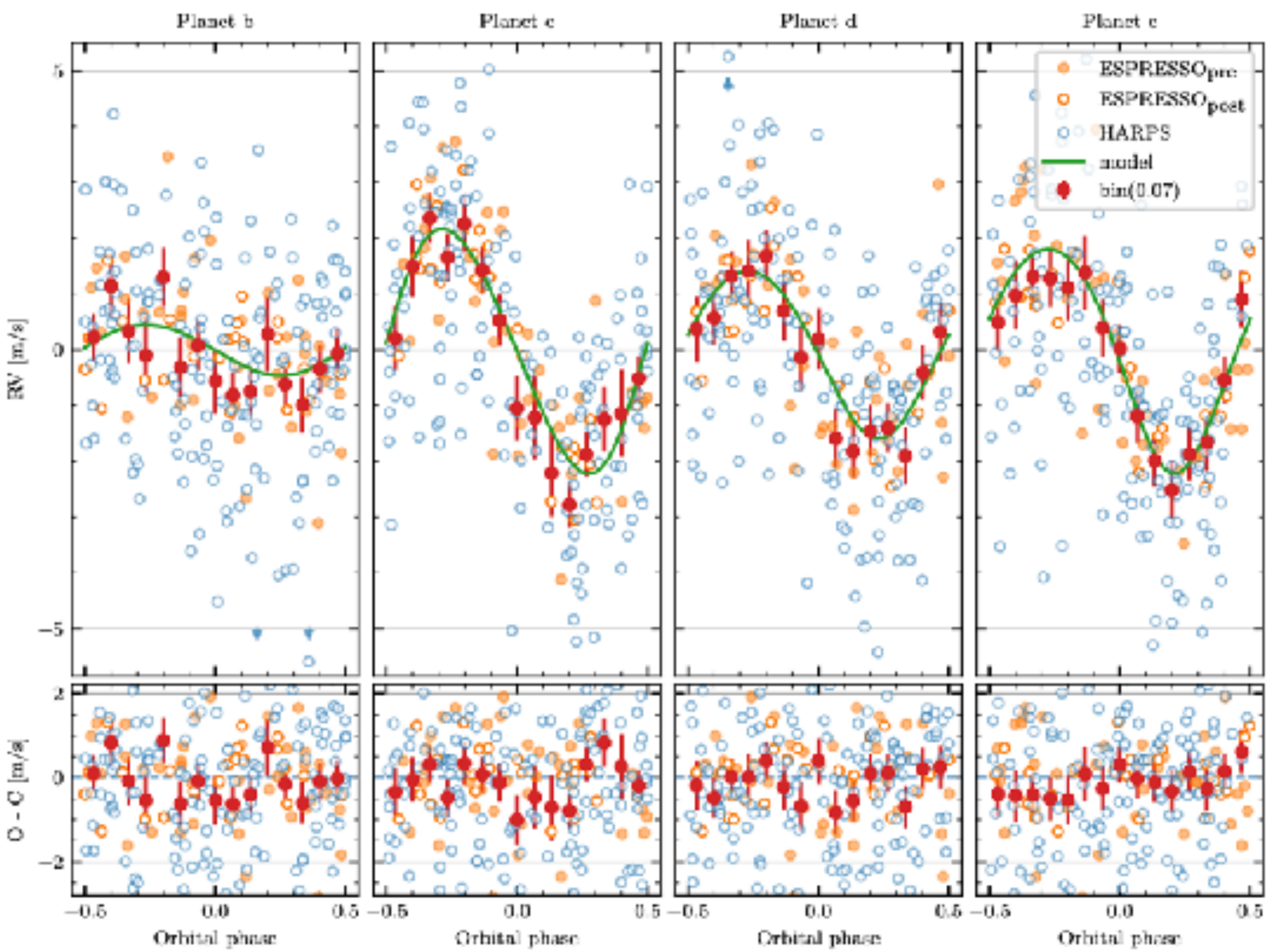

- ESPRESSO
- 4th; possibly 5th planet
- $m_b = 0.4 M_\oplus$
- Lowest mass of RV planets

Demangeon et al. (2021)

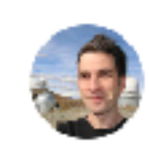

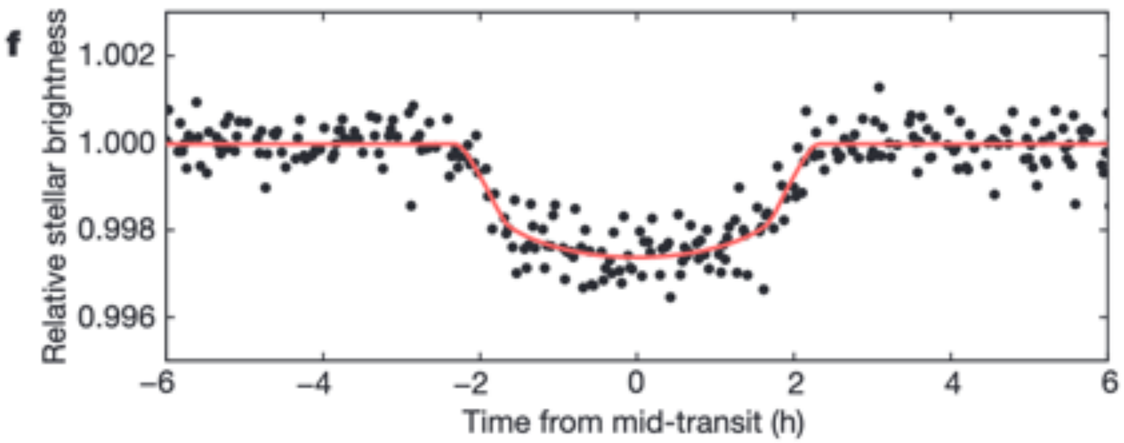

K2-33b

doi:10.1038/nature18293

A Neptune-sized transiting planet closely orbiting a 5–10-million-year-old star

Trevor J. David[1], Lynne A. Hillenbrand[1], Erik A. Petigura[2], John M. Carpenter[3], Ian J. M. Crossfield[4], Sasha Hinkley[5], David R. Ciardi[6], Andrew W. Howard[7], Howard T. Isaacson[8], Ann Marie Cody[9], Joshua E. Schlieder[9], Charles A. Beichman[6] & Scott A. Barenfeld[1]

The Astronomical Journal, 152:61 (13pp), 2016 September
doi:10.3847/0004-6256/152/3/61

CrossMark

ZODIACAL EXOPLANETS IN TIME (ZEIT). III. A SHORT-PERIOD PLANET ORBITING A PRE-MAIN-SEQUENCE STAR IN THE UPPER SCORPIUS OB ASSOCIATION

Andrew W. Mann[1,9], Elisabeth R. Newton[2,10], Aaron C. Rizzuto[1], Jonathan Irwin[2], Gregory A. Feiden[3], Eric Gaidos[4], Gregory N. Mace[1], Adam L. Kraus[1], David J. James[5], Megan Ansdell[6], David Charbonneau[2], Kevin R. Covey[7], Michael J. Ireland[8], Daniel T. Jaffe[1], Marshall C. Johnson[1], Benjamin Kidder[1], and Andrew Vanderburg[2,10]

+ simulations by Klein & Donati (2020) showing mass can be measured w/ SPIROU :0)

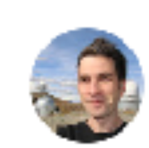

Article

A planet within the debris disk around the pre-main-sequence star AU Microscopii

https://doi.org/10.1038/s41586-020-2400-z

Received: 16 February 2019

Accepted: 17 March 2020

Published online: 24 June 2020

Check for updates

Peter Plavchan[1]✉, Thomas Barclay[2,13], Jonathan Gagné[3], Peter Gao[4], Bryson Cale[1], William Matzko[1], Diana Dragomir[5,6], Sam Quinn[7], Dax Feliz[8], Keivan Stassun[8], Ian J. M. Crossfield[5,9], David A. Berardo[5], David W. Latham[7], Ben Tieu[1], Guillem Anglada-Escudé[10], George Ricker[5], Roland Vanderspek[5], Sara Seager[5], Joshua N. Winn[11], Jon M. Jenkins[12], Stephen Rinehart[13], Akshata Krishnamurthy[5], Scott Dynes[5], John Doty[13], Fred Adams[14], Dennis A. Afanasev[13], Chas Beichman[15,16], Mike Bottom[17], Brendan P. Bowler[18], Carolyn Brinkworth[19], Carolyn J. Brown[20], Andrew Cancino[21], David R. Ciardi[16],

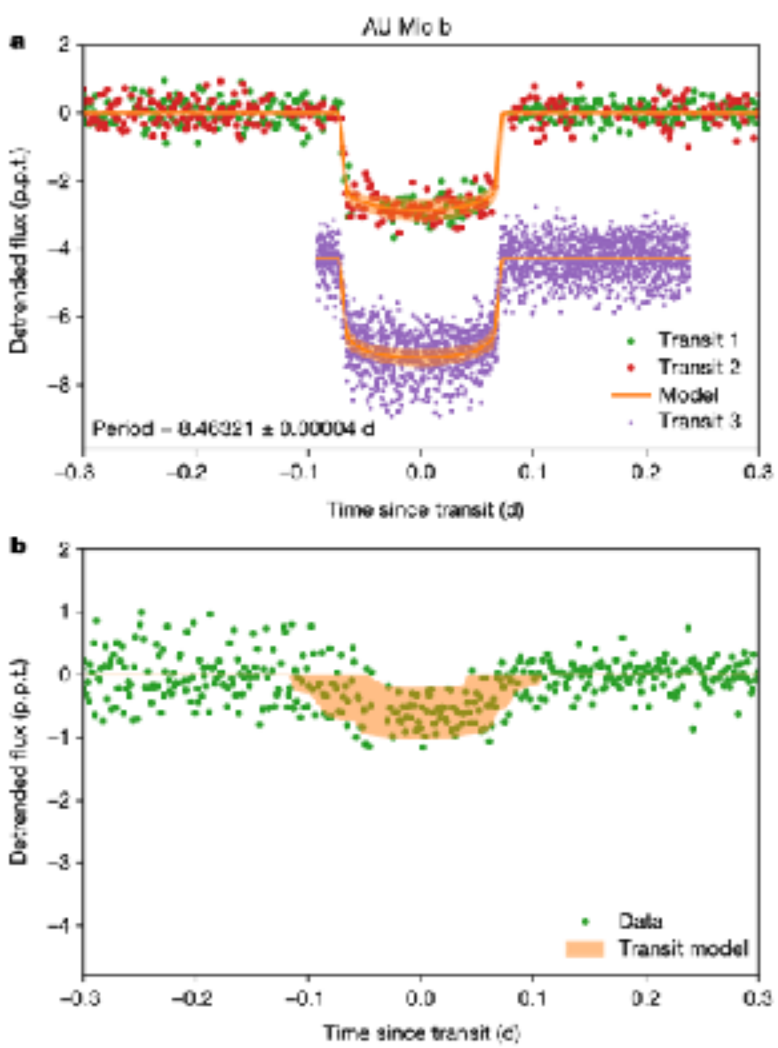

Xavier Bonfils

Article

A planet within the debris disk around the pre-main-sequence star AU Microscopii

https://doi.org/10.1038/s41586-020-2400-z

Received: 16 February 2019

Accepted: 17 March 2020

Published online: 24 June 2020

Check for updates

Peter Plavchan[1✉], Thomas Barclay[2,13], Jonathan Gagné[3], Peter Gao[4], Bryson Cale[1], William Matzko[1], Diana Dragomir[5,6], Sam Quinn[7], Dax Feliz[8], Keivan Stassun[8], Ian J. M. Crossfield[5,9], David A. Berardo[5], David W. Latham[7], Ben Tieu[1], Guillem Anglada-Escudé[10], George Ricker[5], Roland Vanderspek[5], Sara Seager[5], Joshua N. Winn[11], Jon M. Jenkins[12], Stephen Rinehart[13], Akshata Krishnamurthy[5], Scott Dynes[5], John Doty[13], Fred Adams[14], Dennis A. Afanasev[13], Chas Beichman[15,16], Mike Bottom[17], Brendan P. Bowler[18], Carolyn Brinkworth[19], Carolyn J. Brown[20], Andrew Cancino[21], David R. Ciardi[16],

MNRAS 000, 1–16 (2020) Preprint 30 November 2020 Compiled using MNRAS LaTeX style file v3.0

Investigating the young AU Mic system with SPIRou: large-scale stellar magnetic field and close-in planet mass

Baptiste Klein[1★], Jean-François Donati[1], Claire Moutou[1], Xavier Delfosse[2], Xavier Bonfils[2], Eder Martioli[3,4], Pascal Fouqué[1,5], Ryan Cloutier[6], Étienne Artigau[7], René Doyon[7], Guillaume Hébrard[3], Julien Morin[8], Julien Rameau[2], Peter Plavchan[9], Eric Gaidos[10]

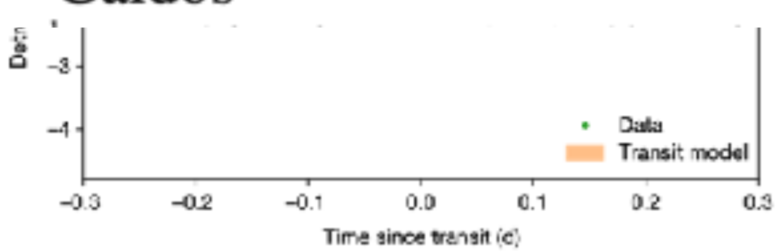

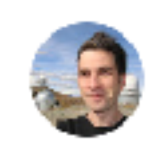

Investigating the young AU Mic system with SPIRou: large-scale stellar magnetic field and close-in planet mass

Baptiste Klein[1★], Jean-François Donati[1], Claire Moutou[1], Xavier Delfosse[2], Xavier Bonfils[2], Eder Martioli[3,4], Pascal Fouqué[1,5], Ryan Cloutier[6], Étienne Artigau[7], René Doyon[7], Guillaume Hébrard[3], Julien Morin[8], Julien Rameau[2], Peter Plavchan[9], Eric Gaidos[10]

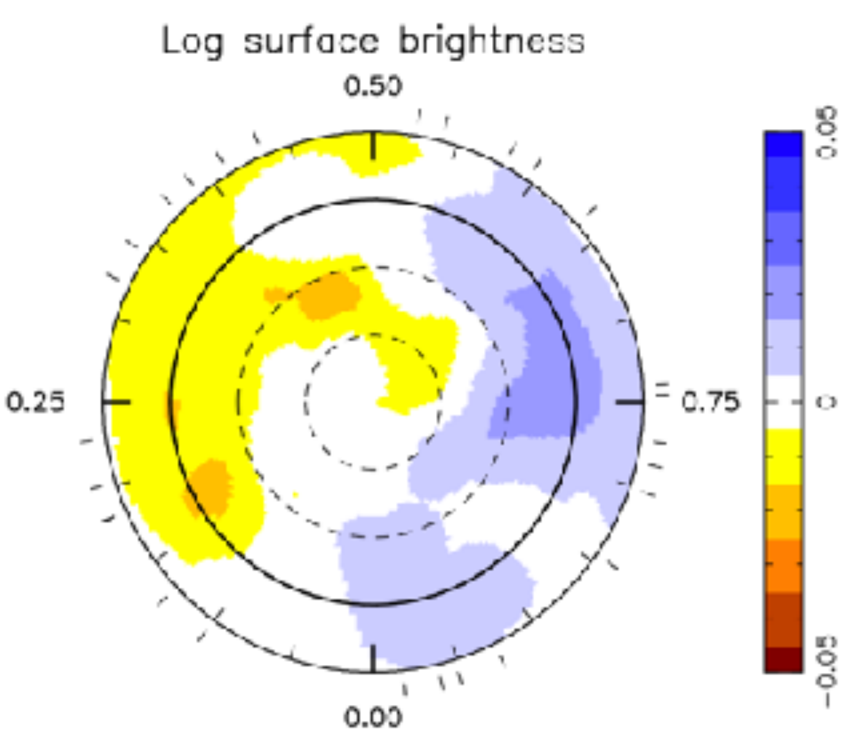

$17M_\oplus$

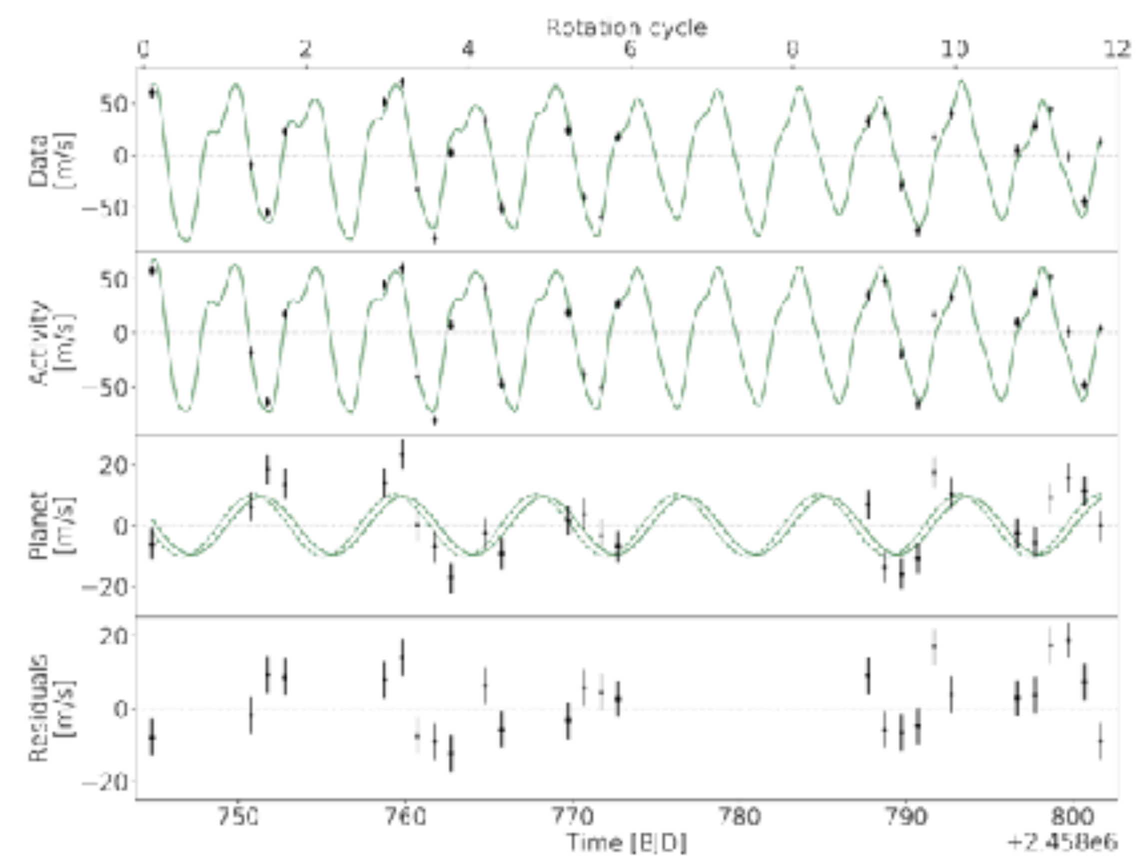

LETTER TO THE EDITOR

Spin-orbit alignment and magnetic activity in the young planetary system AU Mic★

E. Martioli[1,2], G. Hébrard[1,3], C. Moutou[4], J.-F. Donati[4], É. Artigau[5], B. Cale[6], N. J. Cook[5], S. Dalal[1], X. Delfosse[7], T. Forveille[7], E. Gaidos[9], P. Plavchan[6], J. Berberian[6], A. Carmona[7], R. Cloutier[13], R. Doyon[5], P. Fouqué[8,4], B. Klein[4], A. Lecavelier des Etangs[1], N. Manset[8], J. Morin[10], A. Tanner[11], J. Teske[12], and S. Wang[12]

E. Martioli et al.: Spin-orbit alignment and magnetic activity in the young planetary system AU Mic

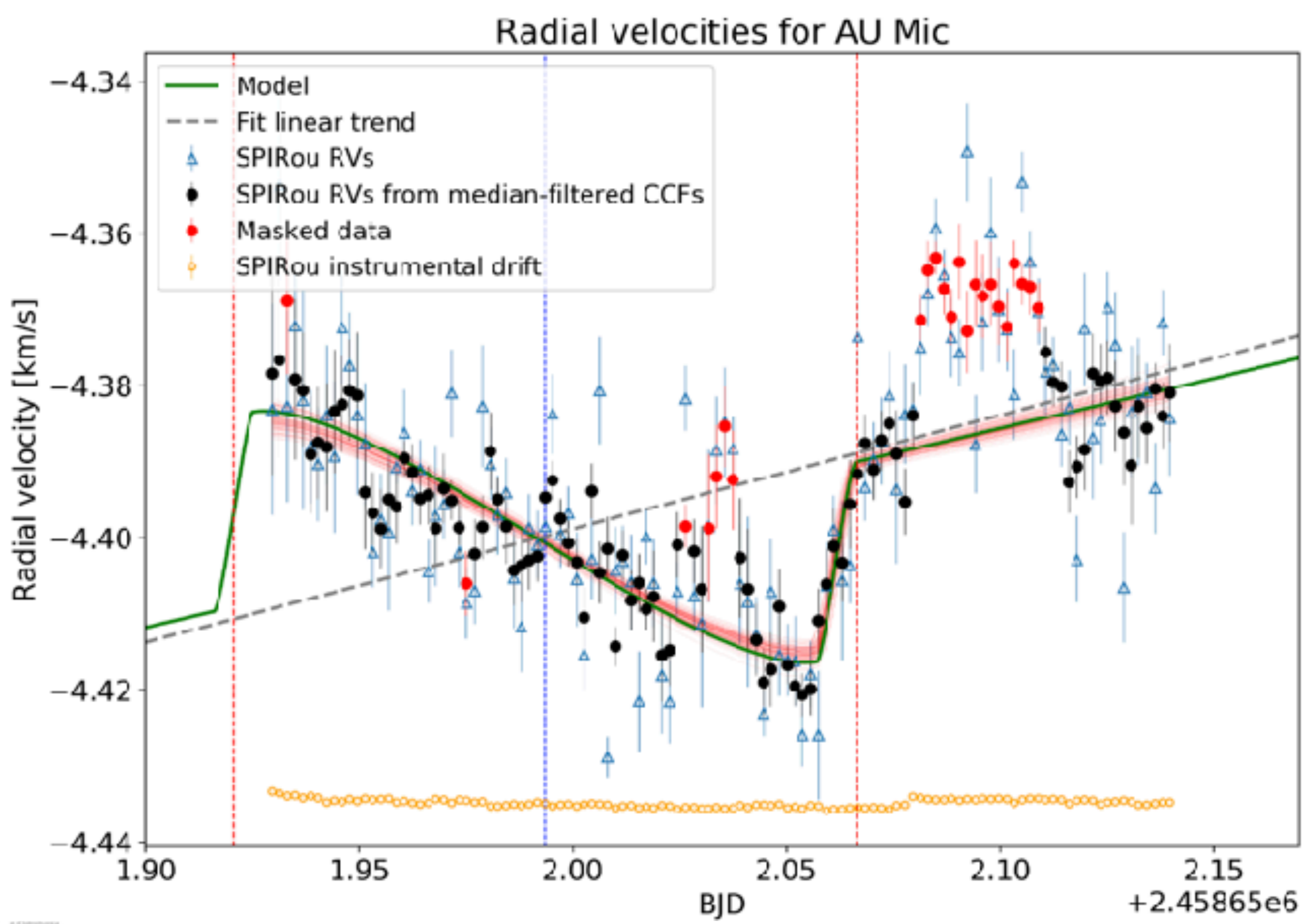

Xavier Bonfils

Draft version August 5, 2020
Typeset using LaTeX **twocolumn** style in AASTeX62

An astrometric planetary companion candidate to the M9 Dwarf TVLM 513−46546

Salvador Curiel,[1] Gisela N. Ortiz-León,[2] Amy J. Mioduszewski,[3] and Rosa M. Torres[4]

[1] *Instituto de Astronomía, Universidad Nacional Autónoma de México (UNAM), Apdo Postal 70-264, México, D.F., México.*
[2] *Max Planck Institut für Radioastronomie, Auf dem Hügel 69, D-53121 Bonn, Germany*
[3] *National Radio Astronomy Observatory, Domenici Science Operations Center, 1003 Lopezville Road, Socorro, NM 87801, USA*
[4] *Centro Universitario de Tonalá, Universidad de Guadalajara, Avenida Nuevo Periférico No. 555, Ejido San José Tatepozco, C.P. 48525, Tonalá, Jalisco, México*

(Received 2020 May 6; Accepted 2020 June 17)

Submitted to AJ

ABSTRACT

Astrometric observations of the M9 dwarf TVLM 513–46546 taken with the VLBA reveal an astrometric signature consistent with a period of 221 ± 5 days. The orbital fit implies that the companion has a mass $m_p = 0.35-0.42\ M_J$, a circular orbit ($e \simeq 0$), a semi-major axis a = 0.28−0.31 AU and an inclination angle i = 71−88°. The detected companion, TVLM 513*b*, is one of the few giant-mass planets found associated to UCDs. The presence of a Saturn-like planet on a circular orbit, 0.3 AU from a 0.06−0.08 $M_\odot$ star, represents a challenge to planet formation theory. This is the first astrometric detection of a planet at radio wavelengths.

Half Jupiter mass planets exist at moderate separation around VLMS
(Although that one is too faint for SPIRou)

Stats

The Staknovist improvement in RV and LC precisions

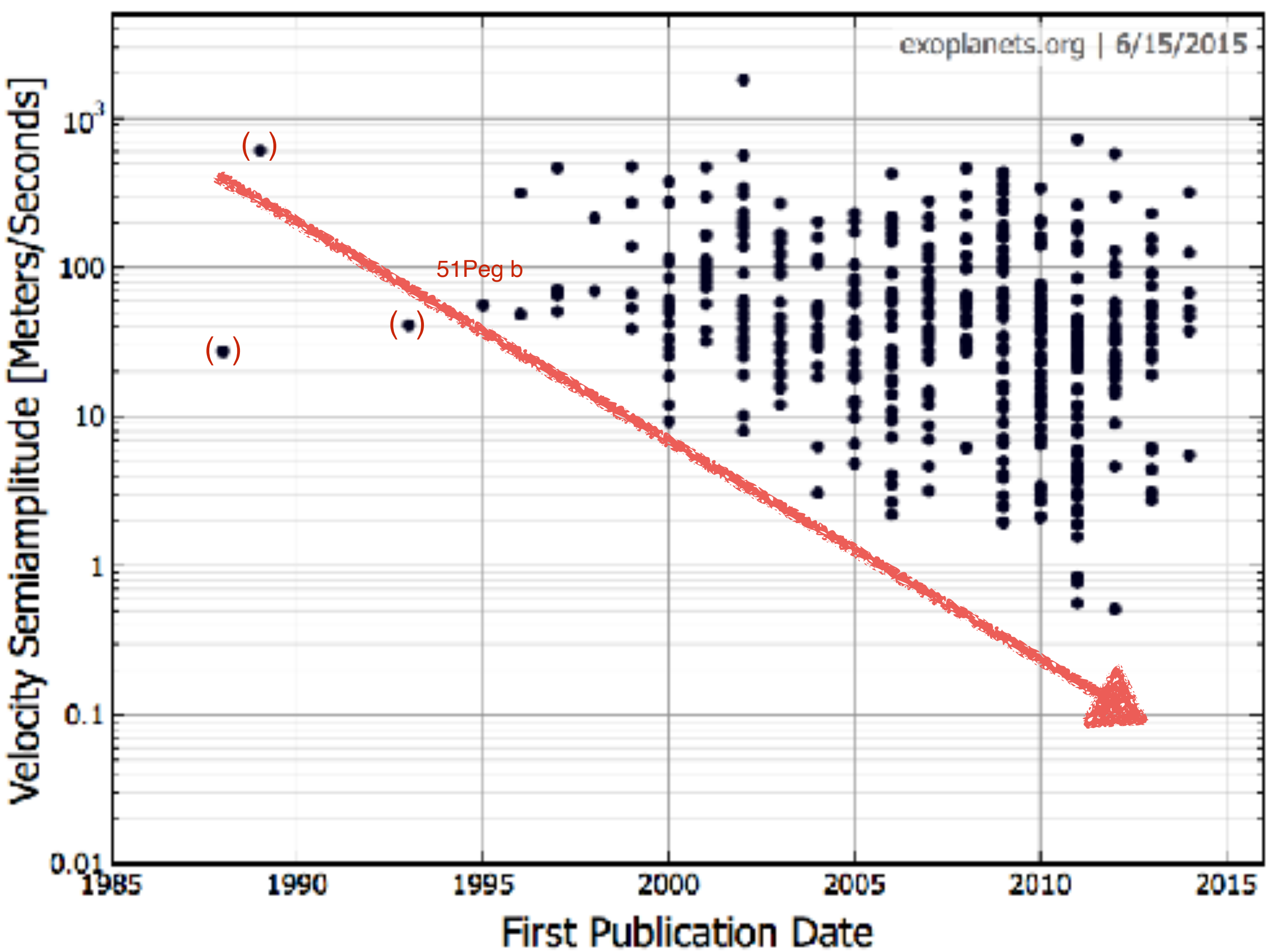

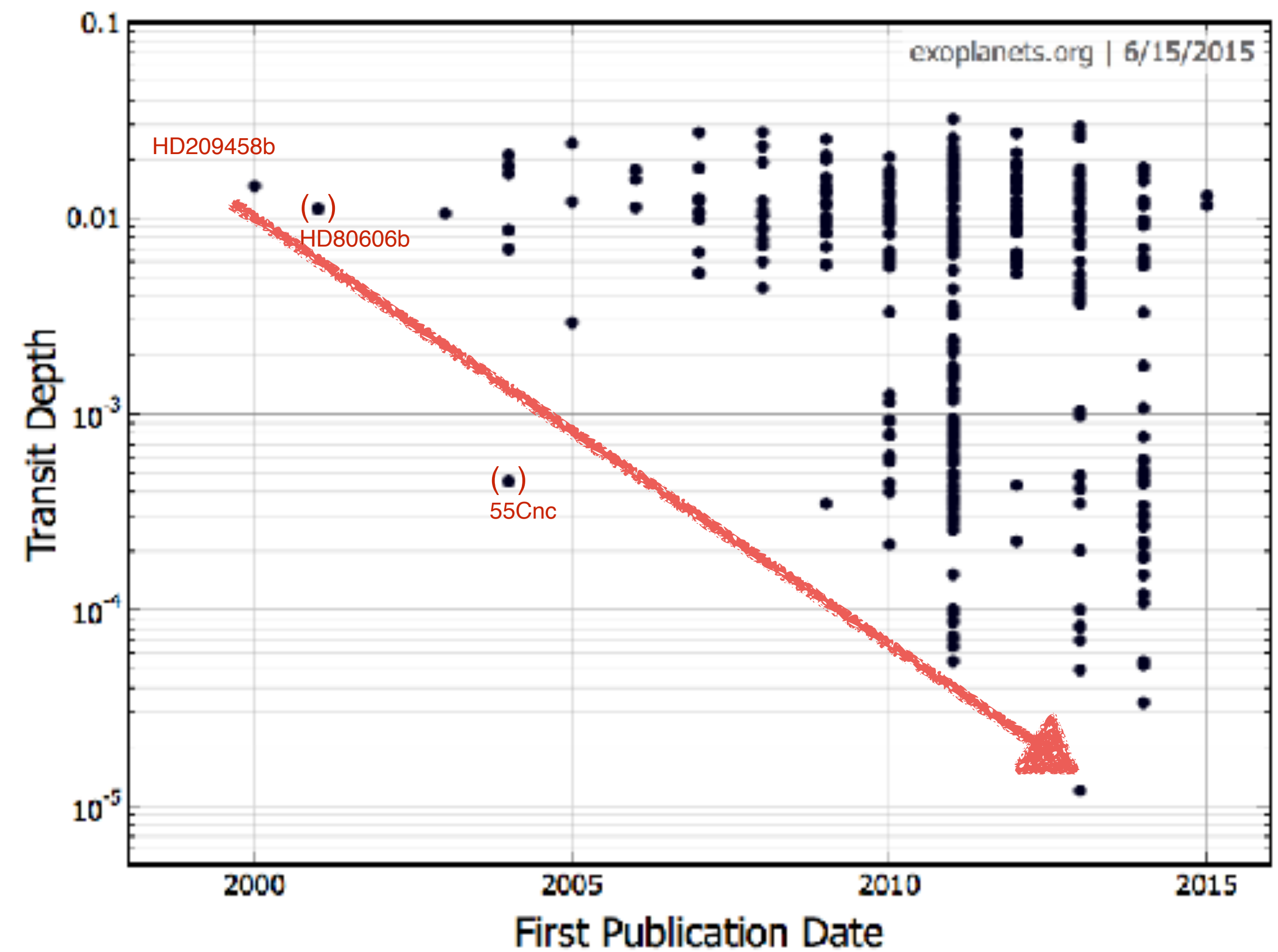

- RV semi-amplitude decreased by ~3 order of magnitudes in 20 years
- Transit depths decreased by ~3 order of magnitude in 15 years

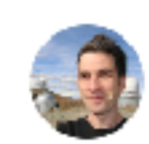

The Staknovist improvement in RV and LC precisions

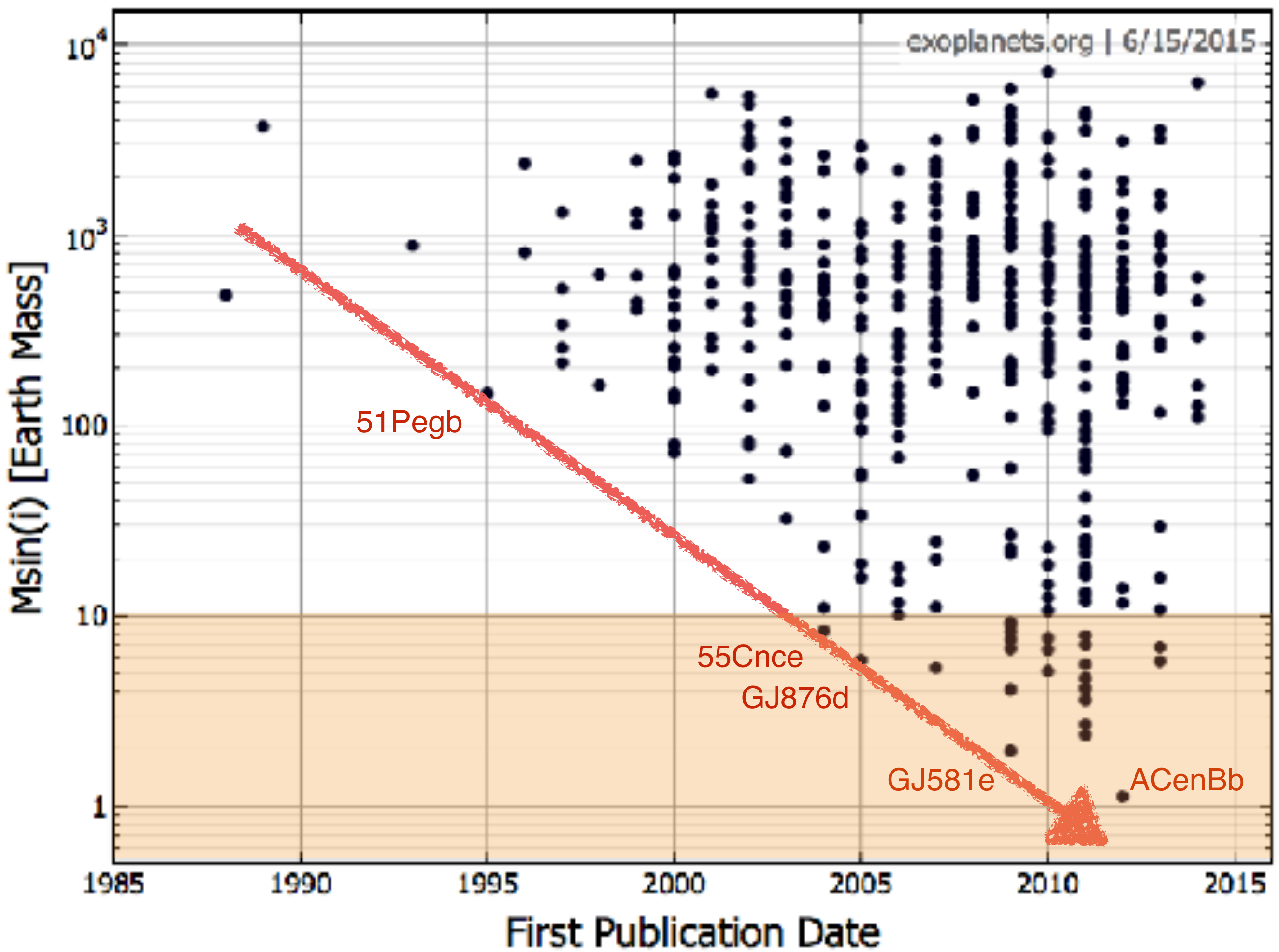

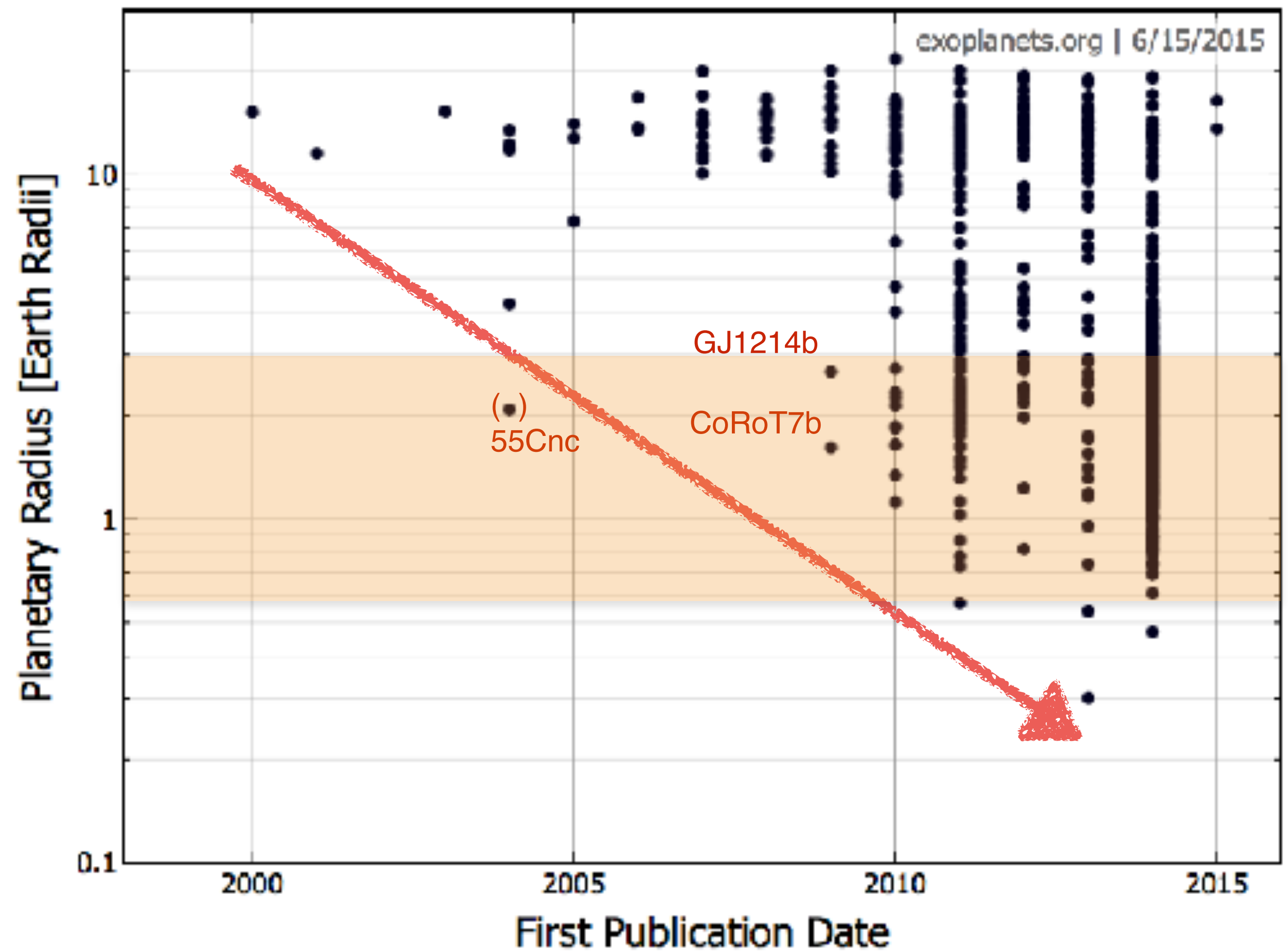

- mass decreased by 3 order of magnitude
- radii decreased by ~2 order of magnitude
- super-Earths domain is now well populated

What have we learned about their statistical properties ?

Stats from RV searches (HARPS+HIRES)

Xavier Bonfils

HARPS

- Observatoire de Genève
- Physikalisches Institut, Bern
- Observatoire Haute-Provence
- Service d'Aéronomie, Paris
- ESO

ΔRV =1 m/s

Δλ=0.00001 A

15 nm

1/10000 pixel

2-fiber feed

ΔRV =1 m/s

ΔT =0.01 K

Δp=0.01 mBar

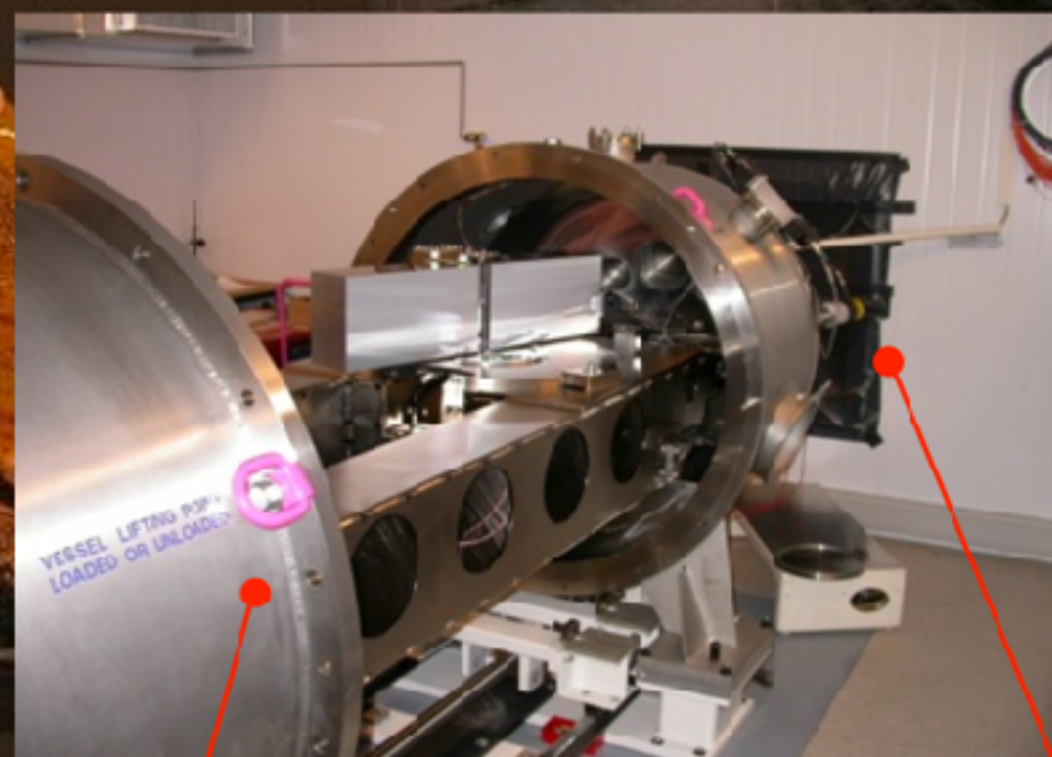

Pressure controlled

Temperature controlled

The HARPS search for southern extra-solar planets

XXXIV. Occurrence, mass distribution and orbital properties of super-Earths and Neptune-mass planets*

M. Mayor[1], M. Marmier[1], C. Lovis[1], S. Udry[1], D. Ségransan[1], F. Pepe[1], W. Benz[2], J.-L. Bertaux[3], F. Bouchy[4], X. Dumusque[1], G. LoCurto[5], C. Mordasini[6], D. Queloz[1], and N.C. Santos[7,8]

Mayor et al. (2011) astro-ph/1109.2497

see also
Lovis et al. (2008) proc. in IAUS253

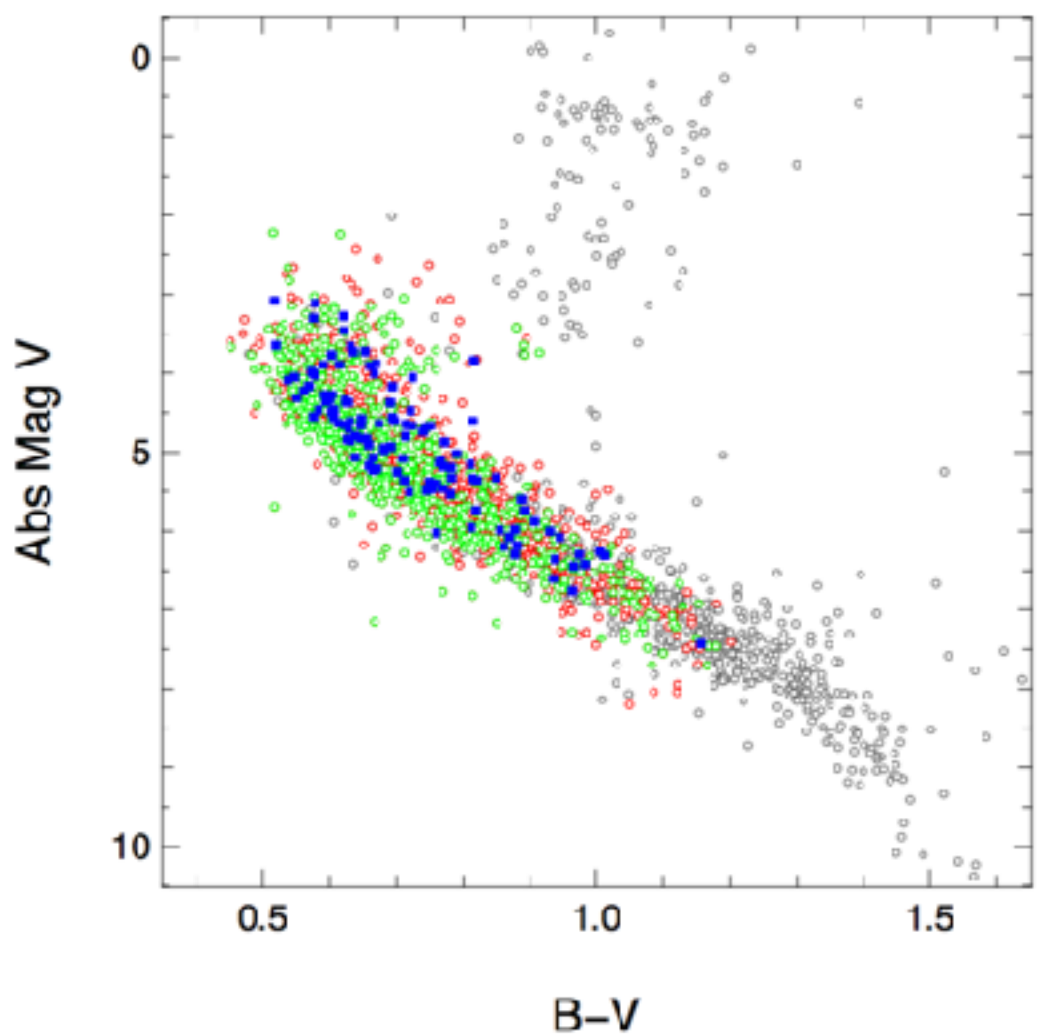

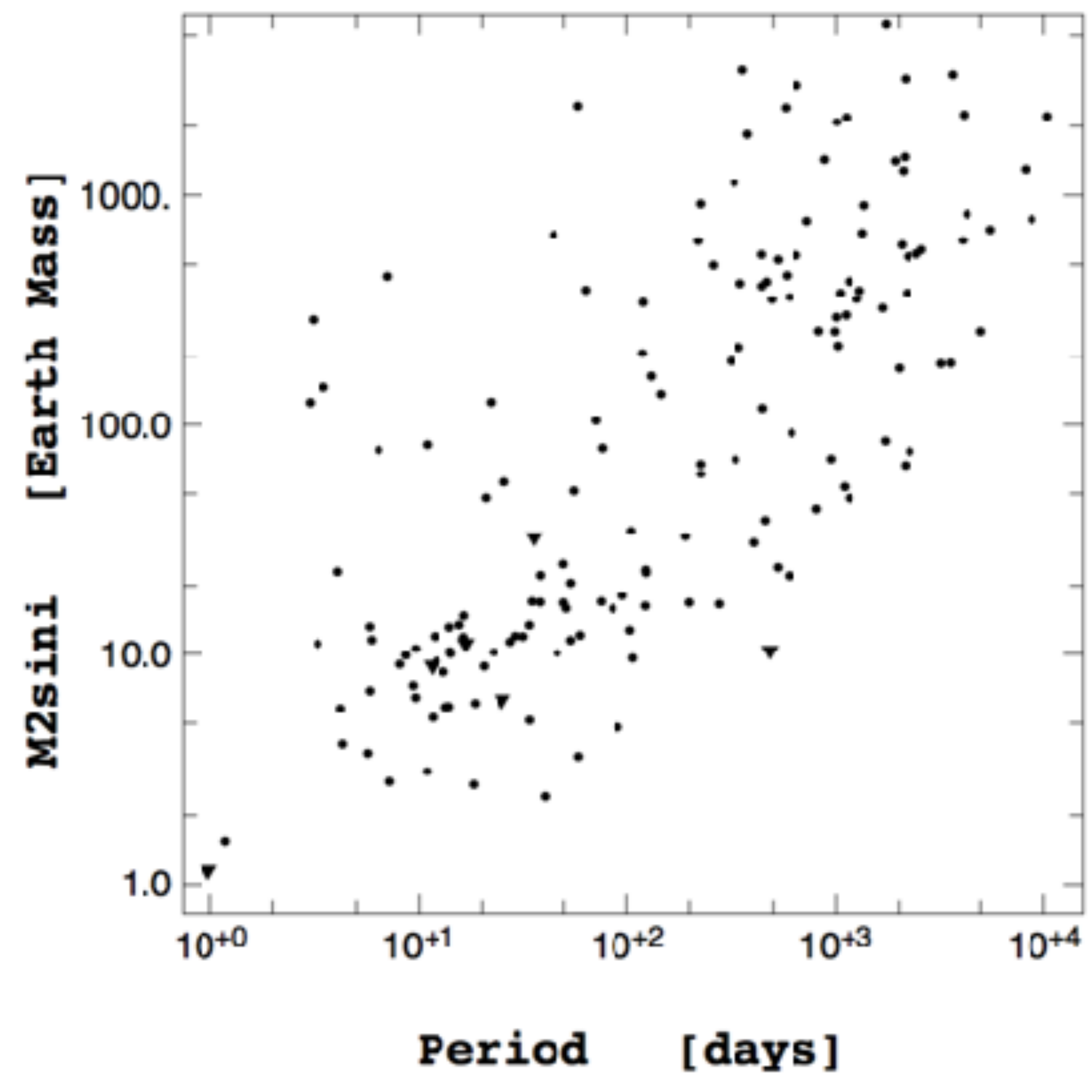

- HARPS: 8 yr, 376 stars
- CORALIE: 13 yr, 1650 stars

- >150 detections
- at the time, >80% of planets with K1<4m/s

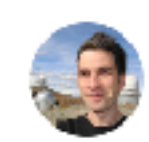

HARPS Mass-Period diagram

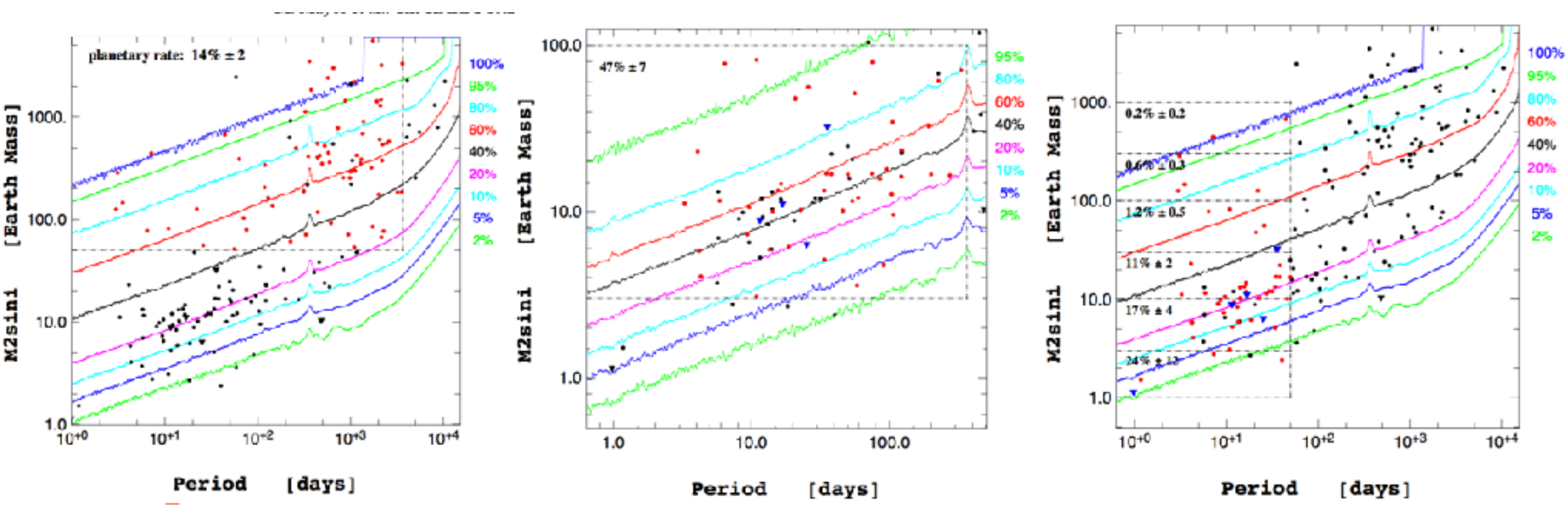

Mass limits	Period limit	Planetary rate based on published planets	Planetary rate including candidates	Comments
$> 50\ M_\oplus$	< 10 years	13.9 ± 1.7 %	13.9 ± 1.7 %	Gaseous giant planets
$> 100\ M_\oplus$	< 10 years	9.7 ± 1.3 %	9.7 ± 1.3 %	Gaseous giant planets
$> 50\ M_\oplus$	< 11 days	0.89 ± 0.36 %	0.89 ± 0.36 %	Hot gaseous giant planets
Any masses	< 10 years	65.2 ± 6.6 %	75.1 ± 7.4 %	All "detectable" planets with $P < 10$ years
Any masses	< 100 days	50.6 ± 7.4 %	57.1 ± 8.0 %	At least 1 planet with $P < 100$ days
Any masses	< 100 days	68.0 ± 11.7 %	68.9 ± 11.6 %	F and G stars only
Any masses	< 100 days	41.1 ± 11.4 %	52.7 ± 13.2 %	K stars only
$< 30\ M_\oplus$	< 100 days	47.9 ± 8.5 %	54.1 ± 9.1 %	Super-Earths and Neptune-mass planets on tight orbits
$< 30\ M_\oplus$	< 50 days	38.8 ± 7.1 %	45.0 ± 7.8 %	As defined in Lovis et al. (2009)

HARPS Mass and Period histograms

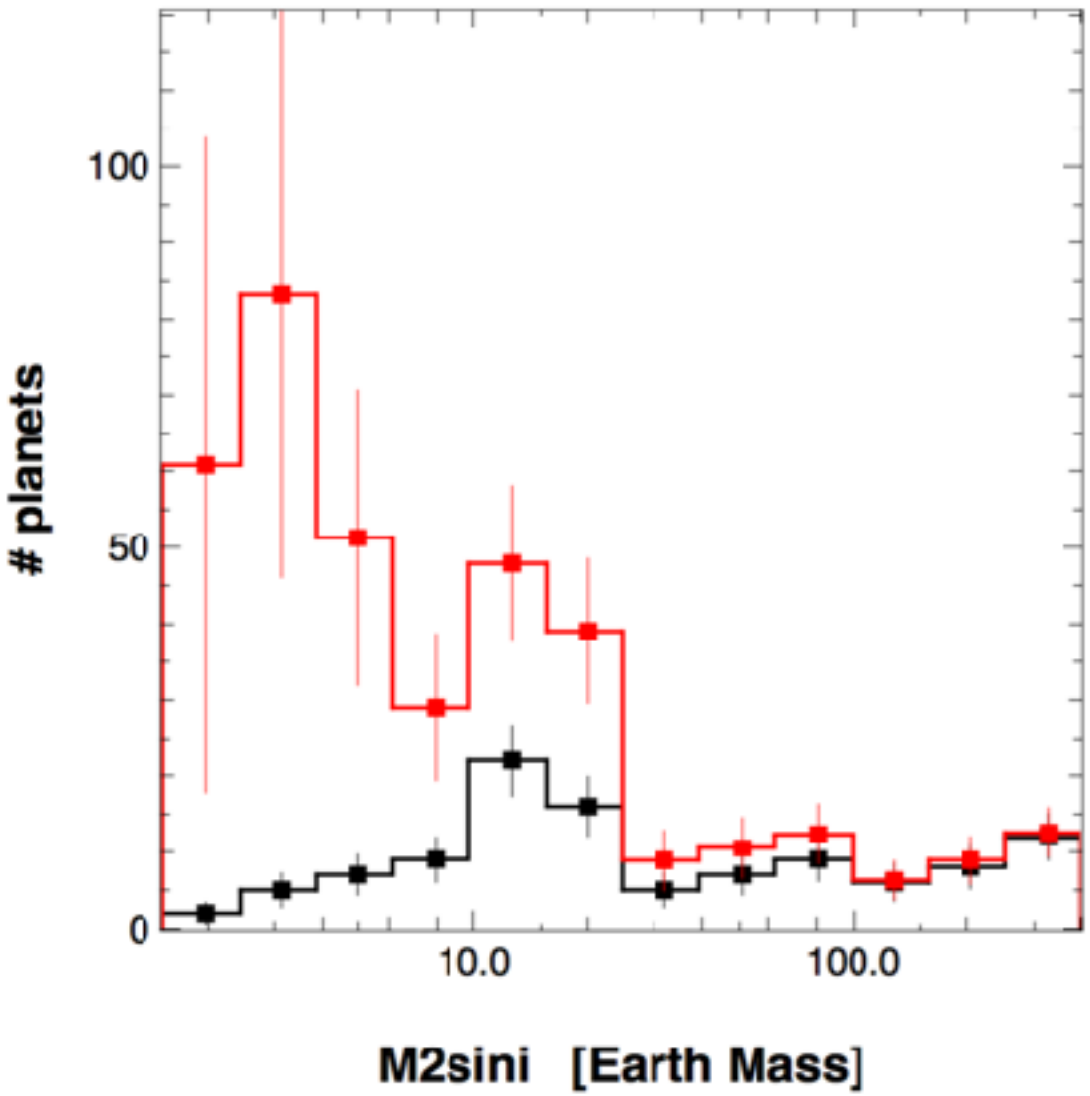

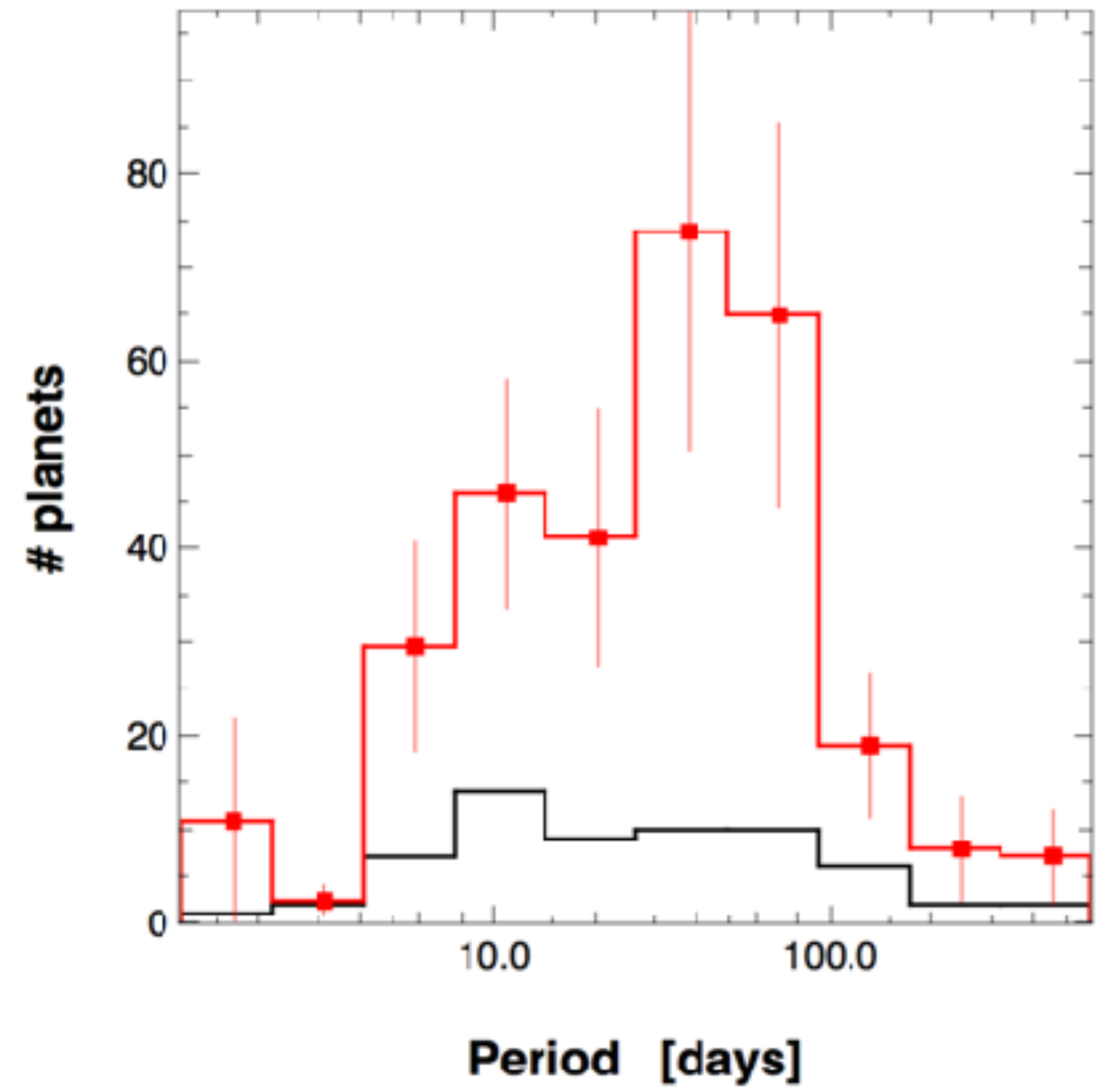

HARPS Multiplicity

- m sin i < 30 Mearth: multiplicity > 70%
- m sin i > 30 Mearth: multiplicity ~ 25%

HARPS [Fe/H] distributions

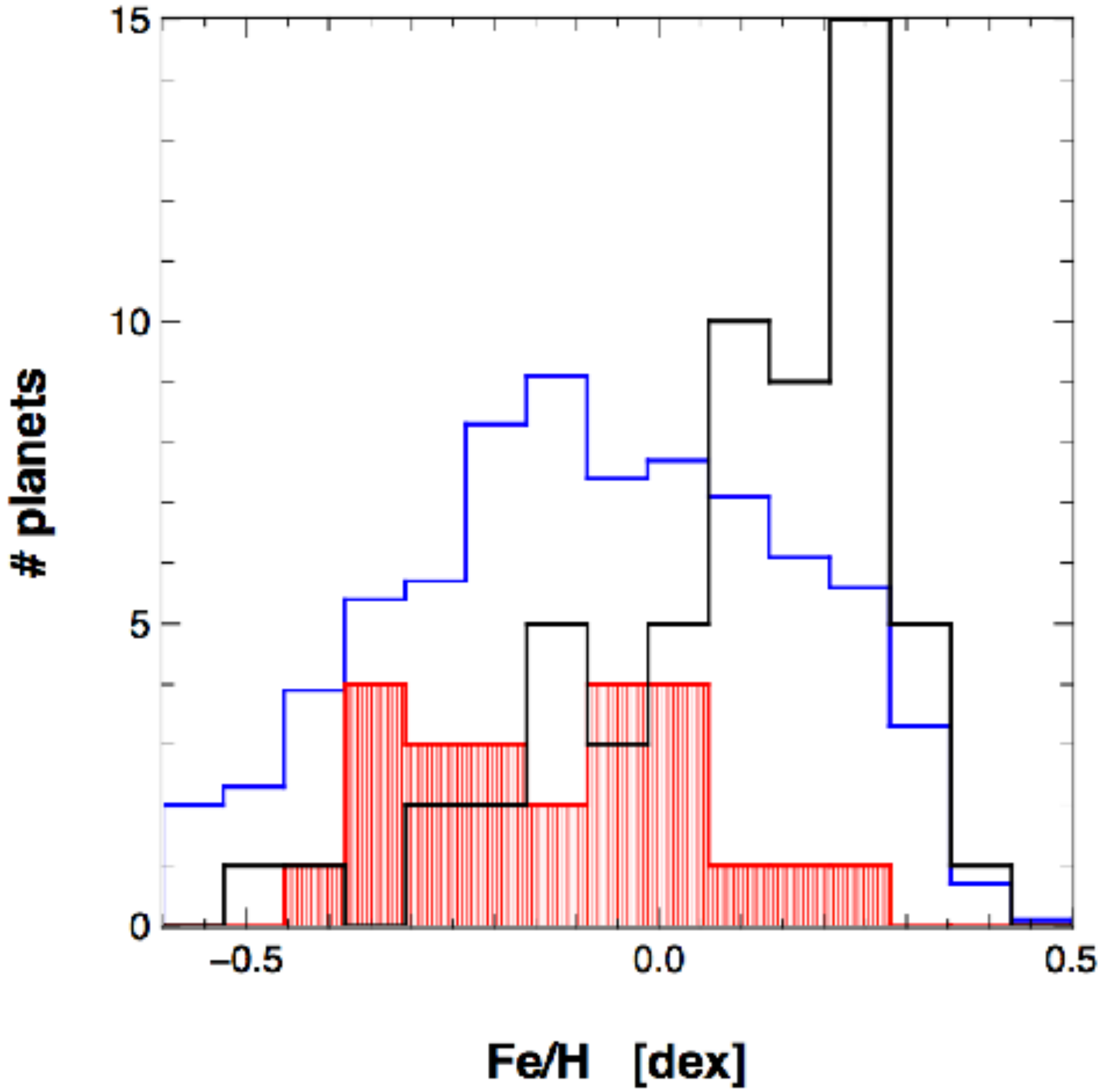

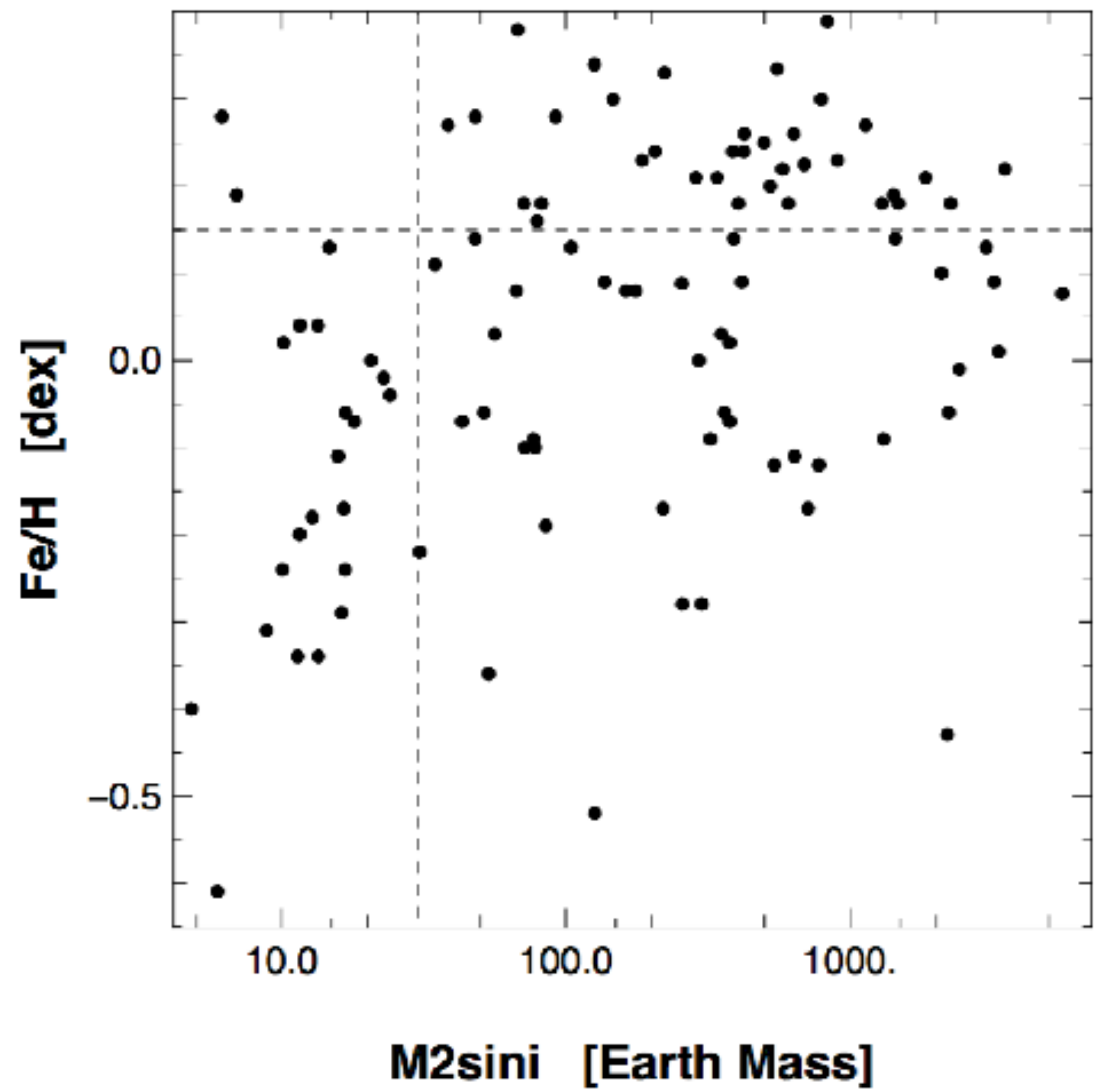

- m sin i > 30 Mearth => planet-metallicity correlation
- m sin i < 30 Mearth => occurrence not correlated w/ [Fe/H]

The HARPS search for southern extra-solar planets*

XXXI. The M-dwarf sample

X. Bonfils[1,2], X. Delfosse[1], S. Udry[2], T. Forveille[1], M. Mayor[2], C. Perrier[1], F. Bouchy[3,4], M. Gillon[5,2], C. Lovis[2], F. Pepe[2], D. Queloz[2], N. C. Santos[6], D. Ségransan[2], and J.-L. Bertaux[7]

Bonfils et al. (2013)
astro-ph/1109.2497

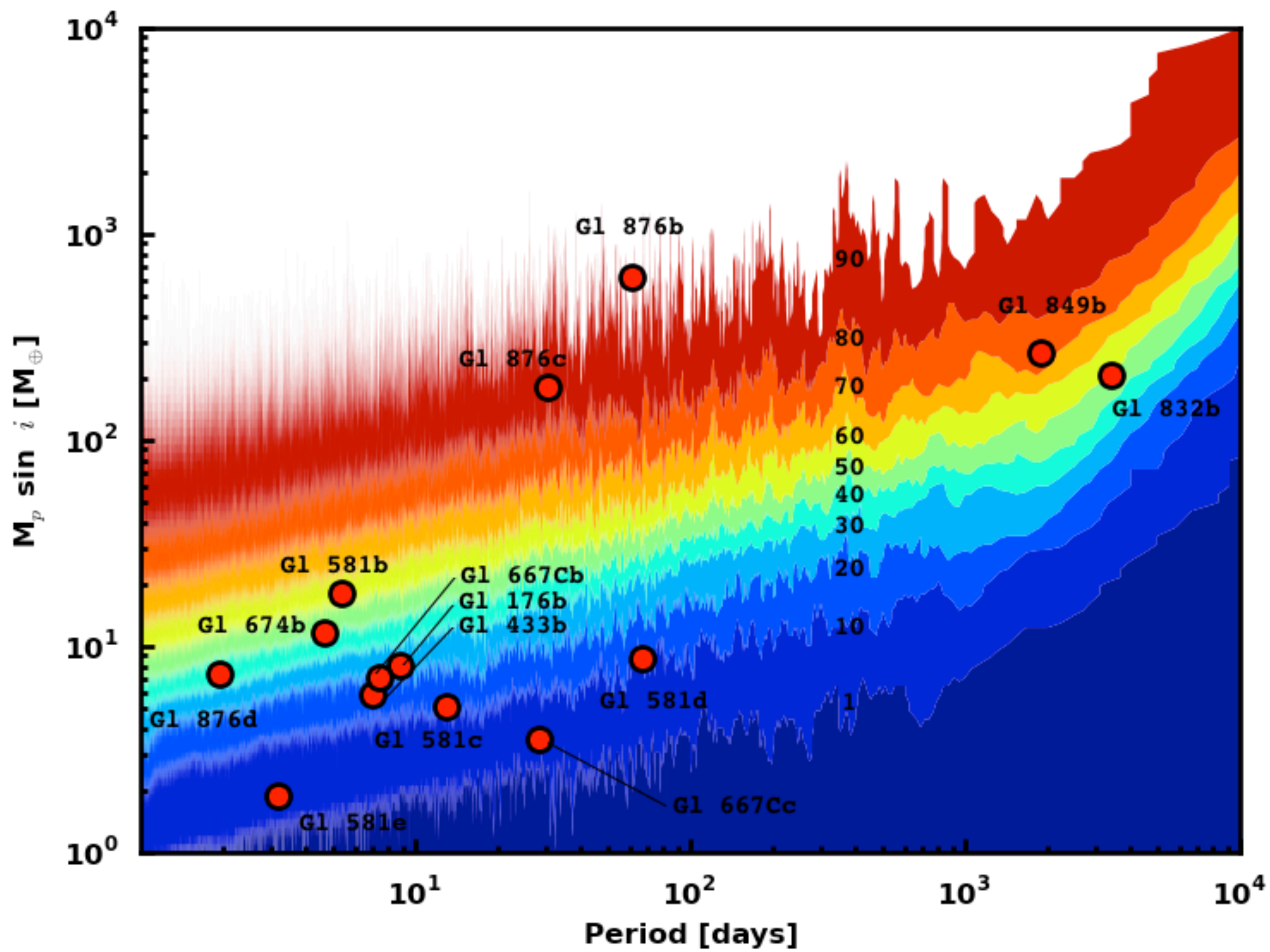

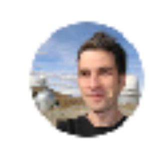

The HARPS search for southern extra-solar planets*

XXXI. The M-dwarf sample

X. Bonfils[1,2], X. Delfosse[1], S. Udry[2], T. Forveille[1], M. Mayor[2], C. Perrier[1], F. Bouchy[3,4], M. Gillon[5,2], C. Lovis[2], F. Pepe[2], D. Queloz[2], N. C. Santos[6], D. Ségransan[2], and J.-L. Bertaux[7]

Bonfils et al. (2013)
astro-ph/1109.2497

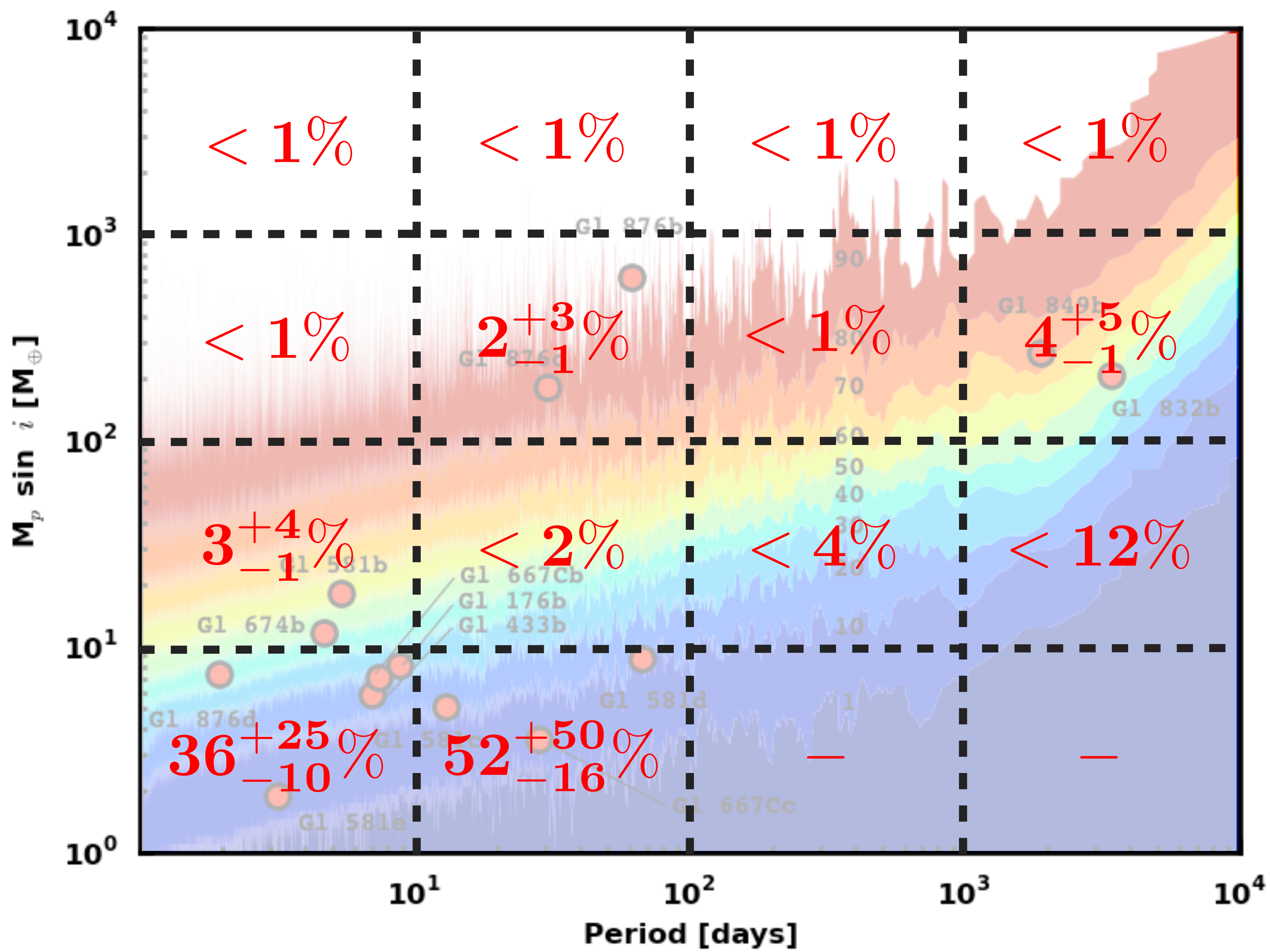

Xavier Bonfils

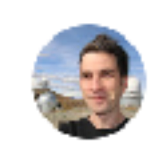

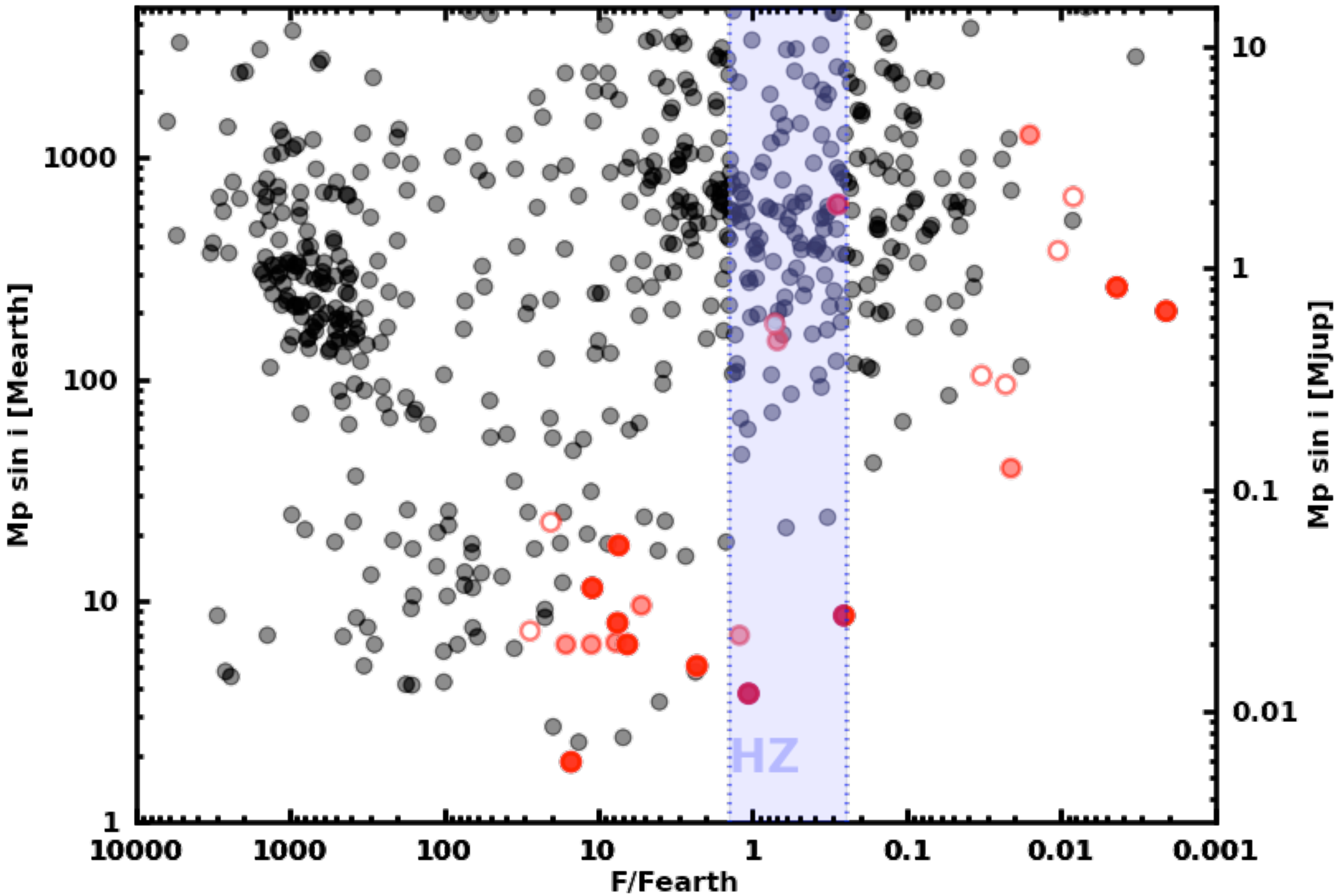

$$\eta_{\oplus} = 0.41^{+0.54}_{-0.13}$$

revised to 30% with GJ581d lost to activity (Robertson et al. 2014)

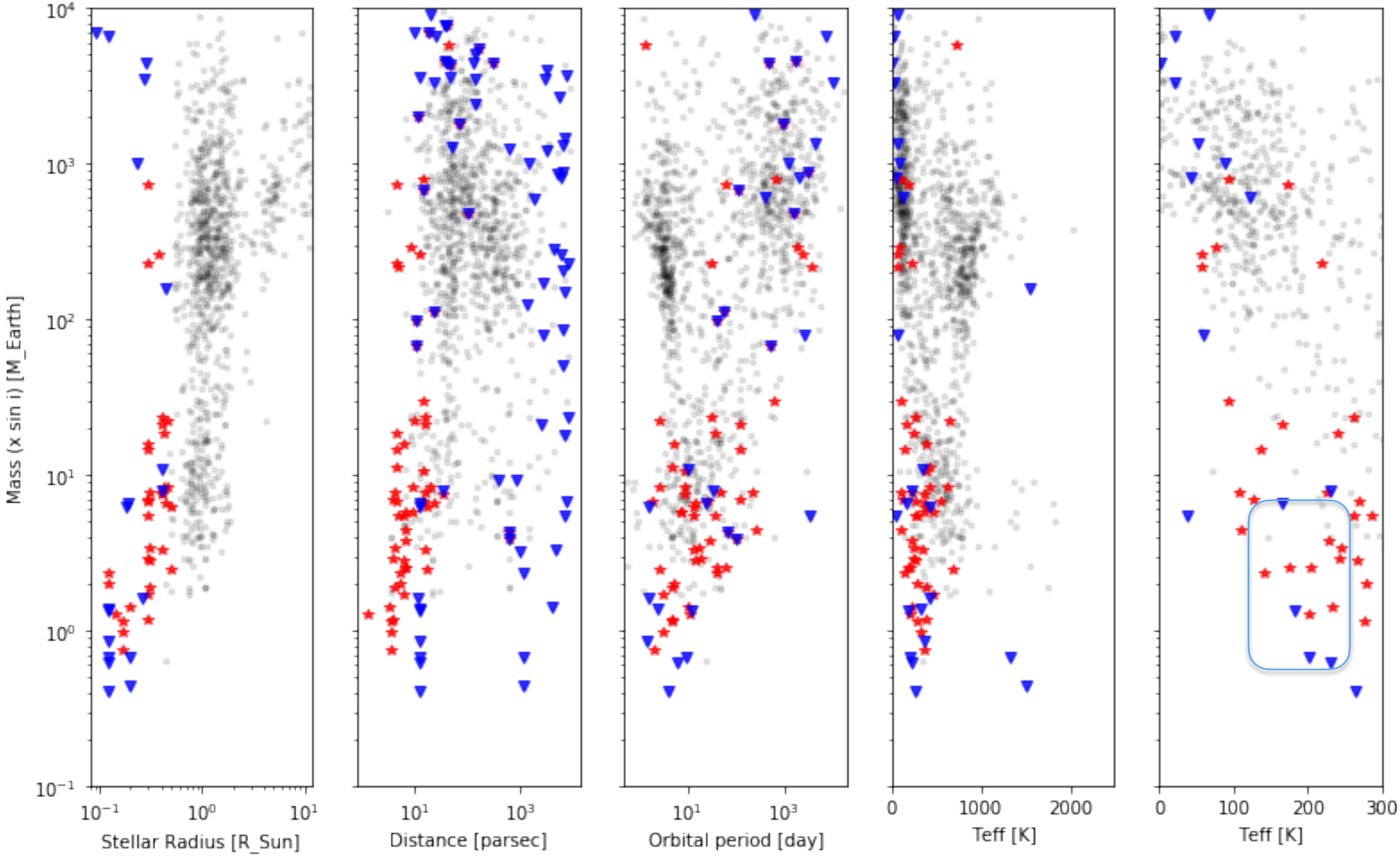

Xavier BONFILS

HIRES @ Keck

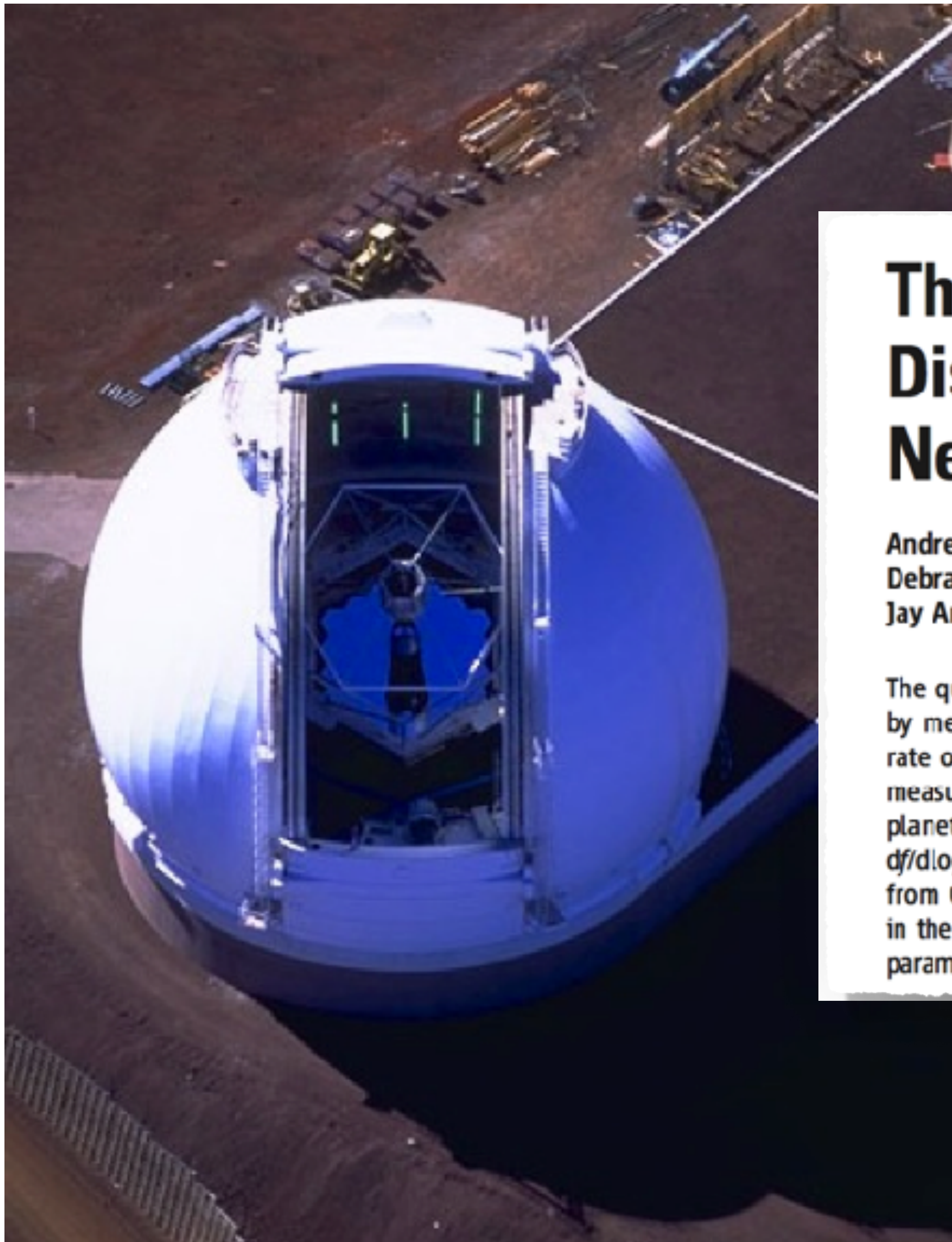

The Occurrence and Mass Distribution of Close-in Super-Earths, Neptunes, and Jupiters

Andrew W. Howard,[1,2]* Geoffrey W. Marcy,[1] John Asher Johnson,[3] Debra A. Fischer,[4] Jason T. Wright,[5] Howard Isaacson,[1] Jeff A. Valenti,[6] Jay Anderson,[6] Doug N. C. Lin,[7,8] Shigeru Ida[9]

The questions of how planets form and how common Earth-like planets are can be addressed by measuring the distribution of exoplanet masses and orbital periods. We report the occurrence rate of close-in planets (with orbital periods less than 50 days), based on precise Doppler measurements of 166 Sun-like stars. We measured increasing planet occurrence with decreasing planet mass (M). Extrapolation of a power-law mass distribution fitted to our measurements, $df/d\log M = 0.39\,M^{-0.48}$, predicts that 23% of stars harbor a close-in Earth-mass planet (ranging from 0.5 to 2.0 Earth masses). Theoretical models of planet formation predict a deficit of planets in the domain from 5 to 30 Earth masses and with orbital periods less than 50 days. This region of parameter space is in fact well populated, implying that such models need substantial revision.

Difference	Keck-HIRES	HARPS/CORALIE
+1.1σ	1.6 ± 1.2 %	0.24 ± 0.17 %
+0.8σ	1.6 ± 1.2 %	0.58 ± 0.29 %
+0.3σ	1.6 ± 1.2 %	1.17 ± 0.52 %
+1.2σ	6.5 ± 3.0 %	11.1 ± 2.4 %
+0.8σ	11.8 ± 4.3 %	16.6 ± 4.4 %
		24 ± 12 %

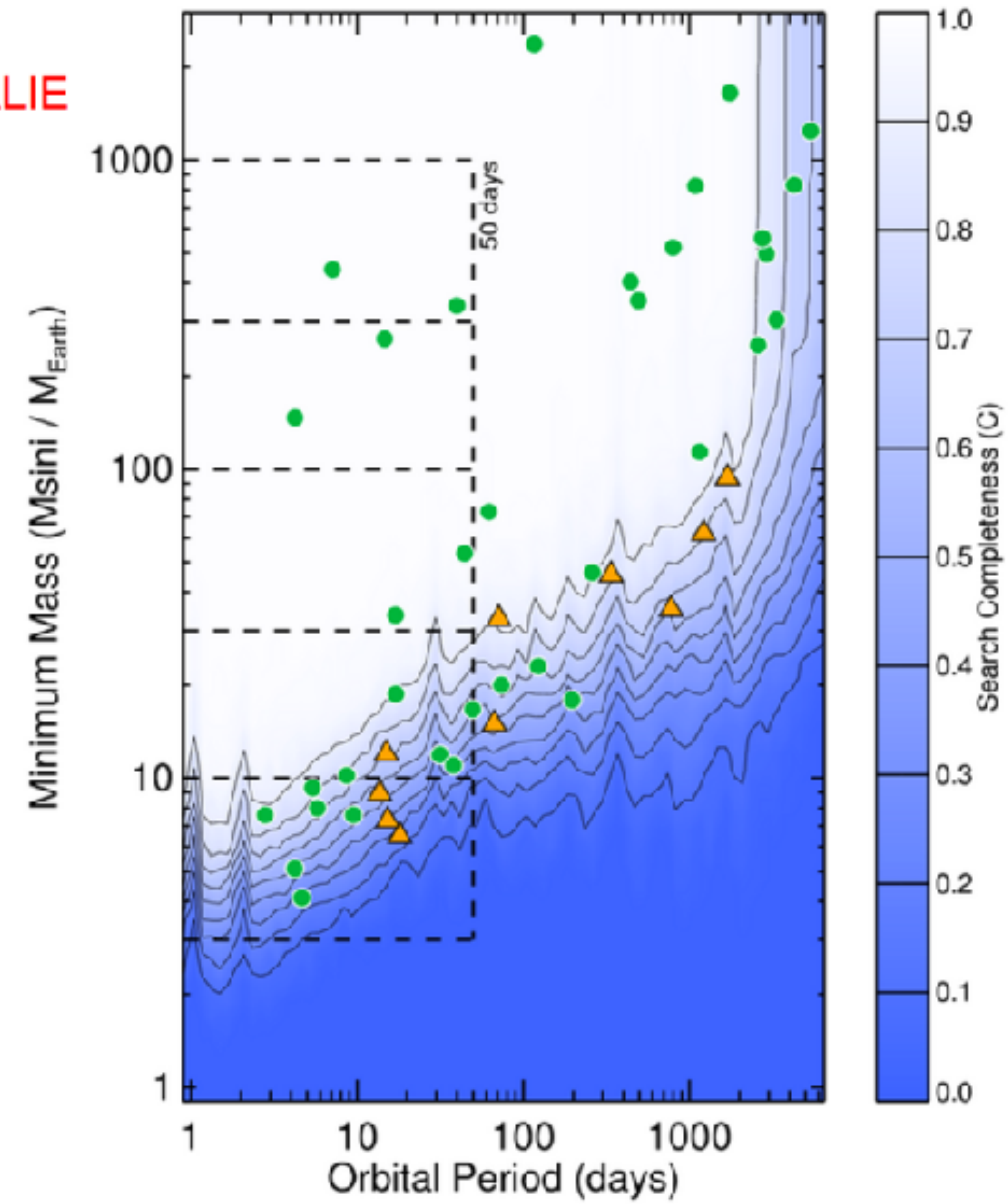

Howard et al. (2010)
Mayor et al. (2011)

slide from Howard et al. (http://www.ipac.caltech.edu/wfir2012/talks/howard_microlens.pdf)

Xavier Bonfils

Other M-dwarf stats from radial-velocity results

(mostly for giant planets)

Endl et al. (2006, AJ 649, 436)

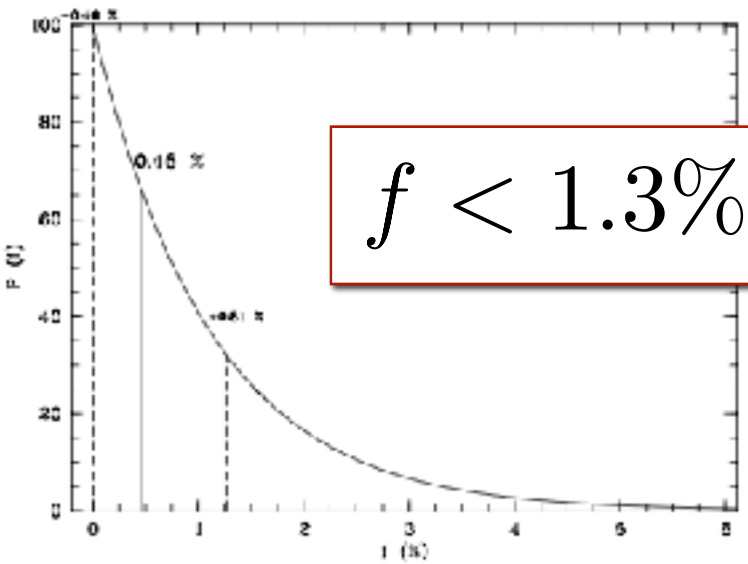

$$f < 1.3\% (1\ \sigma)$$

FIG. 2.—Probability function $P(f)$ for the true companion frequency f based on all our M dwarf data (HET, VLT, HJS, and Keck: $N = 89$ stars) and $d = 0$ detections. We find $f = 0.46^{+1.1}_{-0.46}$ percent. The dashed lines delimit the area of 68% integrated probability ($\pm 1\ \sigma$ Gaussian error).

Johnson et al. (2010, PASP)

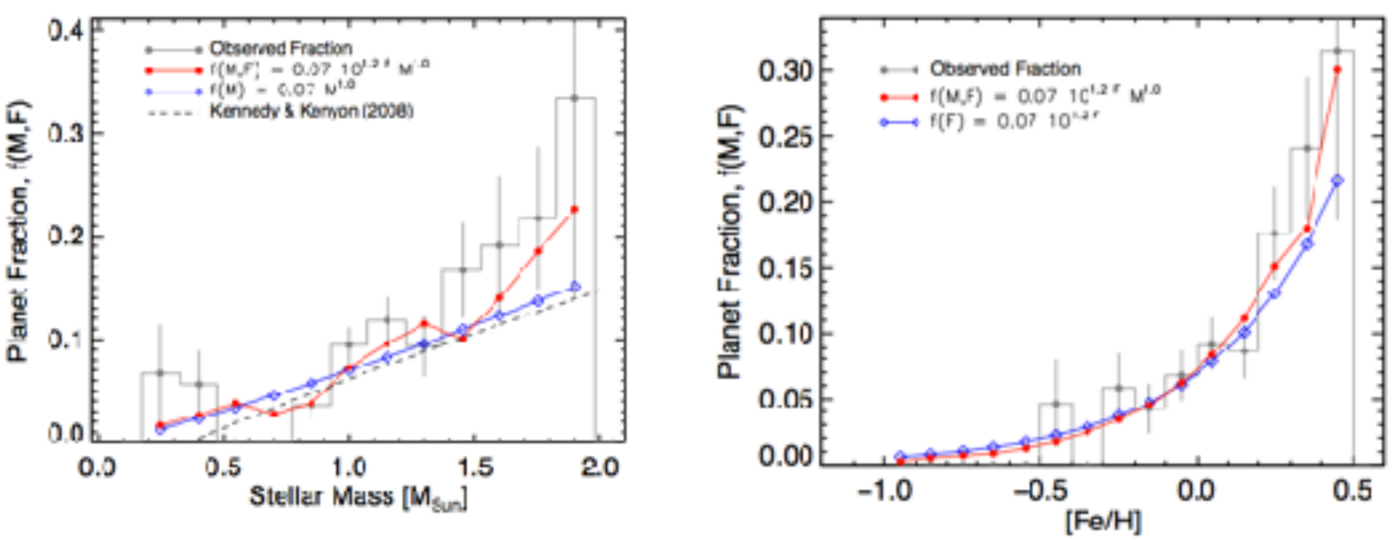

Butler et al. (2006, AJ 649, 436)

$$f = 1.8 \pm 1.2\% \ (> 0.4\ \mathrm{M_{Jup}}; < 2.5\mathrm{AU})$$

Cumming et al. (2008, PASP 120, 531)

> 1 Mjup are x5-10 times under abundant compared to Sun-like stars
f~1% (<5.4% @ 2-sigma)

Johnson et al. (2007, AJ 670, 833)

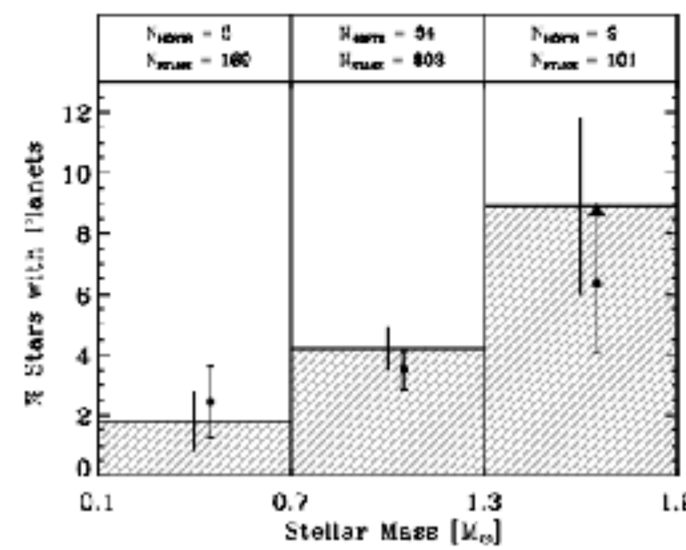

Bonfils et al. (2007, A&A 474, 293)

$$f_{\mathrm{hot\ Nept.}} > f_{\mathrm{hot\ Jup}}$$ (> 97% probability)

$$f(M_\star, [Fe/H]) = 0.07 \pm 0.01 \times (M_\star/M_\odot)^{1.0\pm0.3} \times 10^{1.2\pm0.2[Fe/H]}$$

(Selected) statistics from the Kepler mission

Xavier Bonfils

Howard et al. (2012)

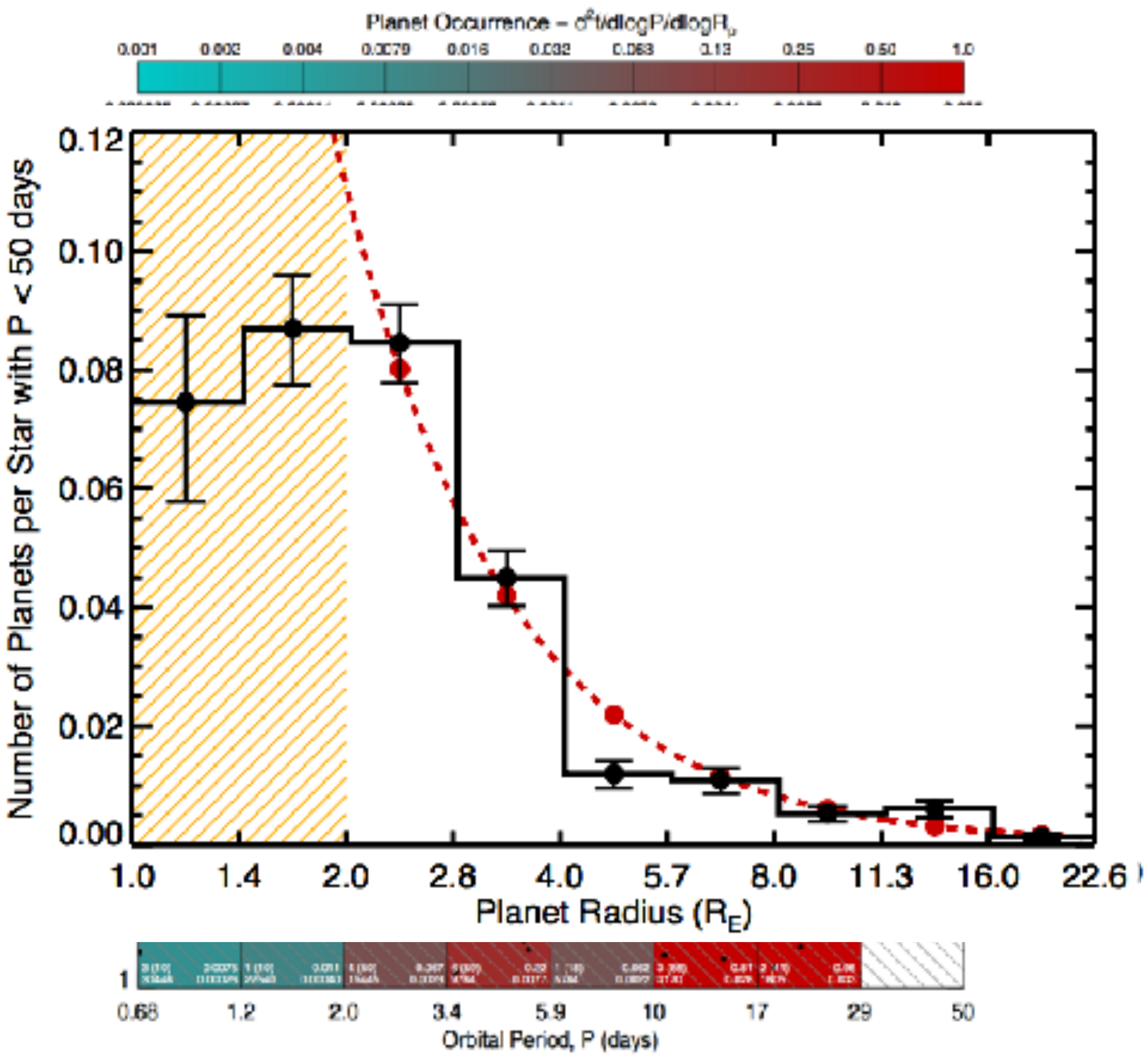

- Q0-Q2 data
- P<50 days
- assumes No false-positives

Morton & Johnson (2011); but see Sauterne et al. (2012)

- S/N threshold on completeness
- P,M distribution for GK dwarfs
- occurrence rate also for F-M

- f increases strongly with lower Rp
- f increases with P
  with some differences with Rp
- for small planets,
  f increases for decreasing Teff

- 0.1 pl./star with P<50d

see also
Batalha et a. (2011)
Cantazarite & Shao (2011)
Traub (2012)
Tremaine & Dong (2012)

Youdin (2011)

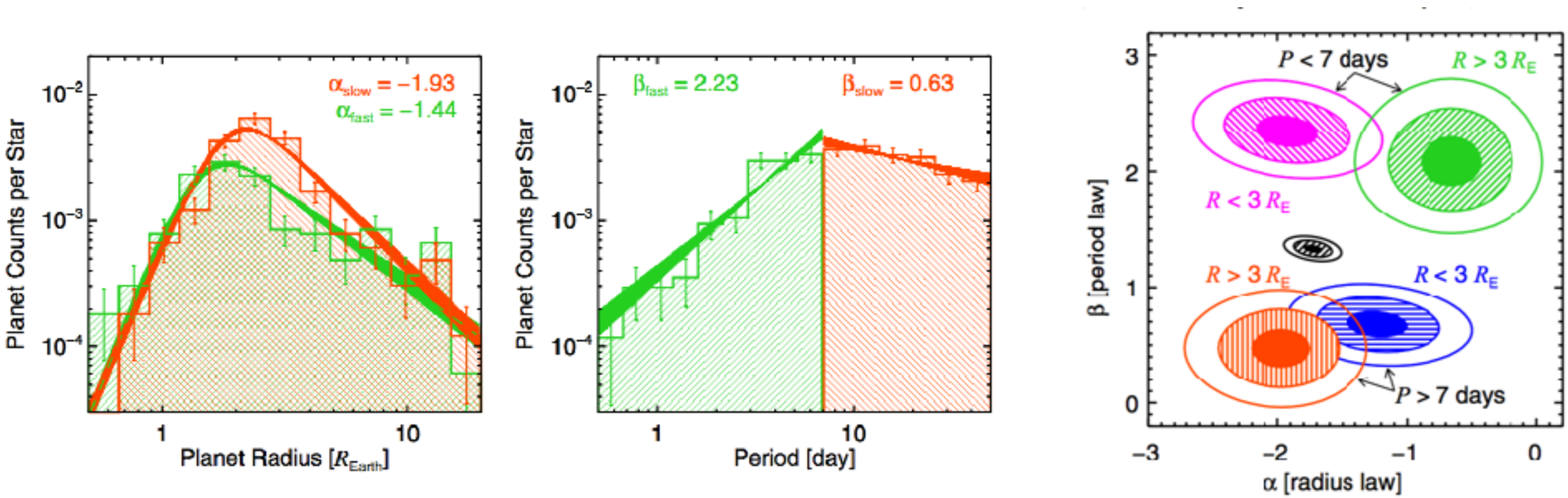

- same data & completeness
- add parameterization

- evidences for different population
- pl. occurrence x2

$$\frac{\partial f}{\partial \ln R \partial \ln P} = C \left(\frac{R}{R_o}\right)^{\alpha} \left(\frac{P}{P_o}\right)^{\beta}$$

Fressin et al. (2013)

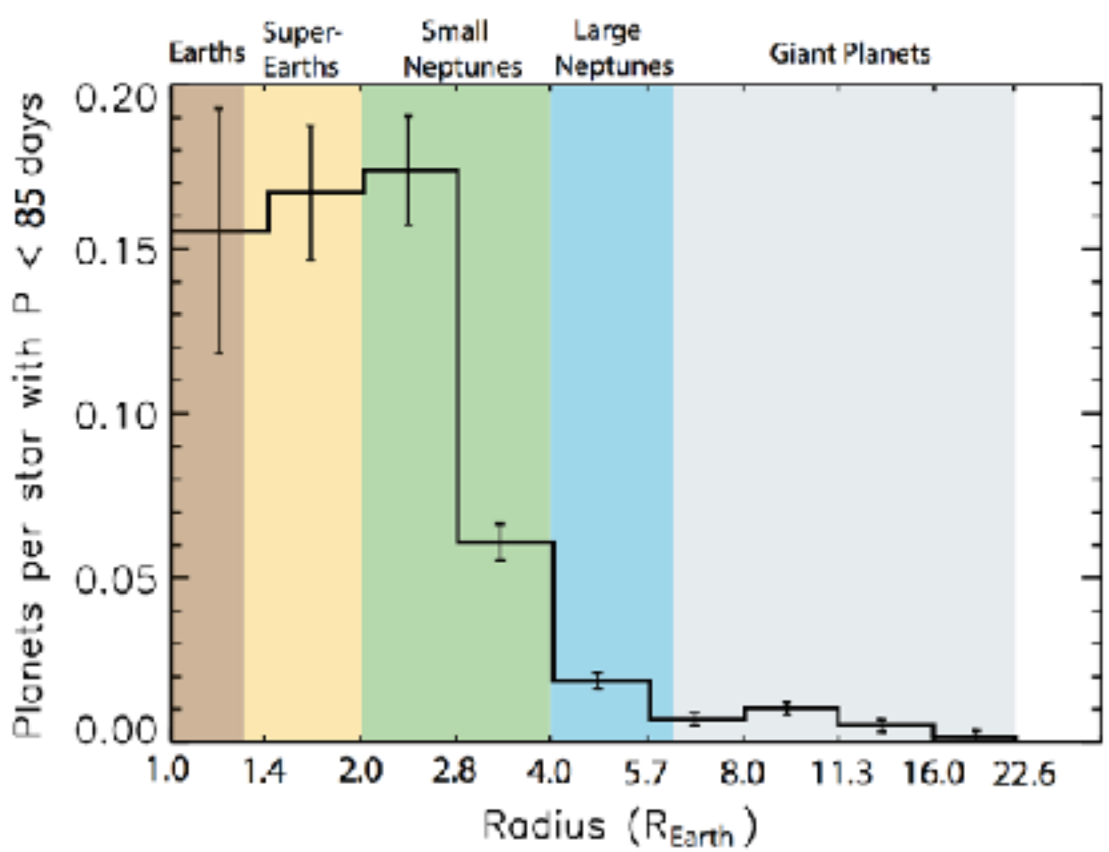

- Q1-Q6 data
- P<85 days
- GK dwarfs
- model the occurrence of both False-Positives and Planets
- completeness is a function of SNR

- FP rate is ~12% for Earth-size
- 16.5% +- 3.6% of GK stars have at least 1 pl. with P<85 d
- found no dependence w/ Teff

see also Dong & Zhu (2013)

Petigura, Howard & Marcy (2013)

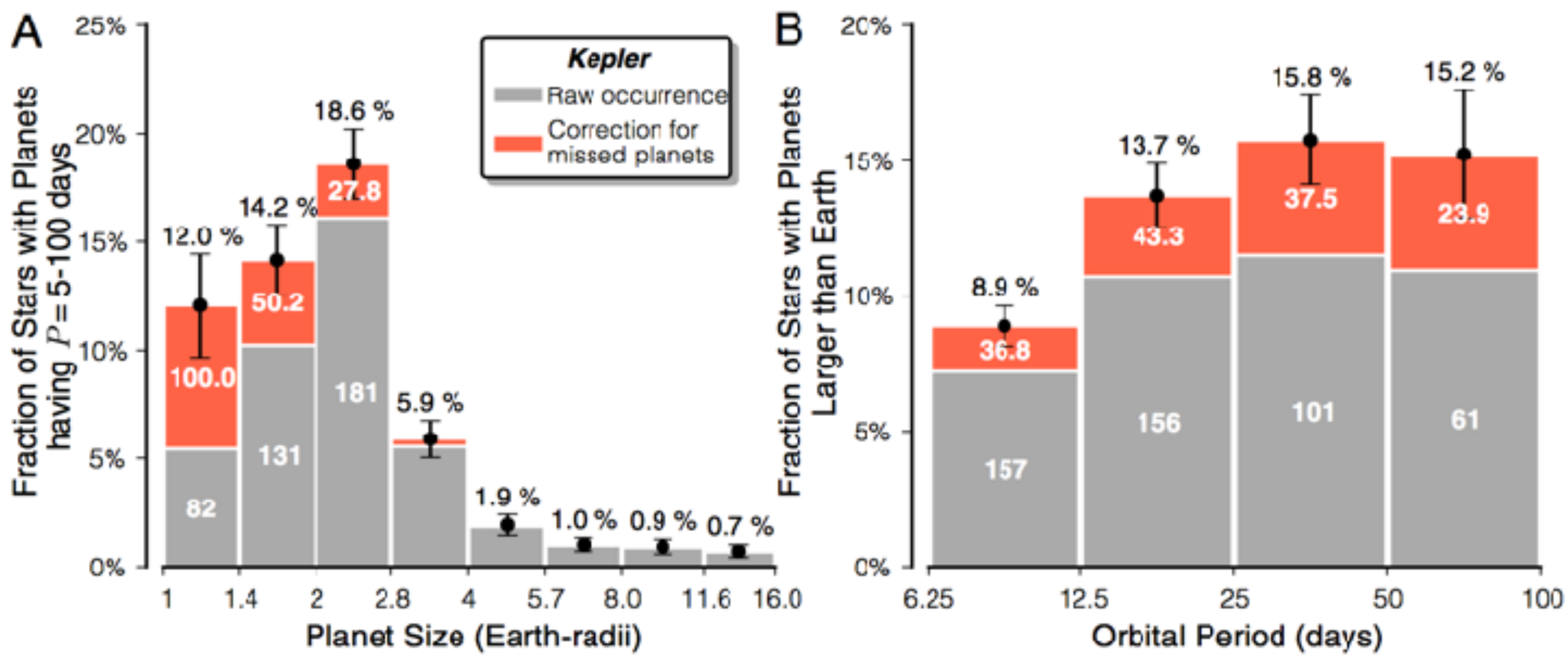

- sub-sample of 42’000 GK dwarfs
- Q1-Q16
- use their own pipeline

- extrapolate to 1-2 Rearth, with 0.25-4x Earth insolation : 22+-8%
- possible peak @ 2Rearth

Foreman-Mackey et al. (2014)

- same sample
- Gaussian process
- no False-Positives

- do not imposes a flat Period distribution
- includes uncertainties in planets and stellar radii

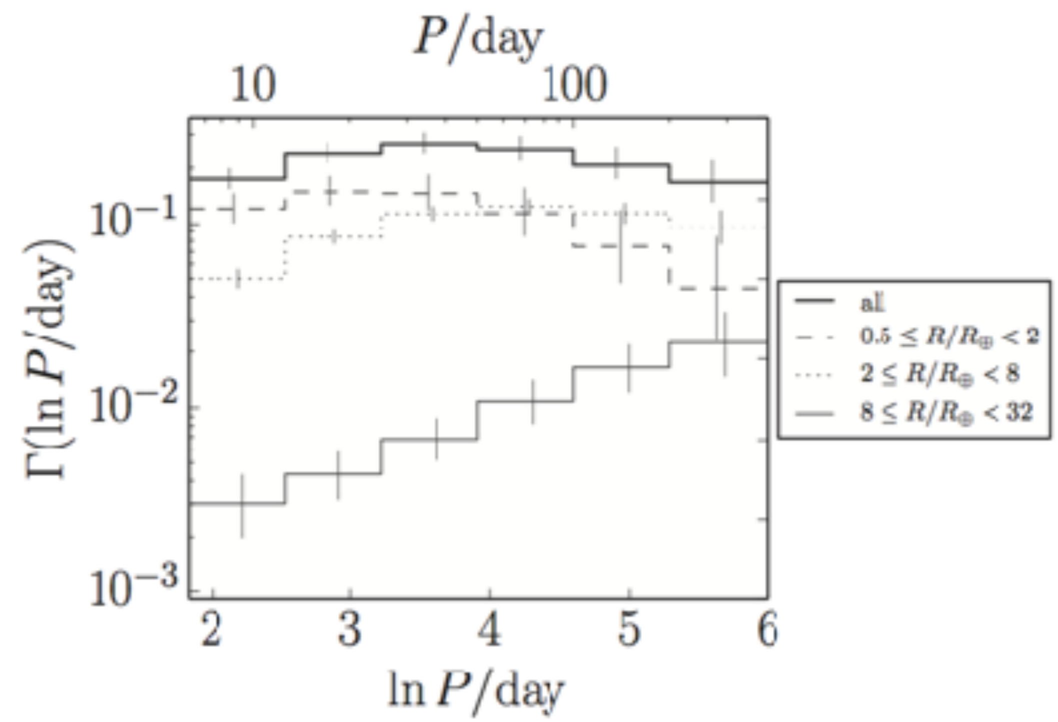

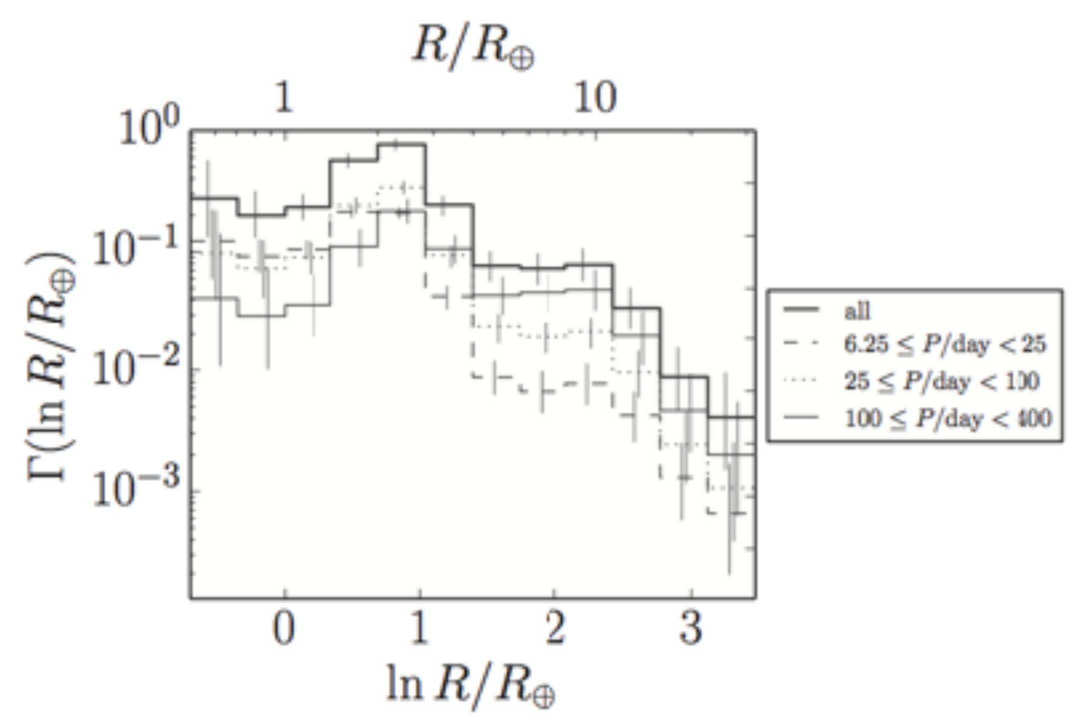

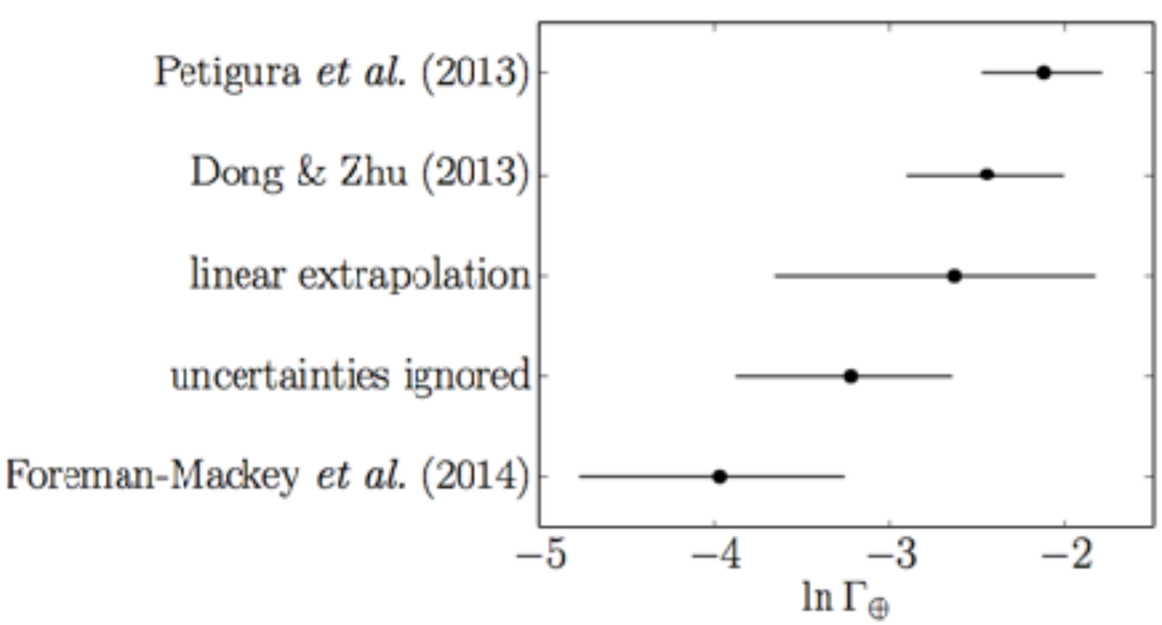

see also Burke et al. (2015)

Dressing & Charbonneau (2015)

see also Dressing & Charbonneau (2013)

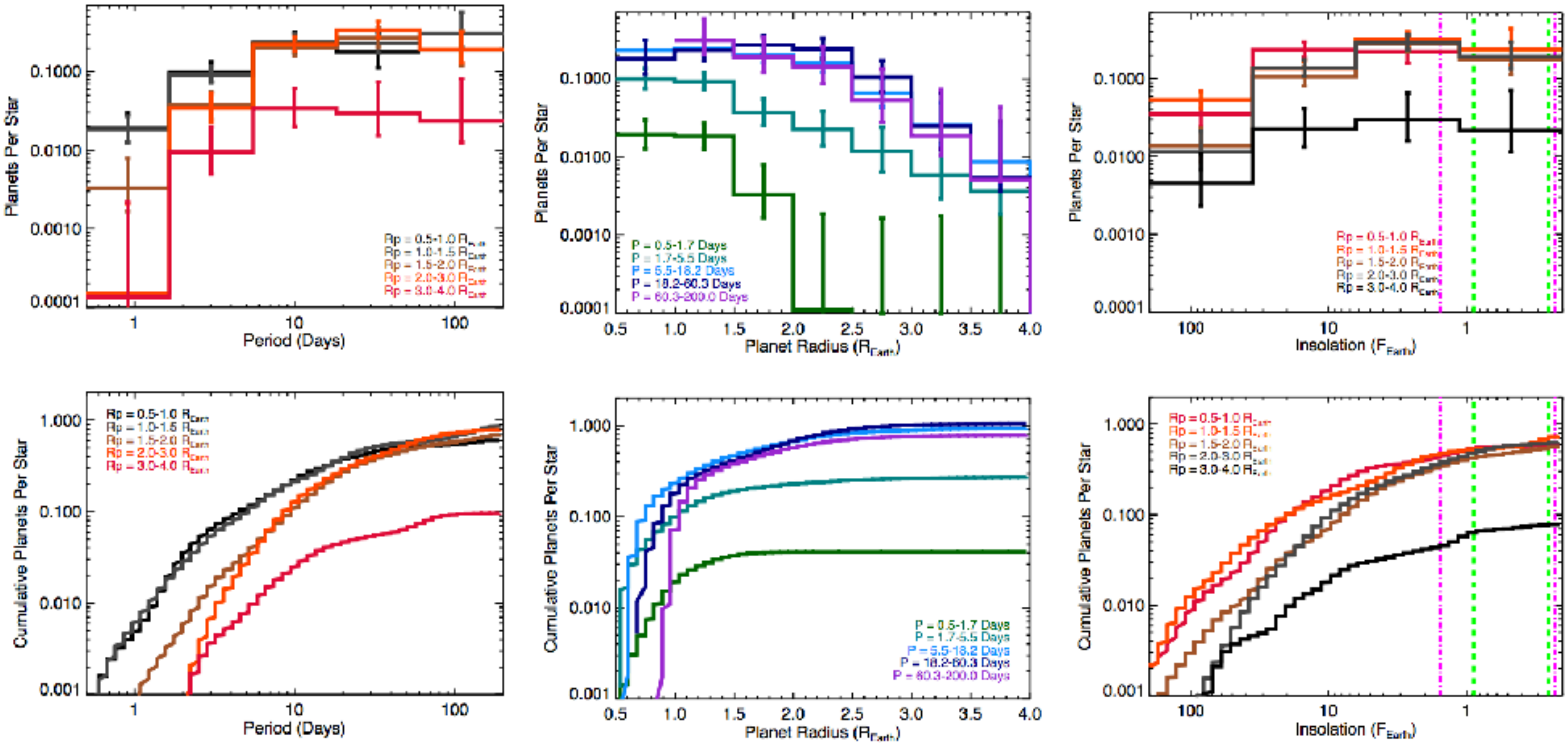

- M dwarfs
- Q0-Q17 data
- own pipeline for completeness
- re-determine stellar parameters

- 1.0-1.5Rearth; f=56%+-5%; P<50d
- 1.5-2.0Rearth; f=45+-6%; P<50d
- confirms that small planets on moderate orbital periods are very abundant

Xavier Bonfils

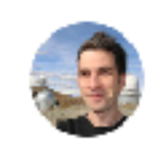

Dressing & Charbonneau (2015)

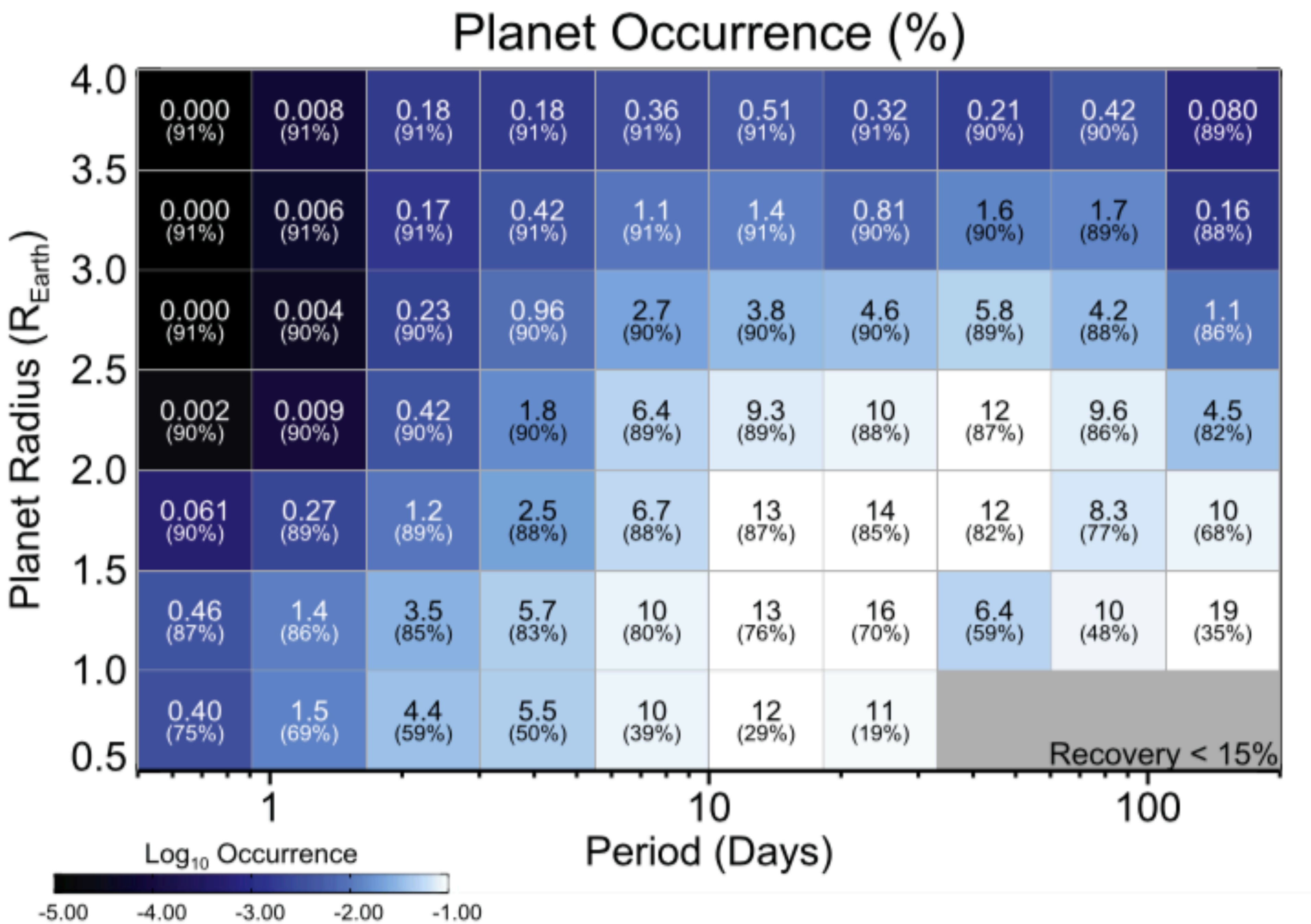

Xavier Bonfils

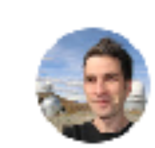

eta_earth summary

taken from a presentation of Charbonneau

http://www.eso.org/sci/meetings/2014/exoelt2014/presentations/Charbonneau.pdf

Number of Earths per HZ

Paper	Eta Earth	HZ Inner Edge	HZ Outer Edge	Planet Properties
Bonfils+ 2013	**0.41** (+0.54/-0.13)	Recent Venus (Selsis +2007)	Early Mars (Selsis+ 2007)	$1 < m \sin i < 10\ M_{Earth}$
Gaidos 2013	**0.46** (+0.18/-0.15)	50% Clouds (Selsis+ 2007)	50% Clouds (Selsis+ 2007)	$R_p > 0.8\ R_{Earth}$
Kopparapu 2013 (Conservative)	**0.48** (+0.12/-0.24)	Moist Greenhouse (Kopparapu+ 2013)	Max Greenhouse (Kopparapu+ 2013)	$0.5 < R_p < 1.4\ R_{Earth}$
Kopparapu 2013 (Optimistic)	**0.61** (+0.07/-0.15)	Recent Venus (Kopparapu+ 2013)	Early Mars (Kopparapu+ 2013)	$0.5 < R_p < 2\ R_{Earth}$
Dressing & Charbonneau 2013	**0.15** (+0.13/-0.06)	Water Loss (Kasting+ 1993)	CO_2 Condensation (Kasting+ 1993)	$0.5 < R_p < 1.4\ R_{Earth}$
Dressing & Charbonneau (in prep)	**0.56** (+0.32/-0.13)	Moist Greenhouse (Kopparapu+ 2013)	Max Greenhouse (Kopparapu+ 2013)	$0.5 < R_p < 1.4\ R_{Earth}$
Dressing & Charbonneau (in prep)	**0.66** (+0.25/-0.12)	Moist Greenhouse with Clouds (Yang+ 2013)	Max Greenhouse (Kopparapu+ 2013)	$0.5 < R_p < 1.4\ R_{Earth}$

Recent reference : between 0.37-0.88 pl/star depending on HZ
Bryson et al. 2020 arXiv:2010.14812

Where to place HZ limits makes most of the uncertainy !

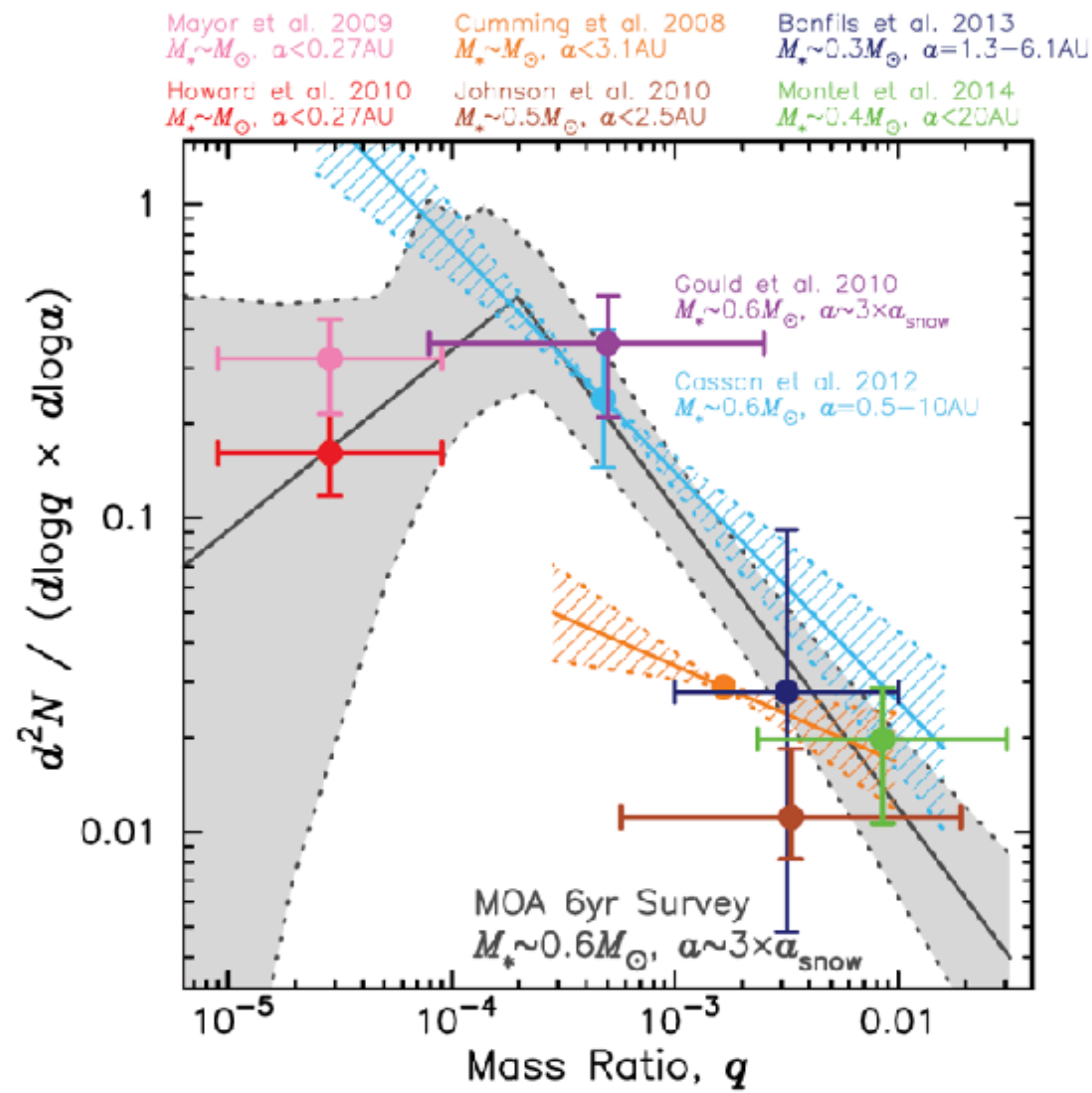

FIGURE 2.5 A broken power-law fit to the frequency of planets per log mass ratio q per log semimajor axis a, as a function of planet/star mass ratio q, as measured by the Microlensing Observations in Astrophysics (MOA) microlensing survey, is shown as the black dotted line. The uncertainty around this fit is shown as the gray shaded region. This frequency is compared to several other results on the frequency of planets in this plane using various methods and for various ranges of mass ratio and semimajor axis, as labeled. SOURCE: Suzuki et al. (2016).

https://exoplanetarchive.ipac.caltech.edu/docs/occurrence_rate_papers.html

NASA Exoplanet Archive
NASA Exoplanet Science Institute

Home | About Us | Data | Tools | Support | Login

Planet Occurrence Rate Papers

This page contains a compilation of published, refereed papers that derive planet occurrence rates. To suggest a paper for inclusion on this page, please submit a Helpdesk ticket.

Author(s) and Publication Year	Title	Publication
Kurimoto et al. (2021)	Combining Transit and Radial Velocity: A Synthesized Population Model	AJ 161 69
Bryson et al. (2021)	The Occurrence of Rocky Habitable-zone Planets around Solar-like Stars from Kepler Data	AJ 161 36
Poleski et al. (2021)	Wide-Orbit Exoplanets are Common. Analysis of Nearly 20 Years of OGLE Microlensing Survey Data	AcA 71 1
Jin, Sheng (2021)	Relative occurrence rates of terrestrial planets orbiting FGK stars	MNRAS 502 5302
Yang, Jia-Yi, Xie, Ji-Wei, & Zhou, Ji-Lin (2020)	Occurrence and Architecture of Kepler Planetary Systems as Functions of Stellar Mass and Effective Temperature	AJ 159 164
Bashi et al. (2020)	Occurrence rates of small planets from HARPS: Focus on the Galactic context	A&A 643 A106
Lu, Schlaufman, & Cheng (2020)	An Increase in Small-planet Occurrence with Metallicity for Late-type Dwarf Stars in the Kepler Field and Its Implications for Planet Formation	AJ 160 253
Bryson et al. (2020) CR	A Probabilistic Approach to Kepler Completeness and Reliability for Exoplanet Occurrence Rates	AJ 159 6
Kurimoto & Bryson (2020) CR	Comparing Approximate Bayesian Computation with the Poisson-Likelihood Method for Exoplanet Occurrence Rates	RNAAS 4 83
Kurimoto & Matthews (2020)	Searching the Entirety of Kepler Data. II. Occurrence Rate Estimates for FGK Stars	AJ 159 248
Bryson (2020)	Exoplanet Occurrence Rates of Mid M-dwarfs Based on Kepler DR25	RNAAS 4 3
Dai et al. (2019)	Planet Occurrence Rate Correlated to Stellar Dynamical History: Evidence from Kepler and Gaia	AJ 162 46
Bashi & Zucker (2019) CR	Small Planets in the Galactic Context: Host Star Kinematics, Iron, and Alpha-element Enhancement	AJ 158 61
Hsu, Ford, & Ragozzine (2019)	Occurrence Rates of Planets Orbiting FGK Stars: Combining Kepler DR25, Gaia DR2, and Bayesian Inference	AJ 158 109
He, Ford, & Ragozzine (2019)	Architectures of exoplanetary systems - I. A clustered forward model for exoplanetary systems around Kepler's FGK stars	MNRAS 490 4575
Herman, Zhu, & Wu (2019)	Revisiting the Long-period Transiting Planets from Kepler	AJ 157 248
Kawahara & Masuda (2019)	Transiting Planets Near the Snow Line from Kepler. I. Catalog	AJ 157 218
Mulders et al. (2019)	The Exoplanet Population Observation Simulator. II. Population Synthesis in the Era of Kepler	ApJ 887 157
Grunblatt et al. (2019)	Giant planet occurrence within 0.2 au of low-luminosity red giant branch stars with K2	AJ 158 227
Fernandes et al. (2019)	Hints for a Turnover at the Snow Line in the Giant Planet Occurrence Rate	ApJ 874 81
Hardegree-Ullman et al. (2019)	Kepler Planet Occurrence Rates for Mid-type M Dwarfs as a Function of Spectral Type	AJ 158 75
Bryan et al. (2018)	An Excess of Jupiter Analogs in Super-Earth Systems	AJ 157 52
van Sluijs, L. and Van Eylen, V. (2018)	The occurrence of planets and other substellar bodies around white dwarfs using K2	MNRAS 474 4603
Mulders et al. (2018)	The Exoplanet Population Observation Simulator. I. The Inner Edges of Planetary Systems	AJ 156 24
Pascucci et al. (2018)	A Universal Break in the Planet-to-star Mass-ratio Function of Kepler MKG Stars	ApJ 856L 28
Narang et al. (2018)	Properties and occurrence rates of Kepler exoplanet candidates as a function of host star metallicity from the DR25 catalog	AJ 156 24
Meyer et al. (2018)	M Dwarf Exoplanet Surface Density Distribution: A Log-Normal Fit from 0.07-400 au	A&A 612 L3
Zhu et al. (2018)	About 30% of Sun-like Stars Have Kepler-like Planetary Systems: A Study of their Intrinsic Architecture	ApJ 860 101

Xavier BONFILS

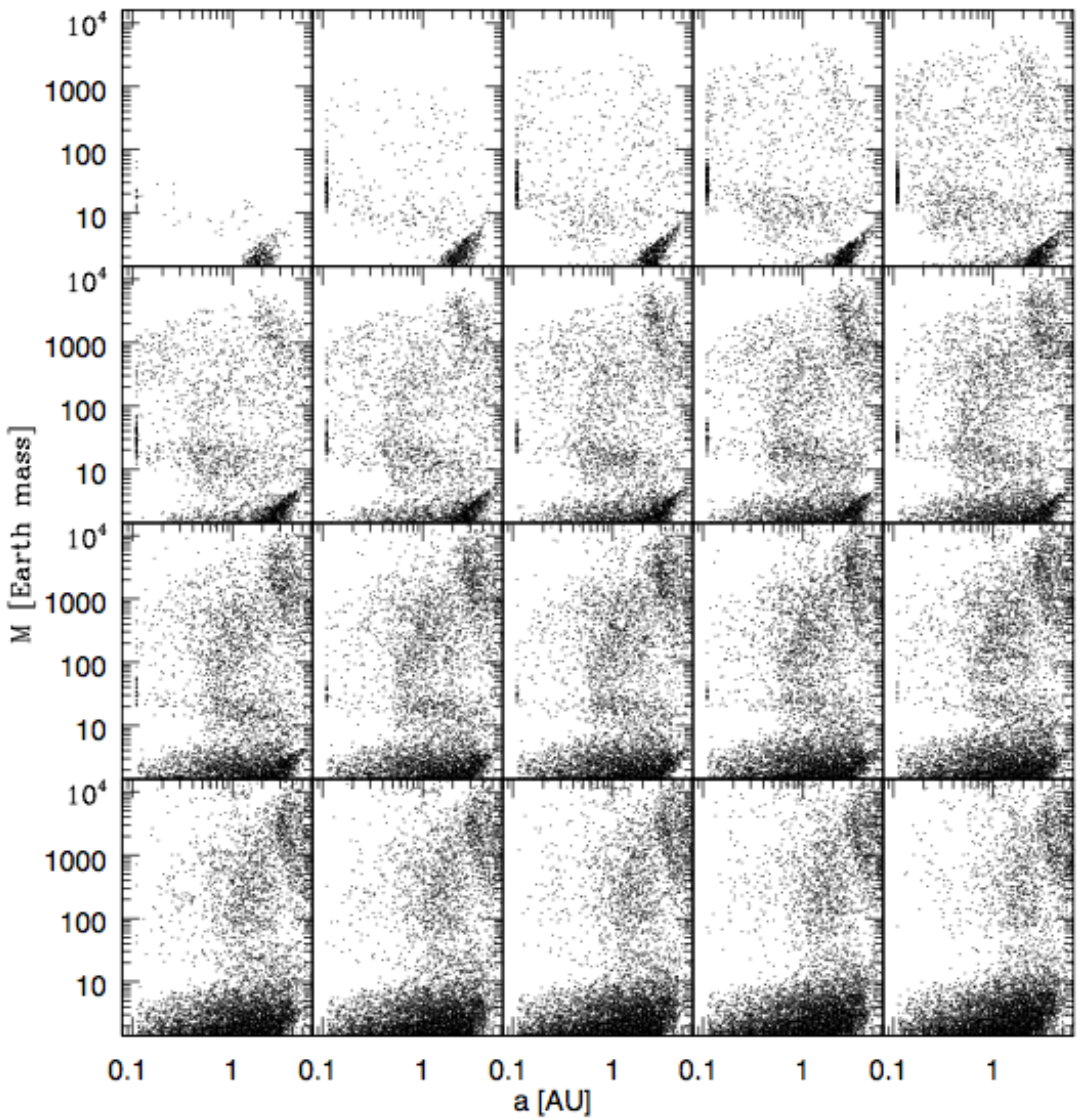

Fig. 12. Mass *versus* semi-major axis for stars between 0.1 $M_\odot$ and 2.0 $M_\odot$. The α_D parameter is equal to 1.2, and disk lifetime are reduced for stars more massive than 1.5 $M_\odot$. 30000 stars are considered in each panel. First line, from left to right, masses between 0.1 $M_\odot$ and 0.5 $M_\odot$, second line, from left to right, masses between 0.6 $M_\odot$ and 1.0 $M_\odot$, third line, from left to right, masses between 1.1 $M_\odot$ and 1.5 $M_\odot$ fourth line, from left to right, masses between 1.6 $M_\odot$ and 2.0 $M_\odot$.

Ida & Lin (2005)

Laughlin et al. (2004)

Kennedy & Kenyon (2008)

Alibert, Mordasini & Benz (2011)

=>matches roughly the theoretical predictions

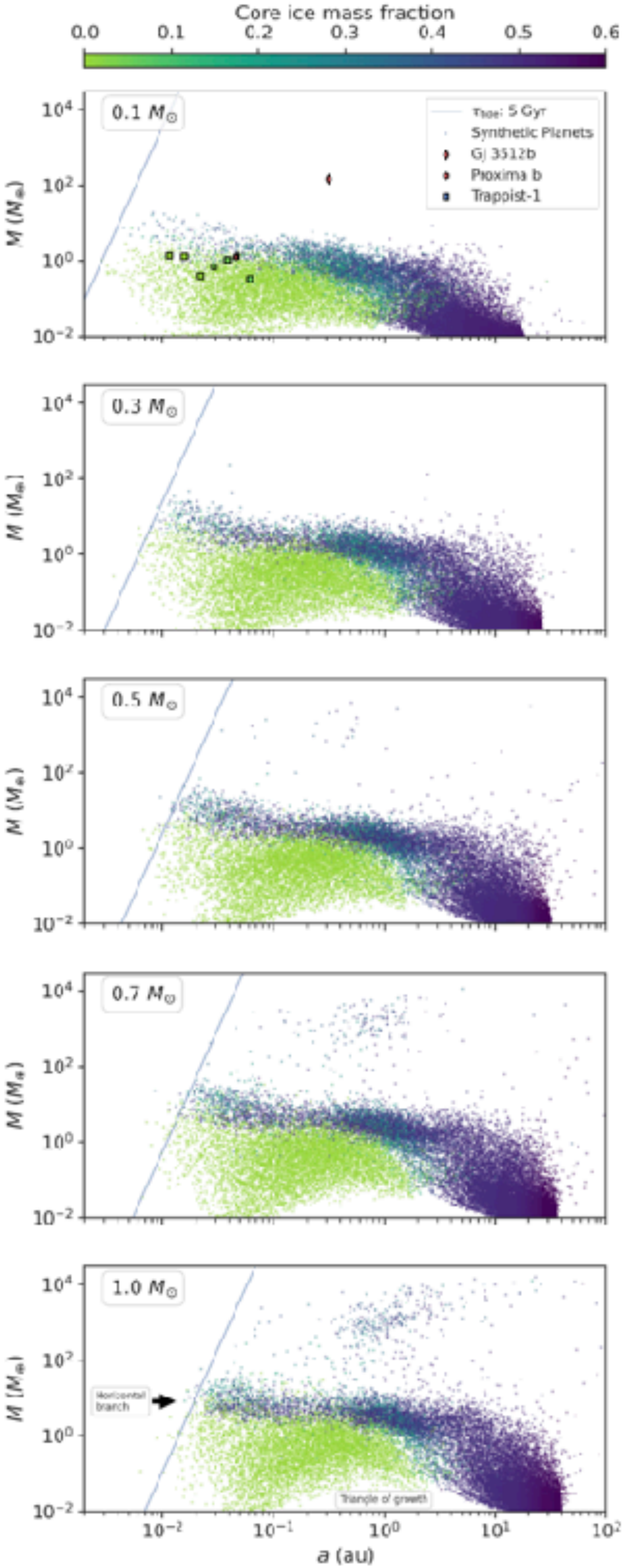

The New Generation Planetary Population Synthesis (NGPPS)

IV. Planetary systems around low-mass stars★

R. Burn[1,2], M. Schlecker[2], C. Mordasini[1], A. Emsenhuber[1,3], Y. Alibert[1], T. Henning[2], H. Klahr[2] and W. Benz[1]

Table 3. Fraction of systems with specific planetary types for the different stellar mass populations with initially 50 lunar-mass embryos

	Stellar mass ($M_\odot$)				
Type	0.1	0.3	0.5	0.7	1.0
$M > 1\ M_\oplus$	0.44	0.77	0.88	0.91	0.95
Earth-like	0.70	0.88	0.89	0.89	0.84
Super Earth	0.19	0.54	0.71	0.78	0.79
Neptunian	0.01	0.08	0.17	0.22	0.27
Sub-giant	0.00	0.00	0.02	0.03	0.05
Giant	0.00	0.00	0.02	0.09	0.19
Temperate zone	0.35	0.66	0.70	0.66	0.57

Combination : Mass-radius relations

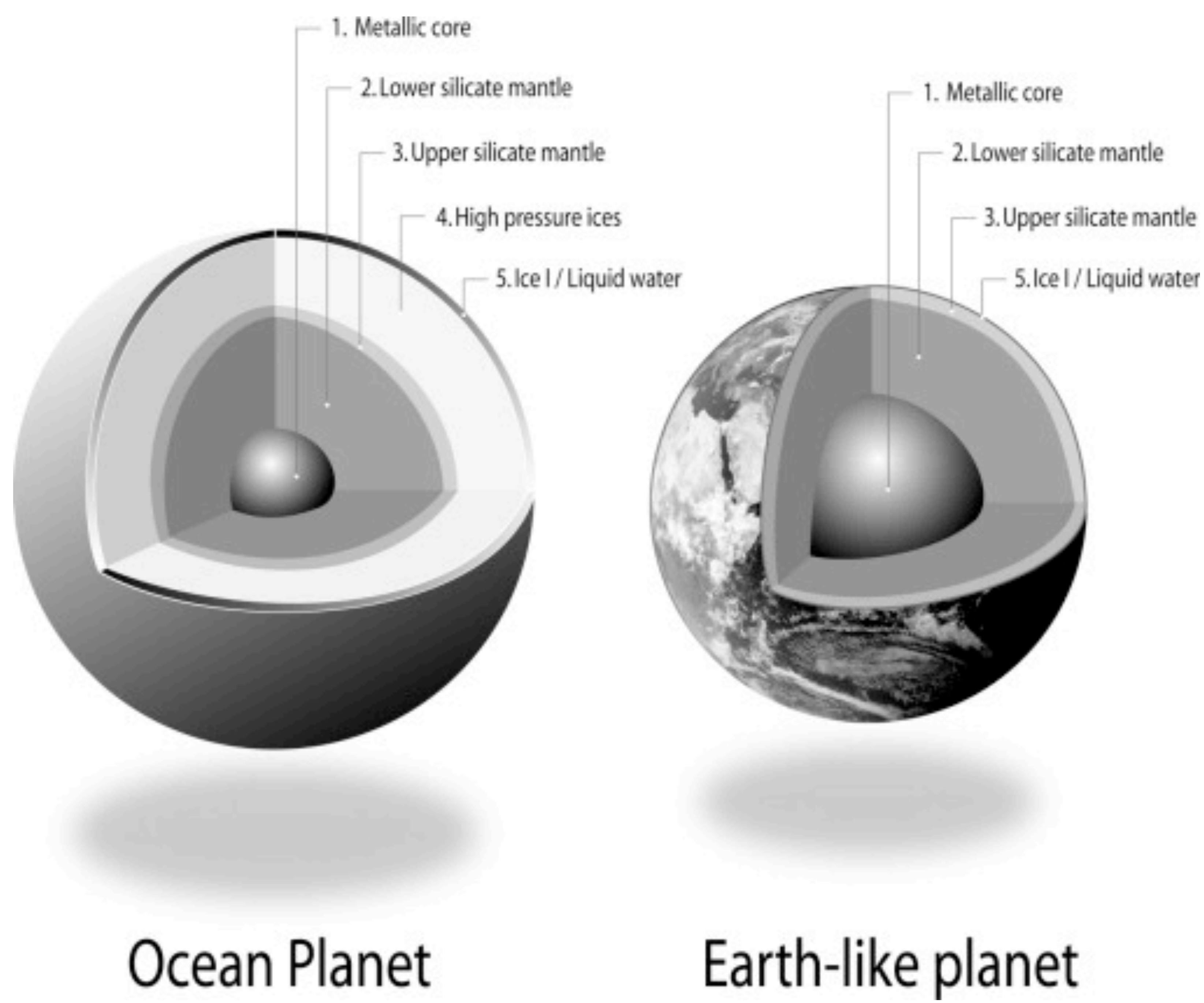

Combination : Mass-radius relations

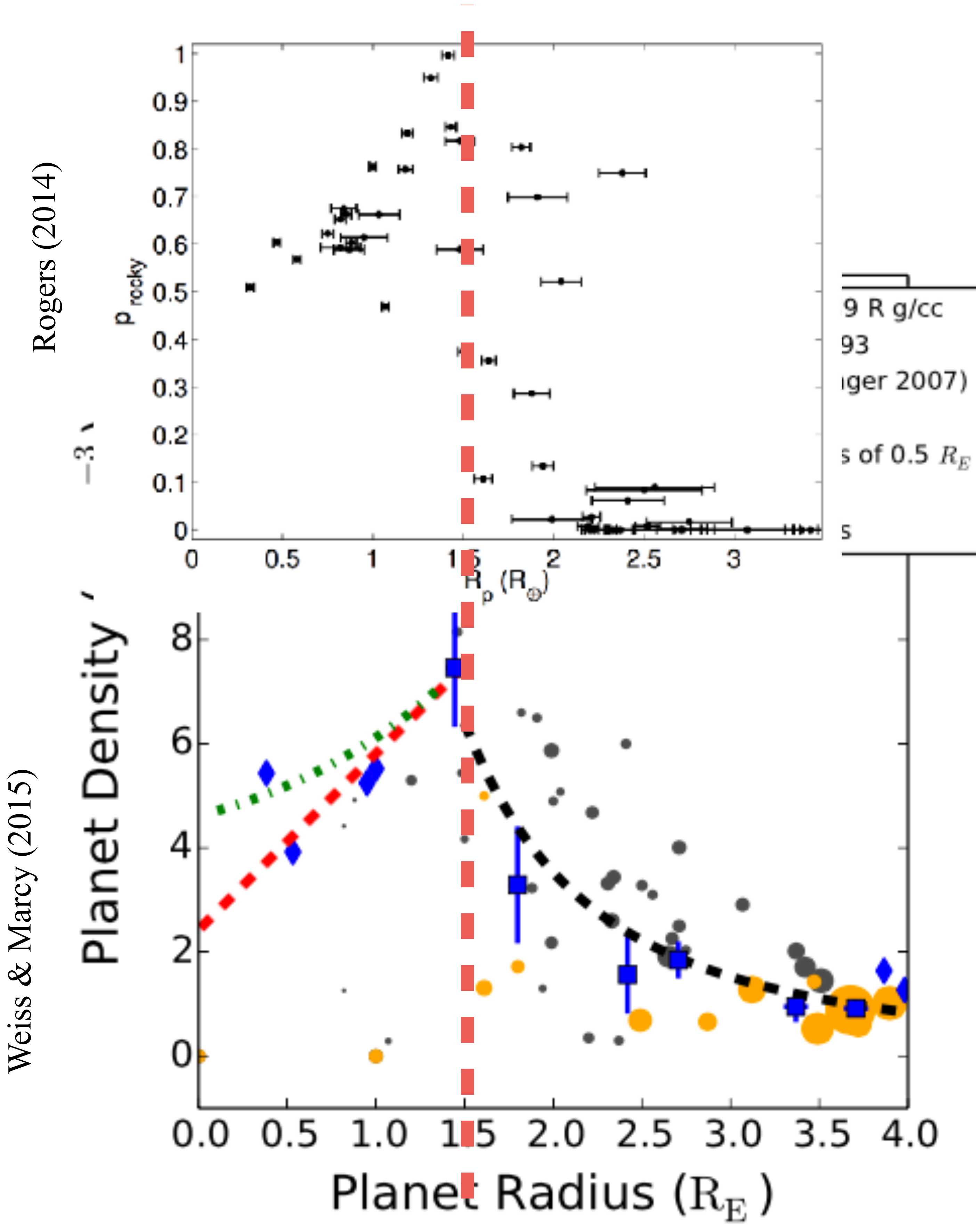

- Rogers (2014); Weiss & Marcy (2015)
- rocky transition @ 1.5-1.8 Rearth
- important consideration for HZ planet searches

- Fulton et al. (2017)
- van Eylen et al. (2018)
- See also Petigura (2020)

- rocky transition @ ~1.8 Rearth
- might correlate with P

- Rocky vs volatile-rich
  + H/He enveloppe

- 1.8 Rp ~ 8 Mearth
- below TESS sensitivity?

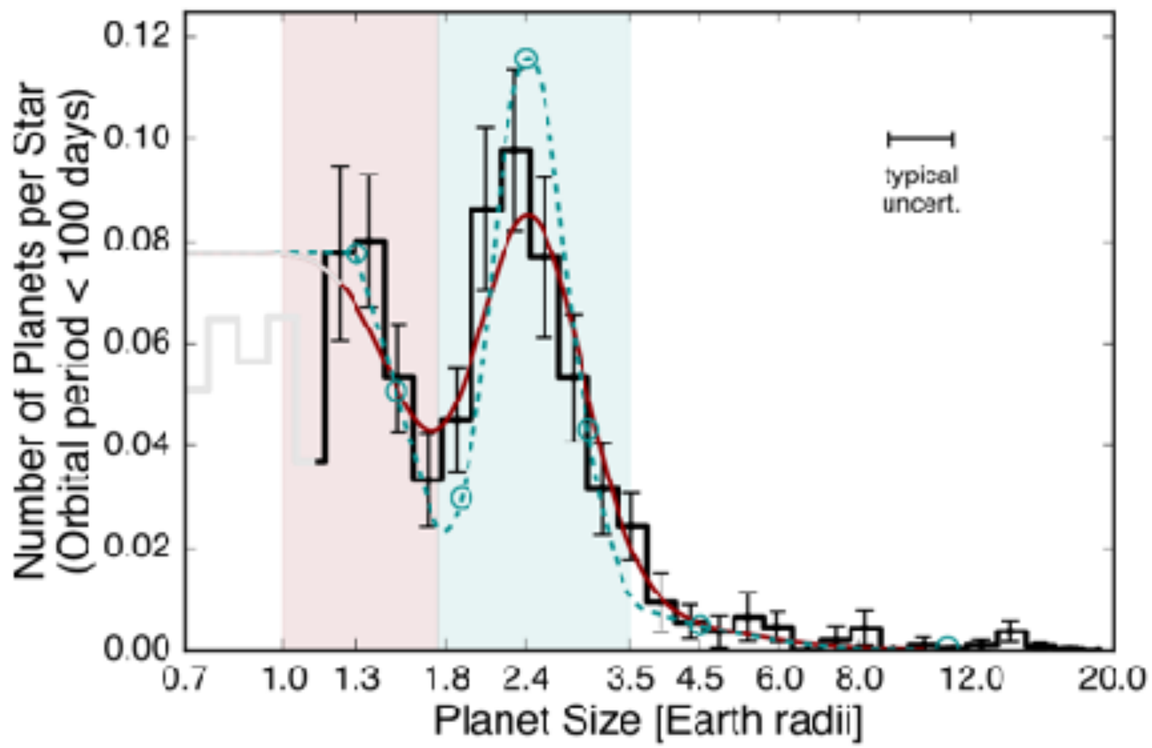

Fulton et al. (2017)

Petigura et al. (2020)

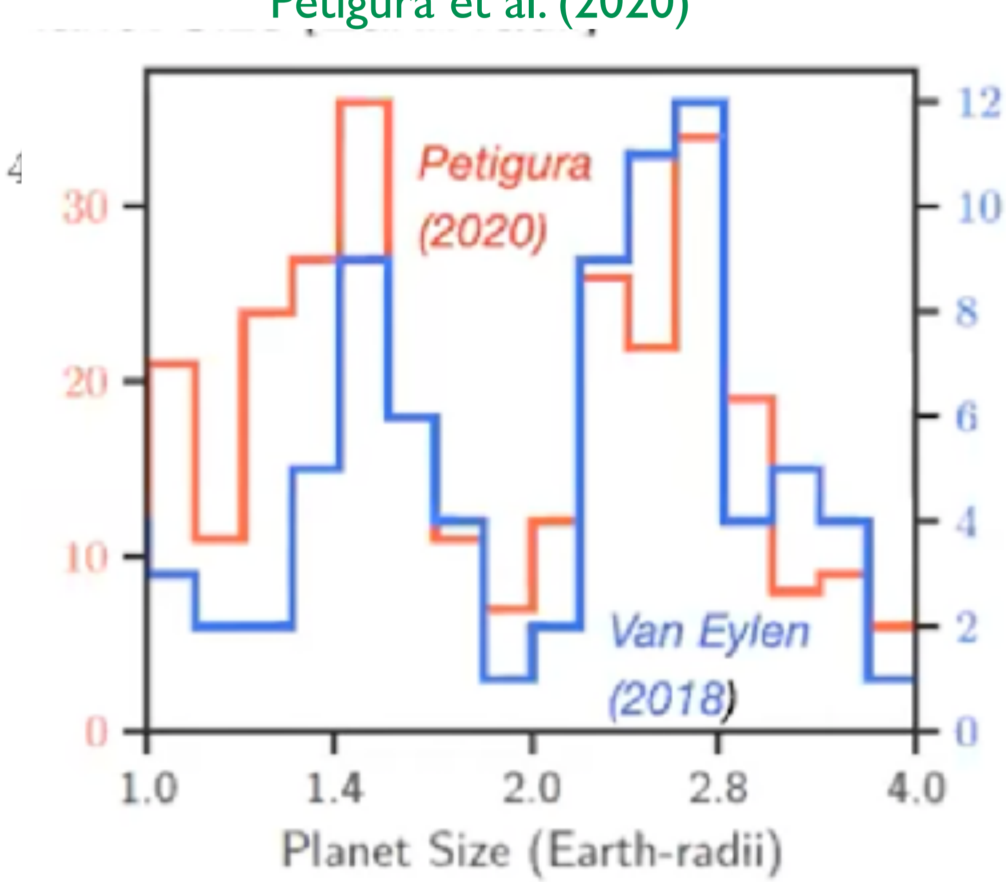

Van Eylen et al. (2018)

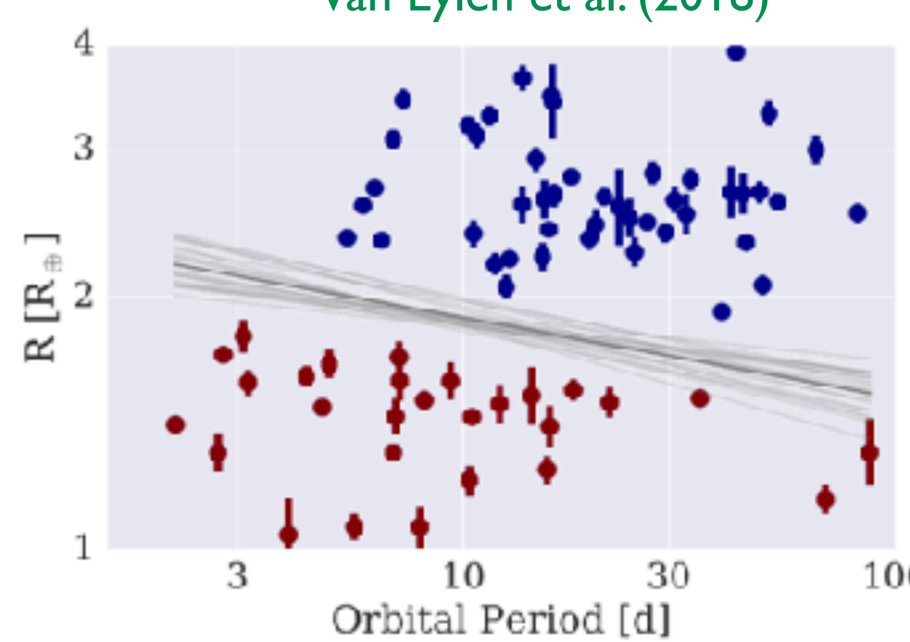

Xavier
BONFILS

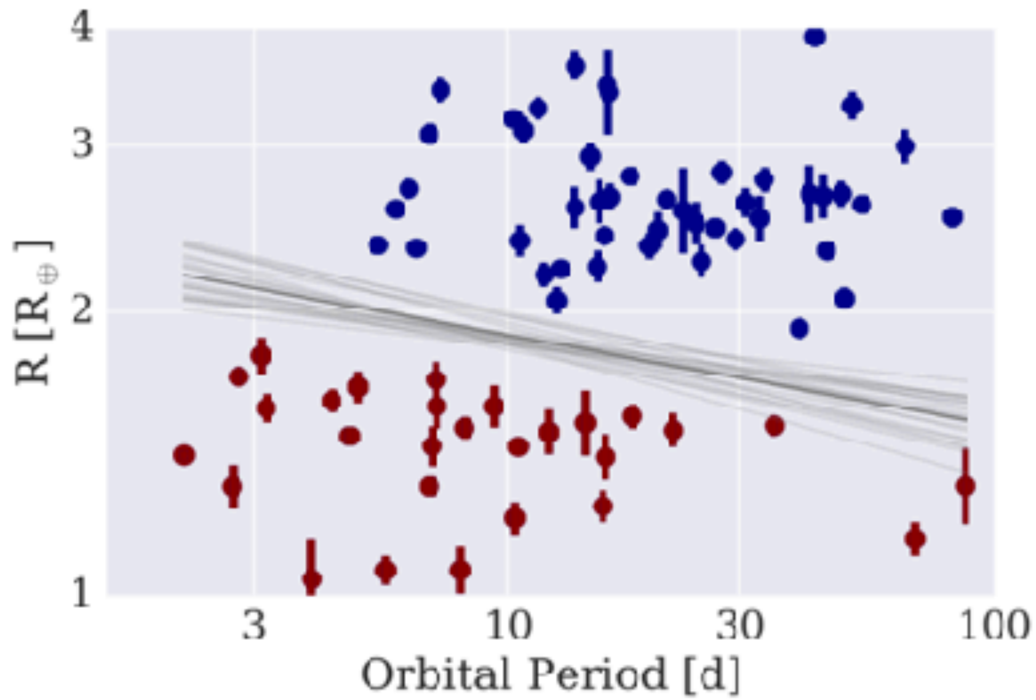

Van Eylen et al. (2020)

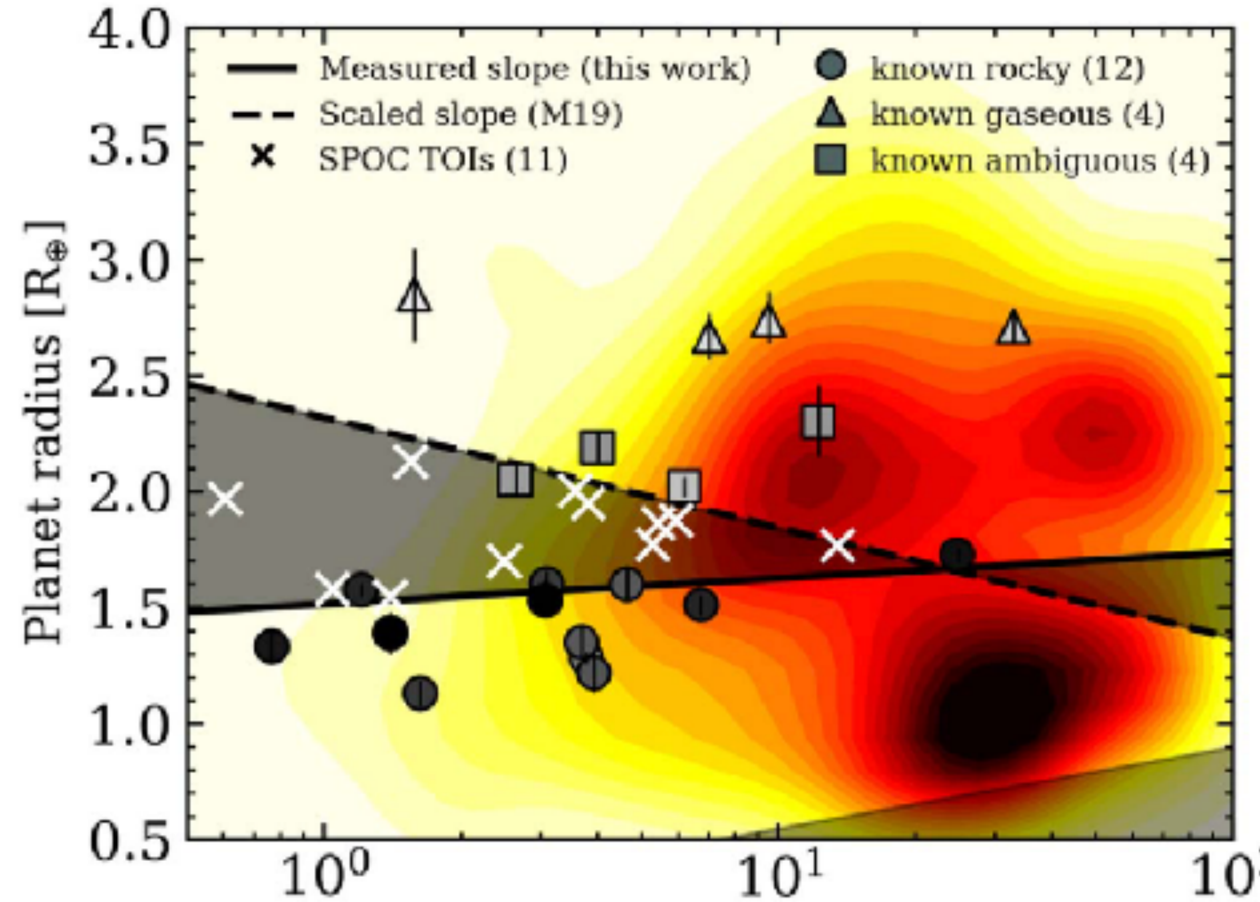

Cloutier & Menou (2020)

Venturini et al. (TESS Science Conf.)

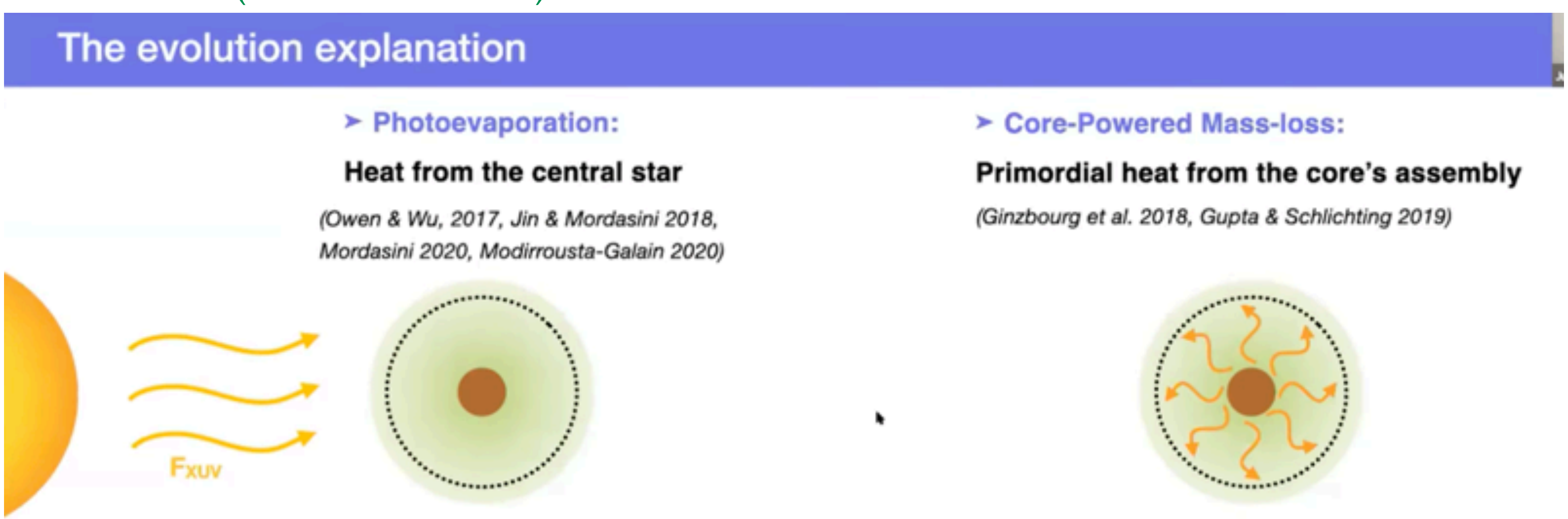

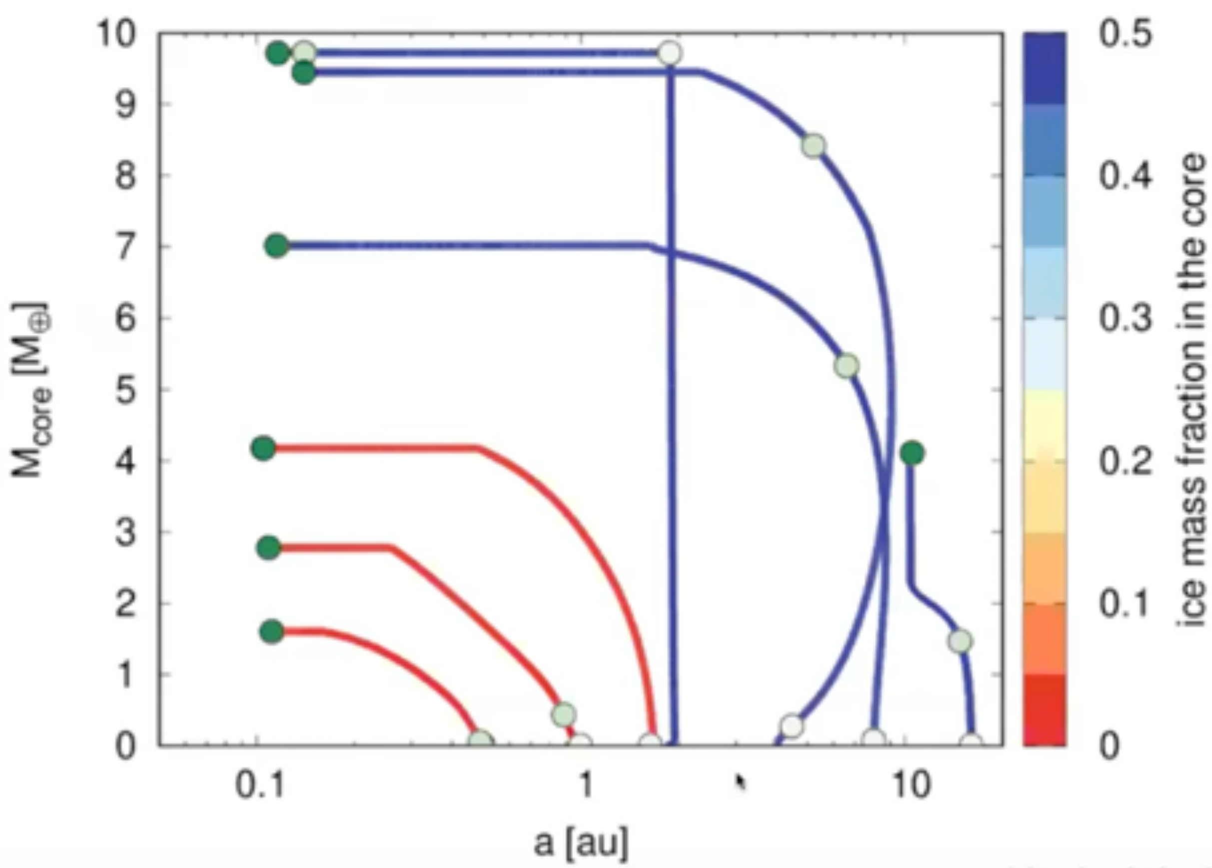

Venturini (TESS Science Conf.)

Venturini et al. (2020, A&A)

- Due to the change of the pebbles' properties at the water ice line, pebble accretion leads to two distinct core populations: icy and large vs. rocky and small cores.
  - **Such bimodality from birth leaves a "valley" imprint on the size distribution of short period exoplanets.**
  - Atmospheric escape after formation must take place the get the bare rocky cores of the first peak.
  - Processes that hinder gas accretion and/or promote atmospheric escape must take place to account for the second peak. Also to better agree with the mass-radius of short period exoplanets.

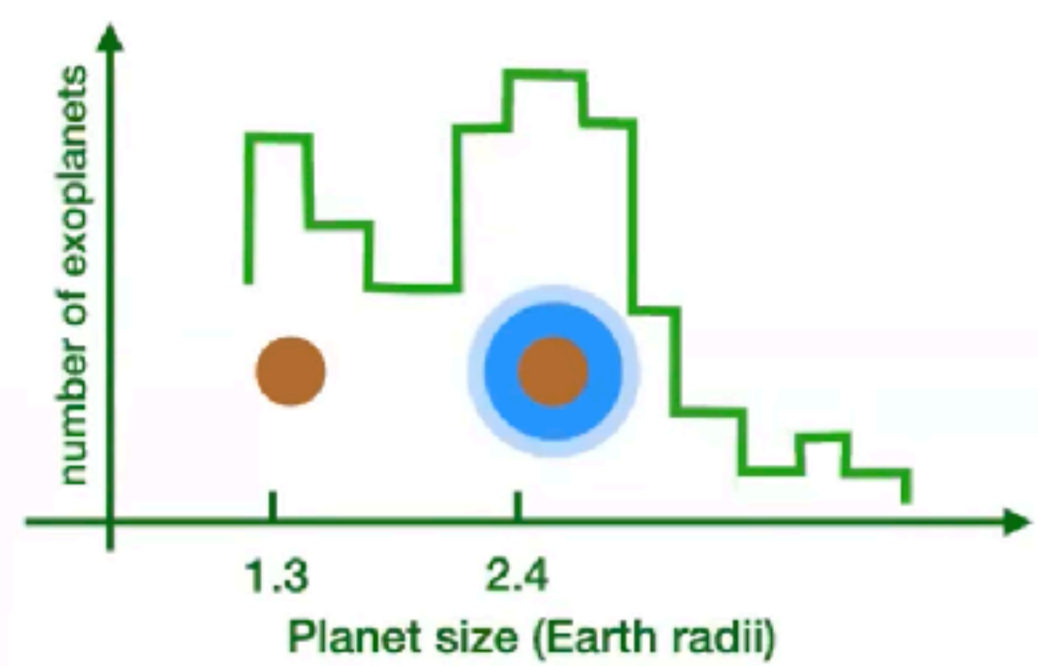

A&A 634, A43 (2020)

Revisited mass-radius relations for exoplanets below 120 $M_\oplus$

J. F. Otegi[1,2], F. Bouchy[2] and R. Helled[1]

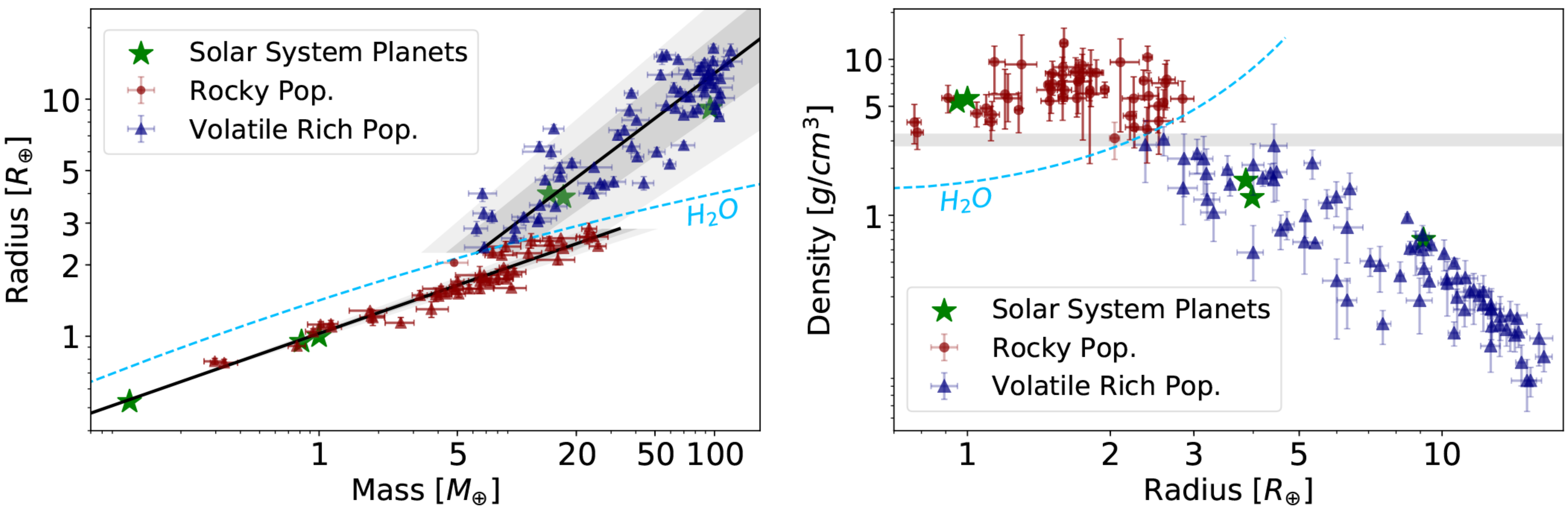

$$R = \begin{cases} (1.03 \pm 0.02)\, M^{(0.29\pm0.01)}, & \text{if } \rho > 3.3\ \mathrm{g\,cm^{-3}} \\ (0.70 \pm 0.11)\, M^{(0.63\pm0.04)}, & \text{if } \rho < 3.3\ \mathrm{g\,cm^{-3}}, \end{cases}$$

$$M = \begin{cases} (0.90 \pm 0.06)\, R^{(3.45\pm0.12)}, & \text{if } \rho > 3.3\ \mathrm{g\,cm^{-3}} \\ (1.74 \pm 0.38)\, R^{(1.58\pm0.10)}, & \text{if } \rho < 3.3\ \mathrm{g\,cm^{-3}}. \end{cases}$$

Multiplicity

Ballard & Johnson (2016)

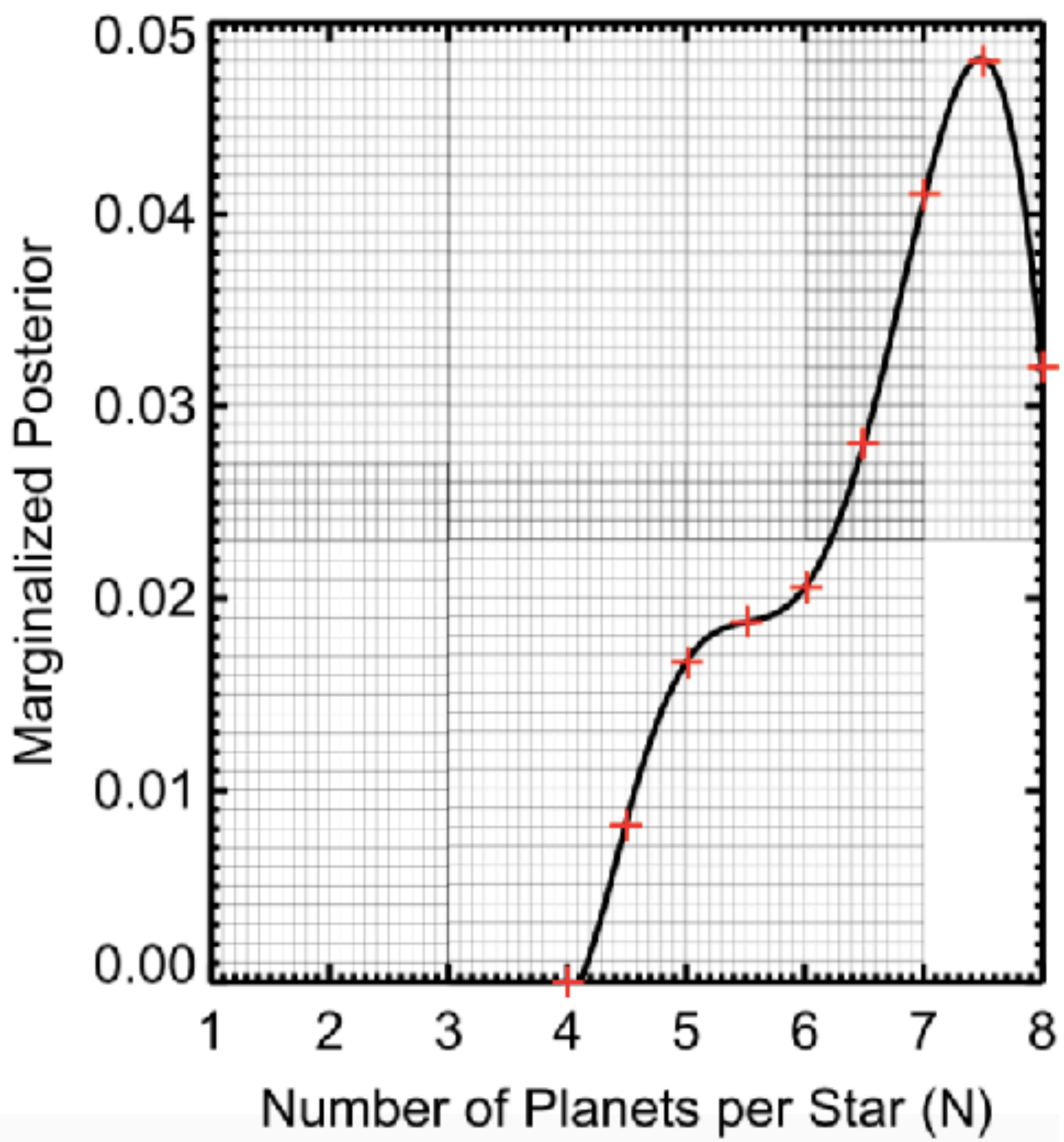

Burn et al. (2020)

Table 4. Multiplicity of specific planetary types for all populations

	Stellar mass ($M_\odot$)				
Type	0.1	0.3	0.5	0.7	1.0
$M > 1\,M_\oplus$	3.04	5.47	6.51	6.89	7.01
Earth-like	4.31	5.58	5.59	5.14	4.89
Super Earth	1.89	3.23	4.06	4.44	4.77
Neptunian	1.00	1.13	1.33	1.39	1.33
Sub-giant	–	1.00	1.14	1.06	1.17
Giant	–	1.00	1.30	1.58	1.63
Temperate zone	1.23	1.53	1.74	1.81	1.98

Mutual inclinations

Ballard & Johnson (2016)

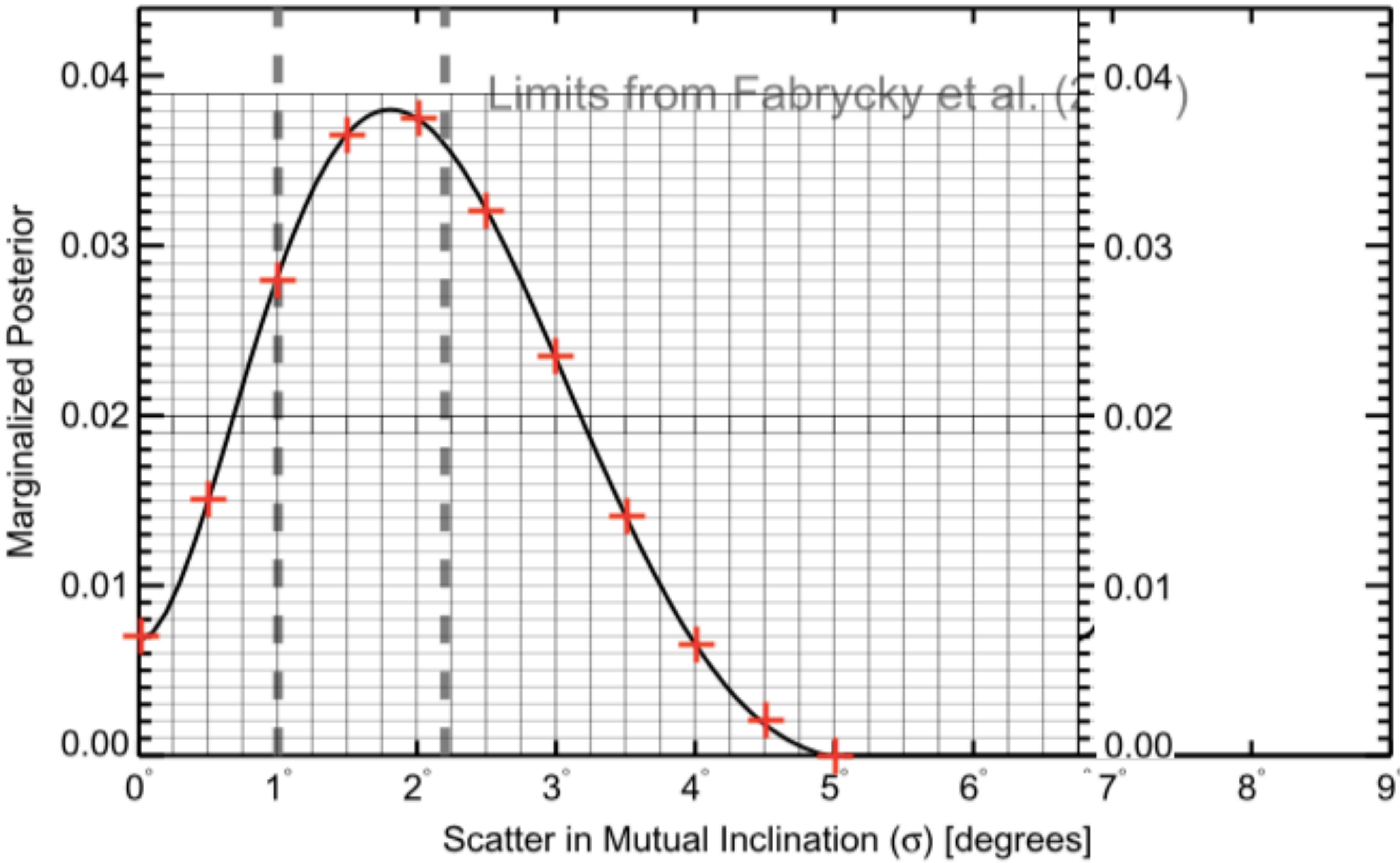

Eccentricities in multis

Linbach & Turner (2015)

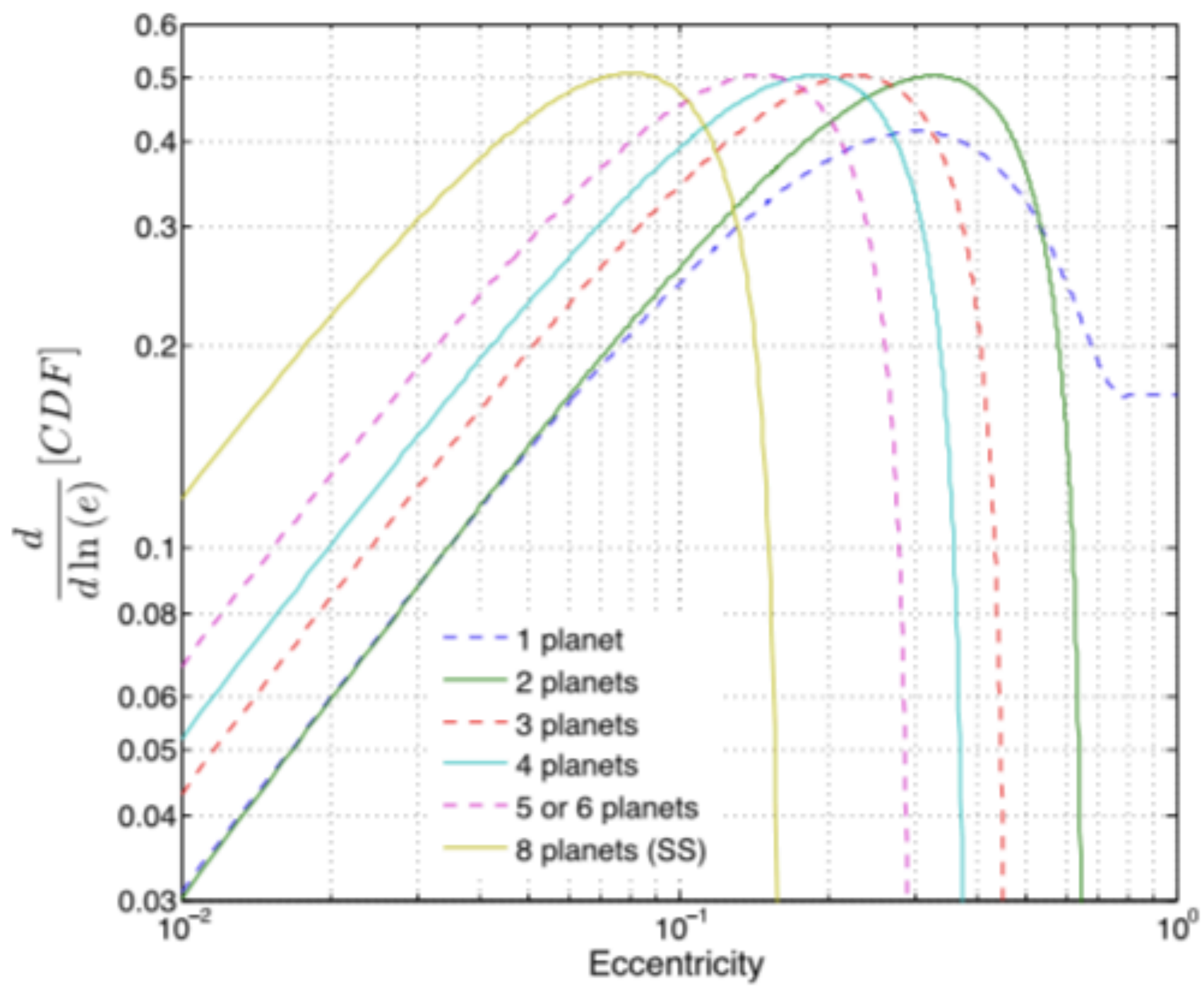

Fig. 4. Eccentricity probability density distributions for various multiplicities based on polynomial fits to the cumulative distribution functions (CDF). Lower-eccentricity systems are more likely to belong to higher-multiplicity systems. Second-order polynomials were fit to the cumulative distributions for all multiplicities except the single-planet systems, in which case a third-order polynomial was used.

Burn et al. (2020)

Table 5. Mean eccentricities of different planetary types for all populations

	Stellar mass ($M_{\odot}$)				
Type	0.1	0.3	0.5	0.7	1.0
$M > 1\,M_{\oplus}$	0.07	0.05	0.04	0.04	0.04
Earth-like	0.07	0.05	0.04	0.04	0.04
Super Earth	0.08	0.05	0.04	0.04	0.03
Neptunian	0.08	0.10	0.10	0.10	0.09
Sub-giant	–	0.05	0.12	0.16	0.13
Giant	–	0.01	0.19	0.14	0.17
Temperate zone	0.11	0.06	0.04	0.03	0.02

s
r

Xavier Bonfils

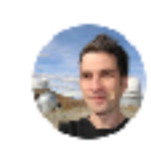

Take home

- Fast progresses from giant exoplanets to temperate exo-Earths
- Many systems w/ unique interests
- Statistics insights :
  - small, low-mass planets are found abundant,
  - with high multiplicity,
  - low eccentricity,
  - low coplanarity
  - Bimodal distribution probably correspond to rocky vs. volatile-rich exoplanets
  - Dominant evaporation process might change toward lower-mass host stars

Xavier Bonfils